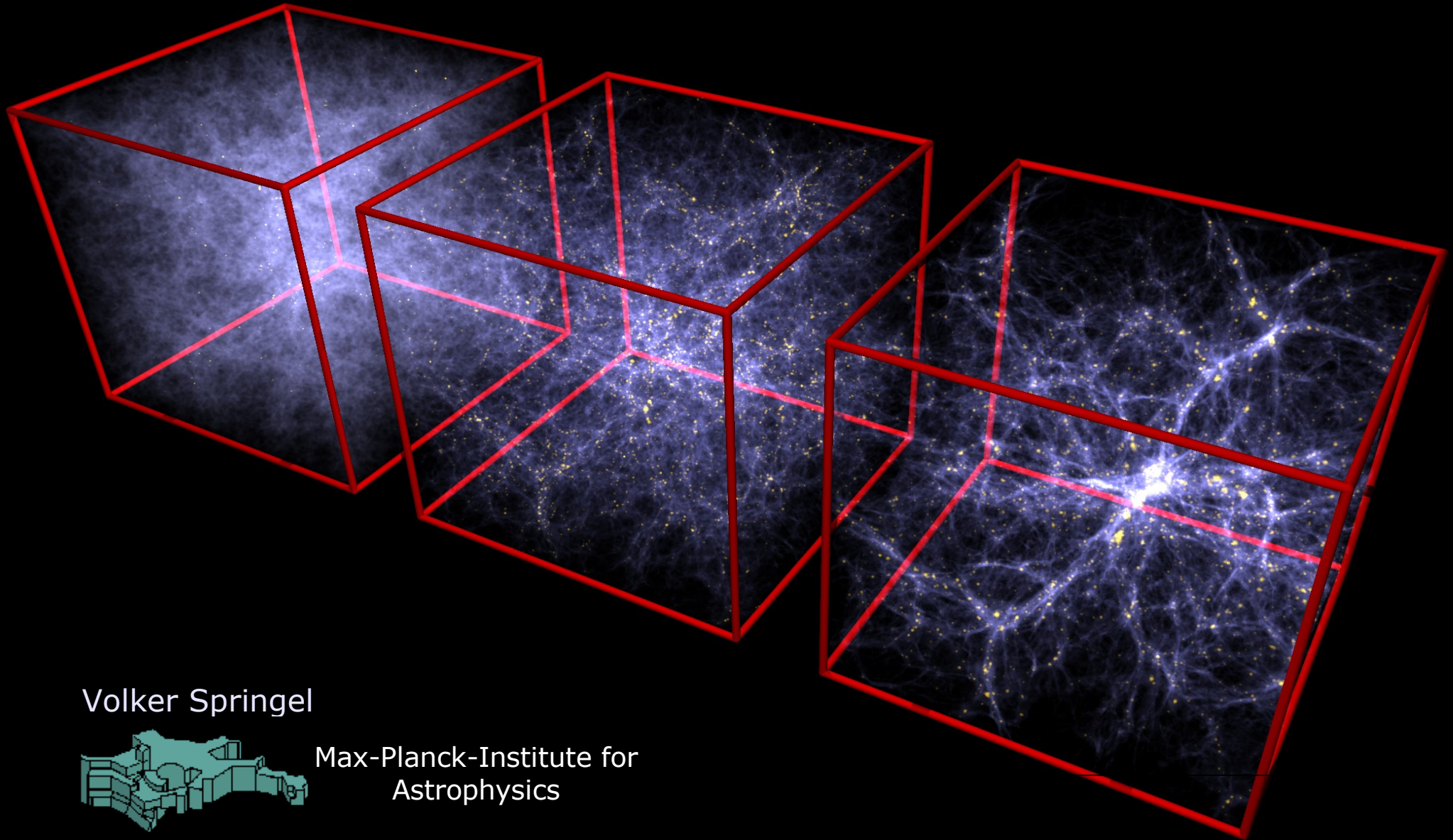


Summer school on cosmological numerical simulations

3rd week – TUESDAY

Helmholtz School of Astrophysics
Potsdam, July/August 2006



Volker Springel



Max-Planck-Institute for
Astrophysics

Smoothed particle hydrodynamics as a tool to model baryonic physics

TUESDAY-Lecture of 3rd week

Volker Springel

- ▶ **Basic of Smoothed Particle Hydrodynamics (SPH)**
- ▶ **Variational formalism and entropy, shock capturing and artificial viscosity**
- ▶ **Strengths and weaknesses of SPH with respect to Eulerian hydrodynamics**
- ▶ **Non-standard physics in SPH**
 - ▶ **Thermal conduction**
 - ▶ **Magnetic fields**
 - ▶ **Cosmic rays**
 - ▶ **Star formation and supernovae**



Basics of SPH

The baryons in the universe can be modelled as an *ideal gas*

BASIC HYDRODYNAMICAL EQUATIONS

Euler equation:

$$\frac{d\mathbf{v}}{dt} = -\frac{\nabla P}{\rho} - \nabla\Phi$$

Continuity equation:

$$\frac{d\rho}{dt} + \rho\nabla \cdot \mathbf{v} = 0$$

First law of thermodynamics:

$$\frac{du}{dt} = -\frac{P}{\rho}\nabla \cdot \mathbf{v} - \frac{\Lambda(u, \rho)}{\rho}$$

Equation of state of ideal monoatomic gas:

$$P = (\gamma - 1)\rho u, \quad \gamma = 5/3$$

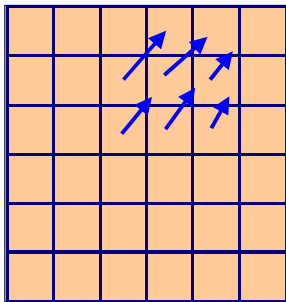
What is smoothed particle hydrodynamics?

DIFFERENT METHODS TO DISCRETIZE A FLUID

Eulerian

discretize space

representation on a mesh
(volume elements)



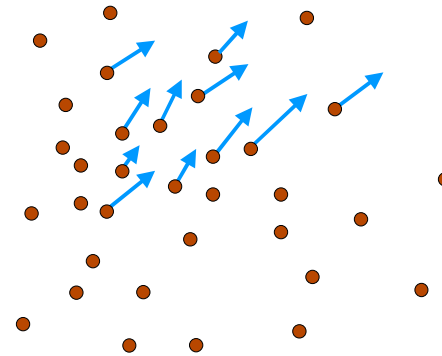
principle advantage:

high accuracy (shock capturing), low numerical viscosity

Lagrangian

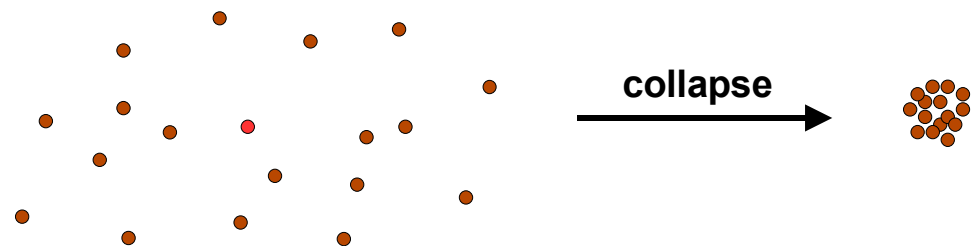
discretize mass

representation by fluid elements
(particles)



principle advantage:

resolutions adjusts automatically to the flow



Kernel interpolation is used in smoothed particle hydrodynamics (SPH) to build continuous fluid quantities from discrete tracer particles

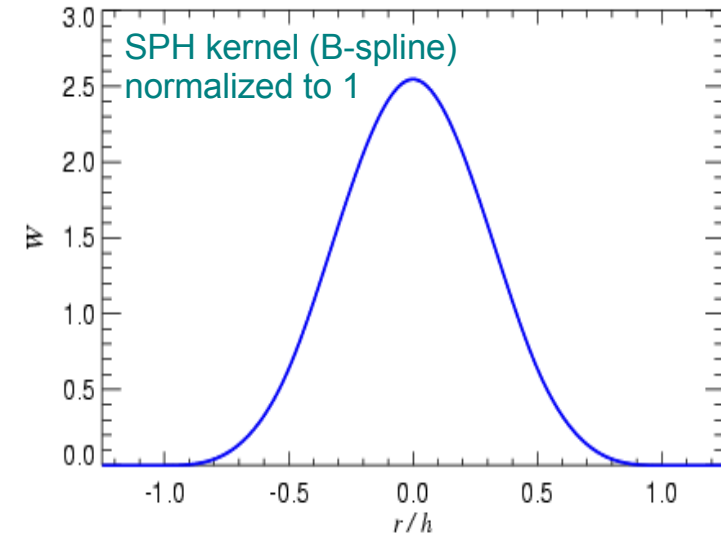
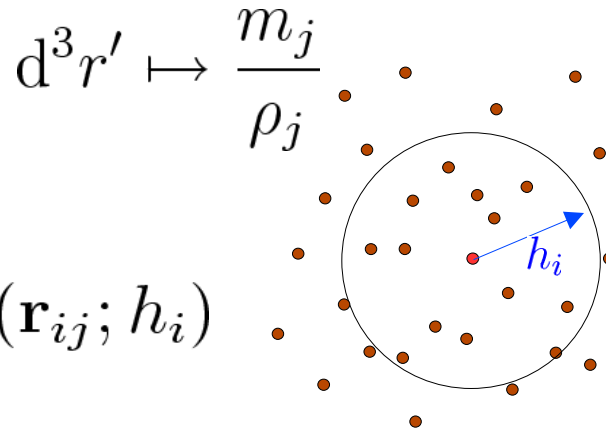
DENSITY ESTIMATION IN SPH BY MEANS OF ADAPTIVE KERNEL ESTIMATION

Kernel interpolant of an arbitrary function:

$$\langle A(\mathbf{r}) \rangle = \int W(\mathbf{r} - \mathbf{r}', h) A(\mathbf{r}') d^3 r'$$

If the function is only known at a set of discrete points, we approximate the integral as a sum, using the replacement:

$$\langle A_i \rangle = \sum_{j=1}^N \frac{m_j}{\rho_j} A_j W(\mathbf{r}_{ij}; h_i)$$



This leads to the SPH density estimate, for $A_i = \rho_i$

$$\rho_i = \sum_{j=1}^N m_j W(|\mathbf{r}_{ij}|, h_i)$$

→ **This can be differentiated !**

Kernel interpolants allow the construction of derivatives from a set of discrete tracer points

EXAMPLES FOR ESTIMATING THE VELOCITY DIVERGENCE

Smoothed estimate for the velocity field:

$$\langle \mathbf{v}_i \rangle = \sum_j \frac{m_j}{\rho_j} \mathbf{v}_j W(\mathbf{r}_i - \mathbf{r}_j)$$

Velocity divergence can now be readily estimated:

$$\nabla \cdot \mathbf{v} = \nabla \cdot \langle \mathbf{v}_i \rangle = \sum_j \frac{m_j}{\rho_j} \mathbf{v}_j \nabla_i W(\mathbf{r}_i - \mathbf{r}_j)$$

But alternative (and better) estimates are possible also:

Invoking the identity

$$\rho \nabla \cdot \mathbf{v} = \nabla \cdot (\rho \mathbf{v}) - \mathbf{v} \cdot \nabla \rho$$

one gets a “pair-wise” formula:

$$\rho_i (\nabla \cdot \mathbf{v})_i = \sum_j m_j (\mathbf{v}_j - \mathbf{v}_i) \nabla_i W(\mathbf{r}_i - \mathbf{r}_j)$$

What is smoothed particle hydrodynamics?

BASIC EQUATIONS OF SMOOTHED PARTICLE HYDRODYNAMICS

Each particle carries either the energy or the entropy per unit mass as independent variable

Density estimate $\rho_i = \sum_{j=1}^N m_j W(|\mathbf{r}_{ij}|, h_i)$ \longrightarrow **Continuity equation automatically fulfilled.**

$\longrightarrow P_i = (\gamma - 1)\rho_i u_i$

Euler equation $\frac{d\mathbf{v}_i}{dt} = - \sum_{j=1}^N m_j \left(\frac{P_i}{\rho_i^2} + \frac{P_j}{\rho_j^2} \right) \nabla_i \bar{W}_{ij}$

Artificial viscosity $+ \Pi_{ij}$

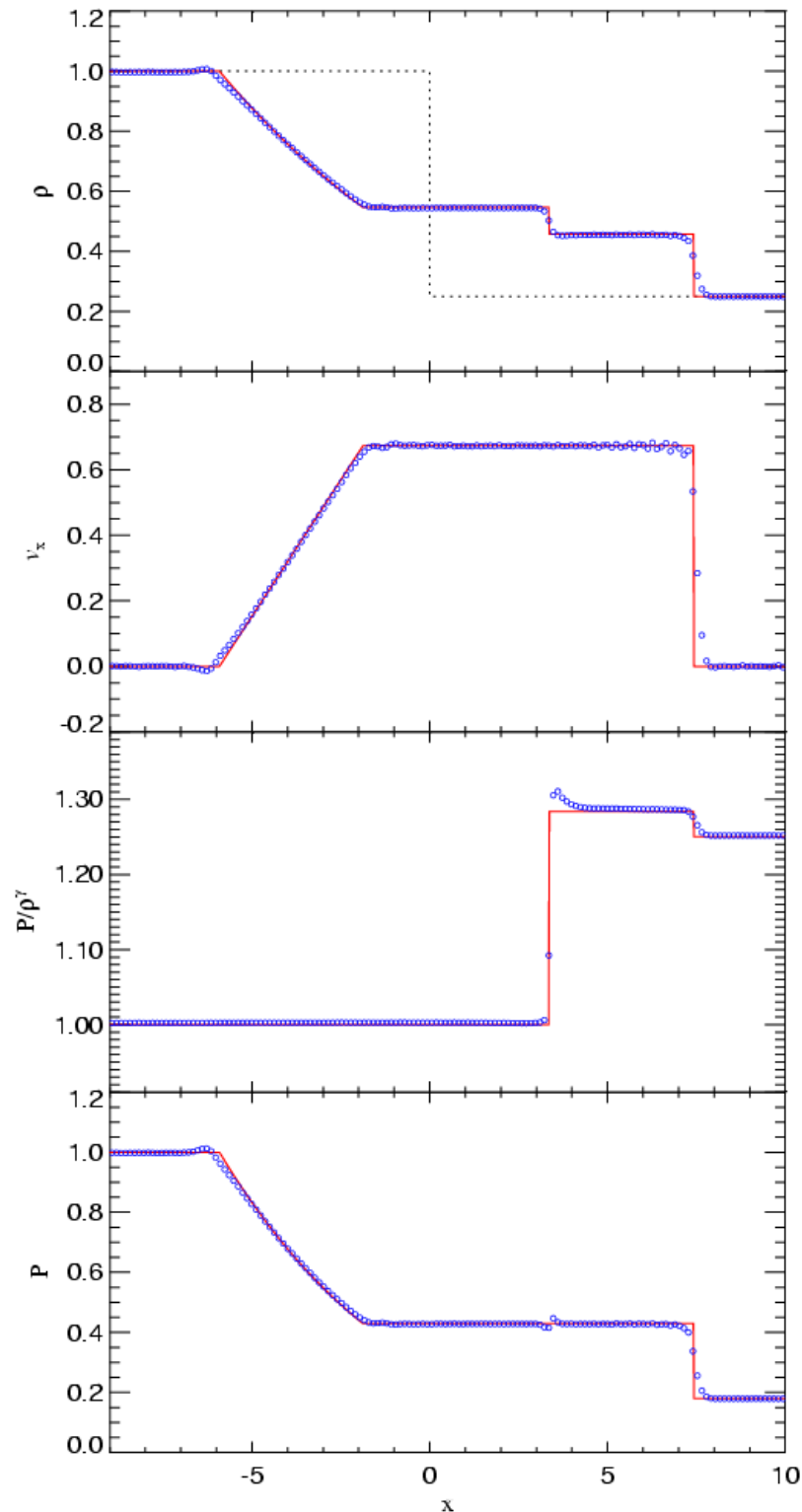
First law of thermodynamics $\frac{du_i}{dt} = \frac{1}{2} \sum_{j=1}^N m_j \left(\frac{P_i}{\rho_i^2} + \frac{P_j}{\rho_j^2} \right) \mathbf{v}_{ij} \cdot \nabla_i \bar{W}_{ij}$

$+ \Pi_{ij}$

Viscosity and shock capturing

An artificial viscosity needs to be introduced to capture shocks

SHOCK TUBE PROBLEM AND VISCOSITY



viscous force:

$$\left. \frac{d\mathbf{v}_i}{dt} \right|_{\text{visc}} = - \sum_{j=1}^N m_j \Pi_{ij} \nabla_i \bar{W}_{ij}$$

parameterization of the artificial viscosity:

$$\Pi_{ij} = \begin{cases} -\frac{\alpha}{2} \frac{[c_i + c_j - 3w_{ij}]w_{ij}}{\rho_{ij}} & \text{if } \mathbf{v}_{ij} \cdot \mathbf{r}_{ij} < 0 \\ 0 & \text{otherwise} \end{cases}$$

$$v_{ij}^{\text{sig}} = c_i + c_j - 3w_{ij},$$

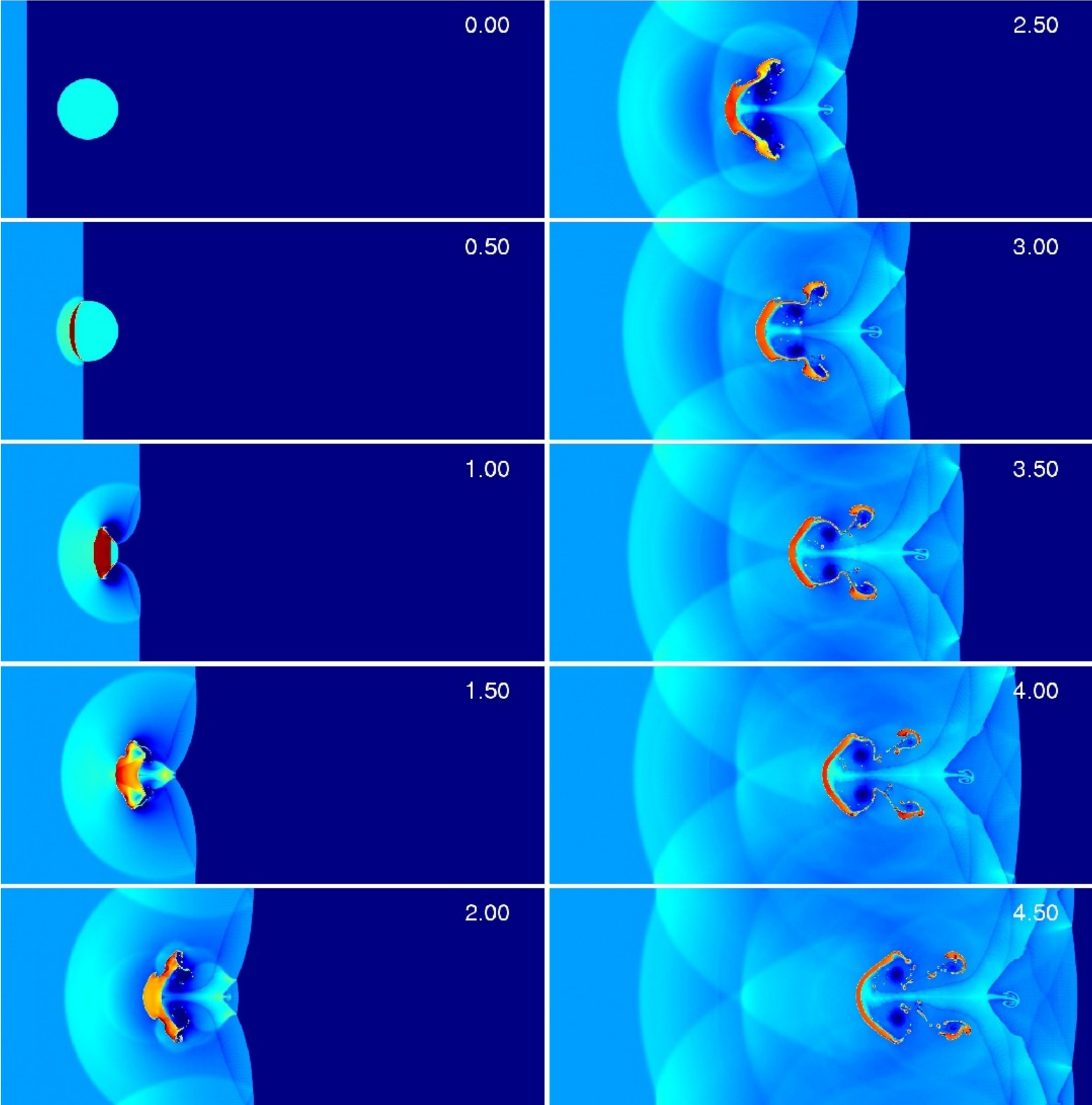
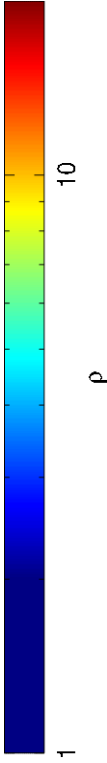
$$w_{ij} = \mathbf{v}_{ij} \cdot \mathbf{r}_{ij} / |\mathbf{r}_{ij}|$$

heat production rate:

$$\frac{du_i}{dt} = \frac{1}{2} \sum_{j=1}^N m_j \Pi_{ij} \mathbf{v}_{ij} \cdot \nabla_i \bar{W}_{ij}$$

SPH can handle strong shocks and vorticity generation

A MACH NUMBER 10 SHOCK THAT STRIKES AN OVERDENSE CLOUD



Variational derivation of SPH

The traditional way to derive the SPH equations leaves room for many different formulations

SYMMETRIZATION CHOICES

$$\overline{W}_{ij} = W(|\mathbf{r}_{ij}|, [h_i + h_j]/2)$$

Symmetrized kernel:

$$\overline{W}_{ij} = \frac{1}{2} [W(|\mathbf{r}_{ij}|, h_i) + W(|\mathbf{r}_{ij}|, h_j)]$$

Symmetrization of pressure terms:

$$\text{Using } \nabla P = 2\sqrt{P}\nabla\sqrt{P} \quad \frac{1}{2} \left(\frac{P_i}{\rho_i^2} + \frac{P_j}{\rho_j^2} \right) \iff \sqrt{\frac{P_i P_j}{\rho_i^2 \rho_j^2}}$$

Is there a best choice?

For an adiabatic flow, temperature can be derived from the specific entropy

ENTROPY FORMALISM

Definition of an entropic function:

$$P_i = A_i \rho_i^\gamma$$

for an adiabatic flow:

$$A_i = A_i(s_i) = \text{const.}$$

don't integrate the temperature, but infer it from:

$$u_i = \frac{A_i}{\gamma - 1} \rho_i^{\gamma-1}$$

Use an artificial viscosity to generate entropy in shocks:

$$\frac{dA_i}{dt} = \frac{1}{2} \frac{\gamma - 1}{\rho_i^{\gamma-1}} \sum_{j=1}^N m_j \Pi_{ij} \mathbf{v}_{ij} \cdot \nabla_i \bar{W}_{ij}$$

None of the adaptive SPH schemes conserves energy and entropy simultaneously

CONSERVATION LAW TROUBLES

Hernquist (1993):

If the **thermal energy** is integrated, **entropy** conservation can be **violated**...

If the **entropy** is integrated, total **energy** is **not** necessarily **conserved**...

The trouble is caused by varying smoothing lengths...

∇h -terms

Do we have to worry about this?

YES

Can we do better?

YES

A fully conservative formulation of SPH

Springel & Hernquist (2002)

DERIVATION

Lagrangian:

$$L(\mathbf{q}, \dot{\mathbf{q}}) = \frac{1}{2} \sum_{i=1}^N m_i \dot{\mathbf{r}}_i^2 - \frac{1}{\gamma - 1} \sum_{i=1}^N m_i A_i \rho_i^{\gamma-1}$$
$$\mathbf{q} = (\mathbf{r}_1, \dots, \mathbf{r}_N, h_1, \dots, h_N)$$

Constraints:

$$\phi_i(\mathbf{q}) \equiv \frac{4\pi}{3} h_i^3 \rho_i - M_{\text{sph}} = 0$$

Equations of motion:

$$\frac{d}{dt} \frac{\partial L}{\partial \dot{q}_i} - \frac{\partial L}{\partial q_i} = \sum_{j=1}^N \lambda_j \frac{\partial \phi_j}{\partial q_i}$$

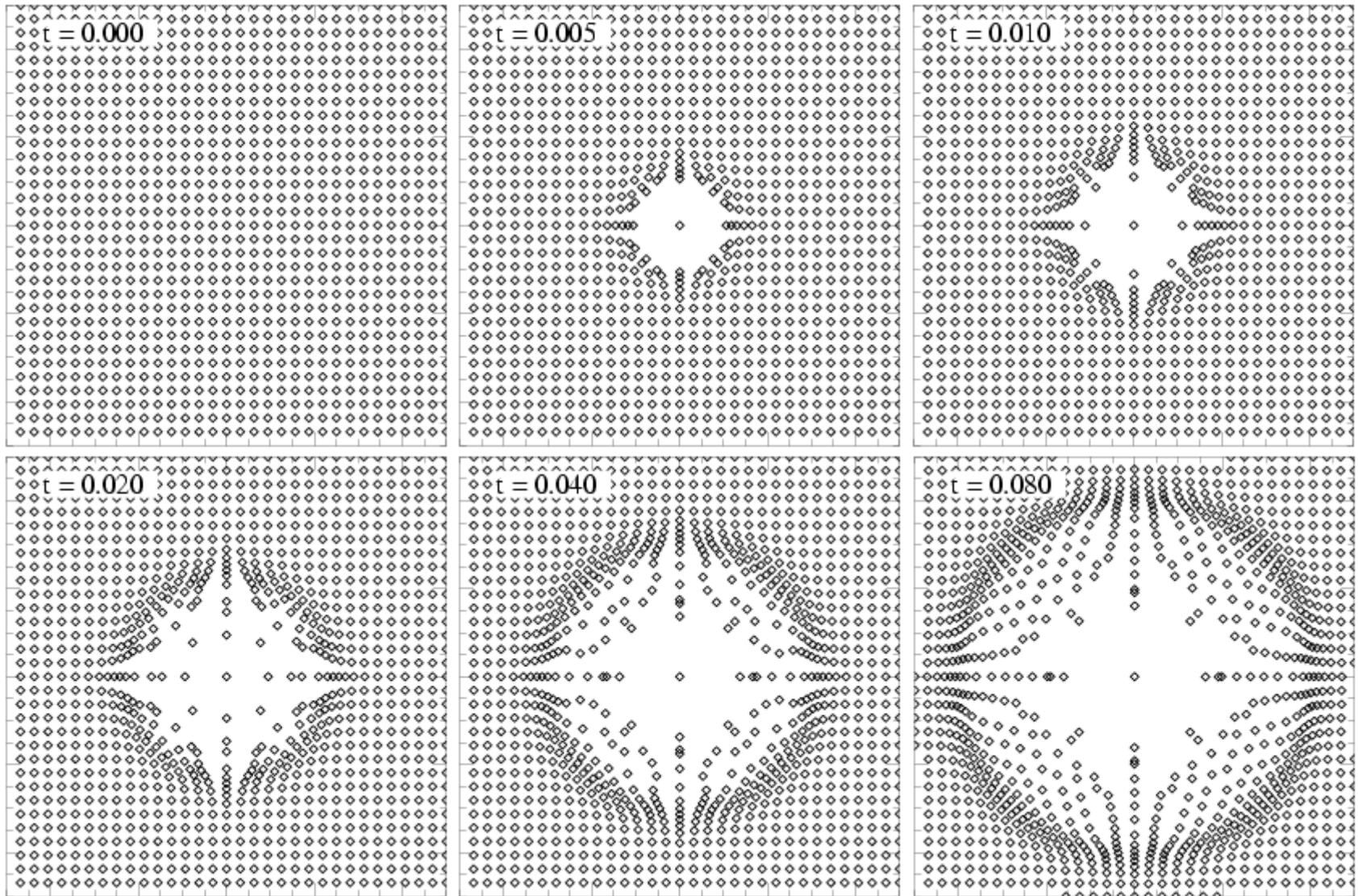
$$\frac{d\mathbf{v}_i}{dt} = - \sum_{j=1}^N m_j \left[f_i \frac{P_i}{\rho_i^2} \nabla_i W_{ij}(h_i) + f_j \frac{P_j}{\rho_j^2} \nabla_i W_{ij}(h_j) \right]$$

$$f_i = \left[1 + \frac{h_i}{3\rho_i} \frac{\partial \rho_i}{\partial h_i} \right]^{-1}$$

Does the entropy
formulation give better
results?

A strong point-explosion is a challenging problem for any hydrodynamical code

EXPLOSIONS IN SPH

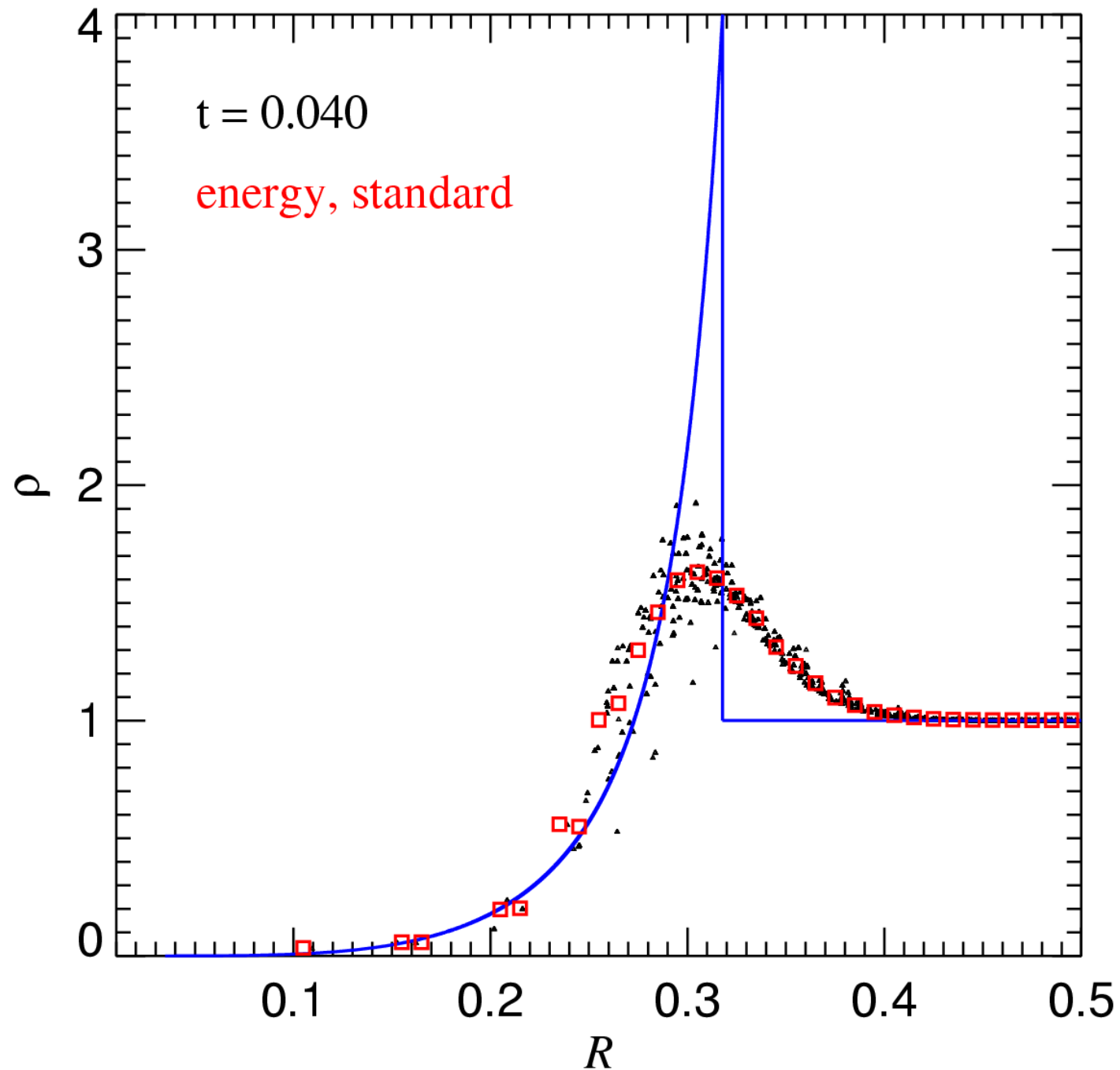


- Geometric formulation gives completely unphysical result (no explosion at all)
- Standard energy formulation produces severe error in total energy, but asymmetric form ok
- Standard entropy formulation ok, but energy fluctuates by several percent

There is a well-known similarity solution for strong point-like explosions

SEDOV-TAYLOR SOLUTIONS FOR SMOOTHED EXPLOSION ENERGY

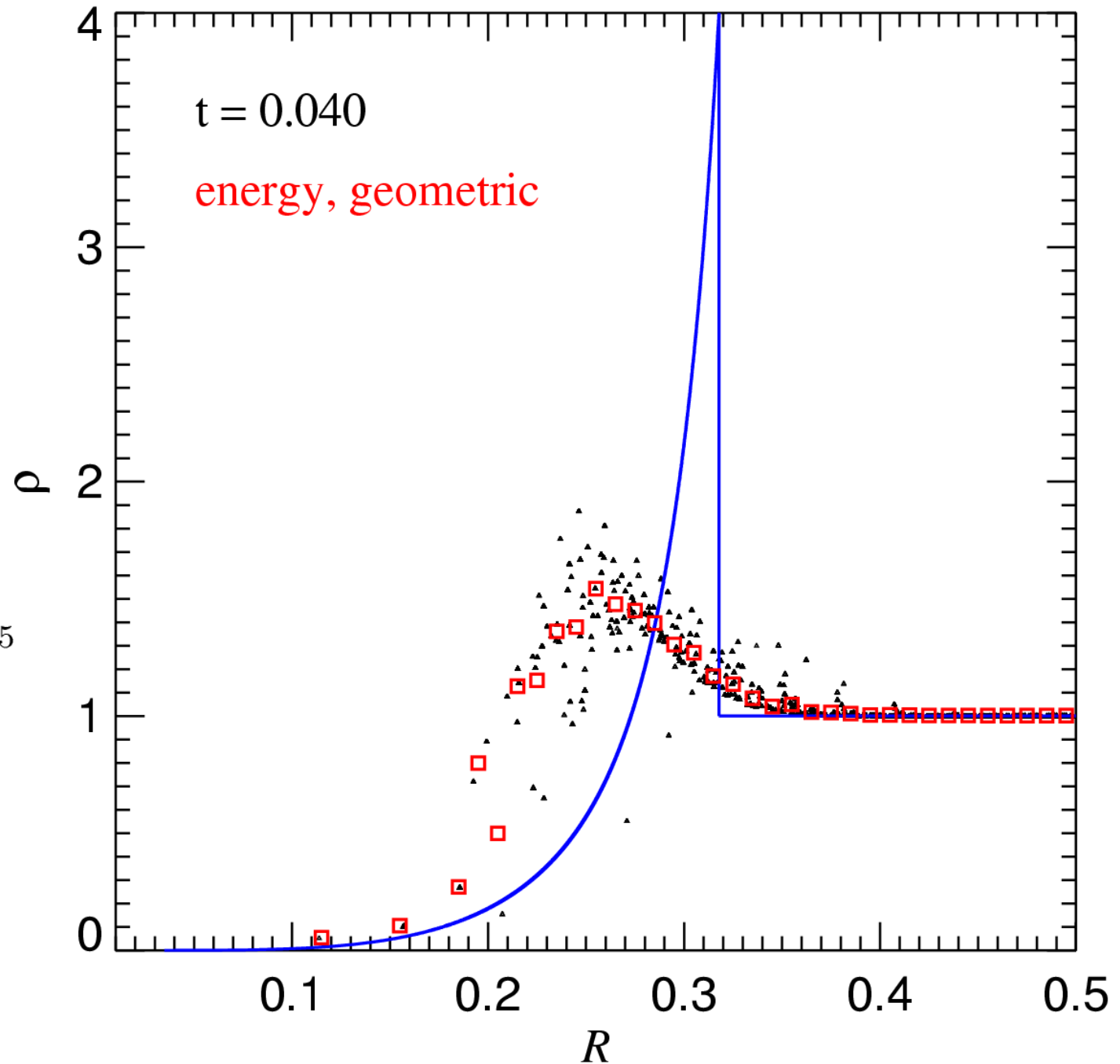
$$R(t) = \beta \left(\frac{Et^2}{\rho} \right)^{1/5}$$



There is a well-known similarity solution for strong point-like explosions

SEDOV-TAYLOR SOLUTIONS FOR SMOOTHED EXPLOSION ENERGY

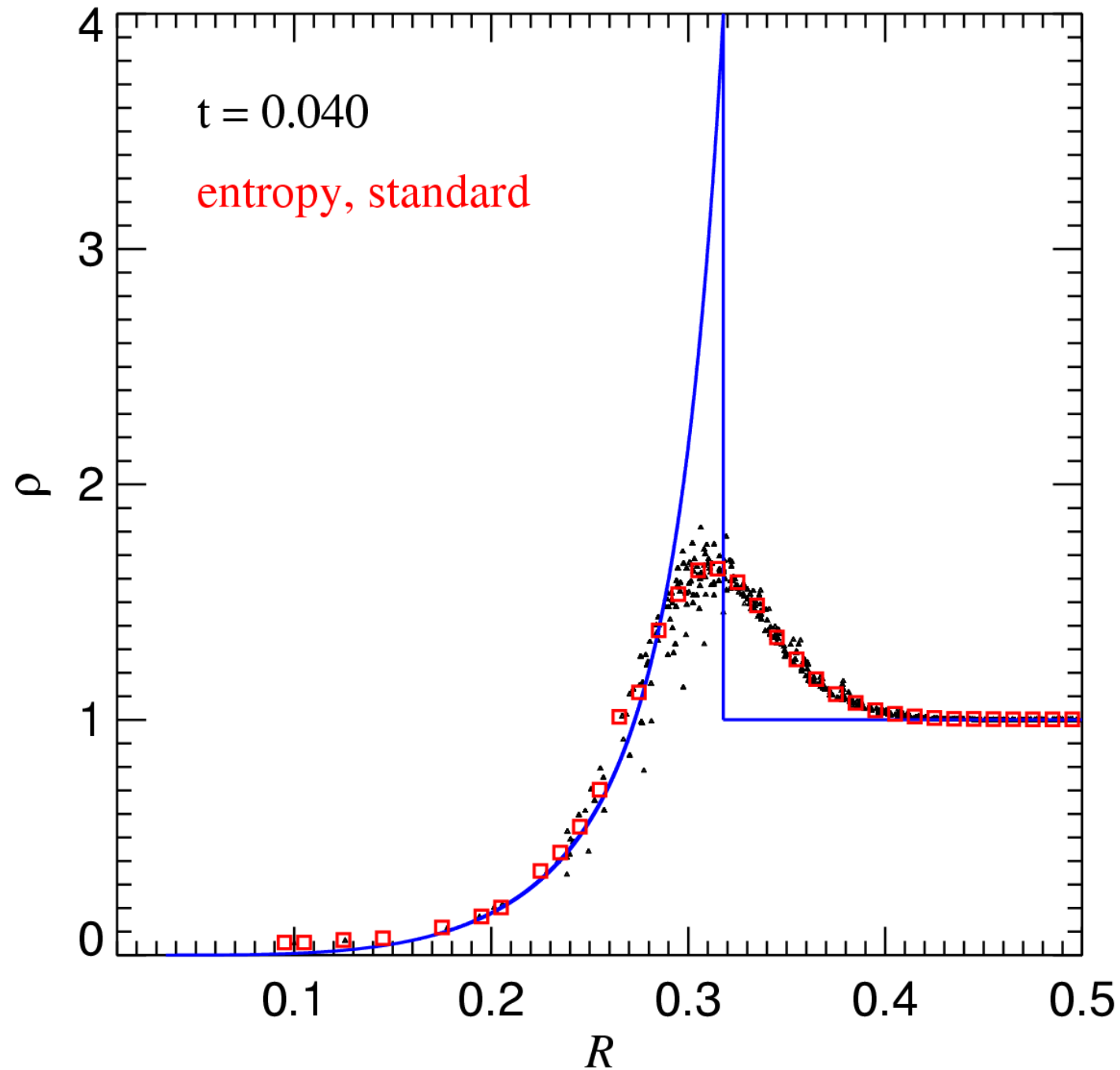
$$R(t) = \beta \left(\frac{Et^2}{\rho} \right)^{1/5}$$



There is a well-known similarity solution for strong point-like explosions

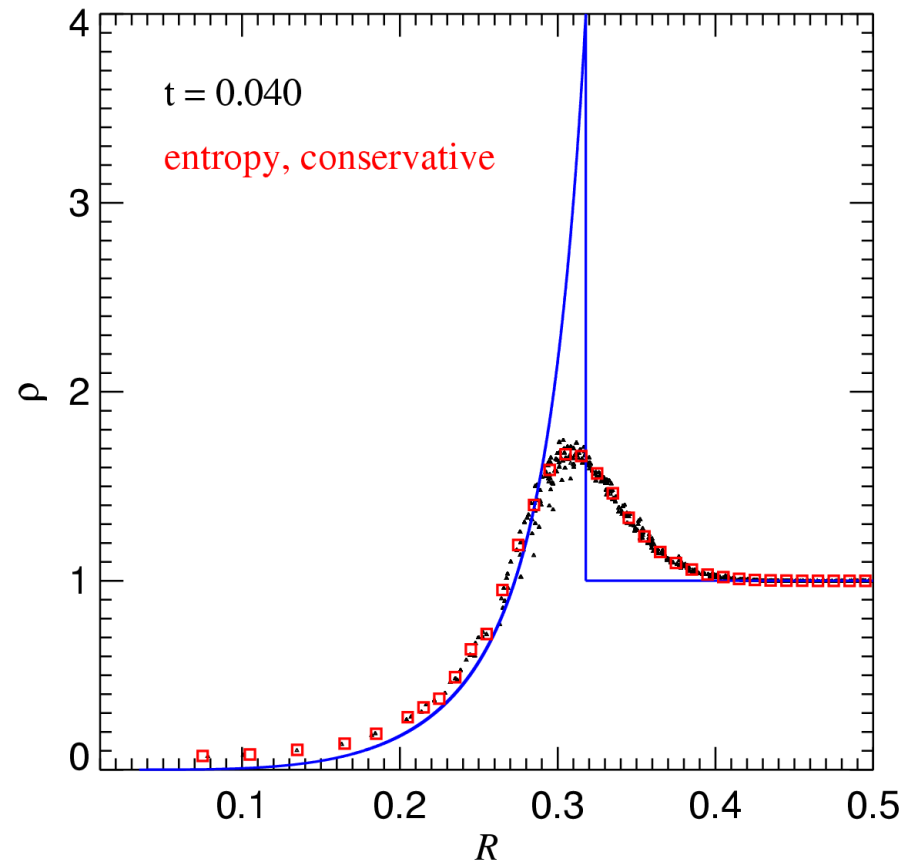
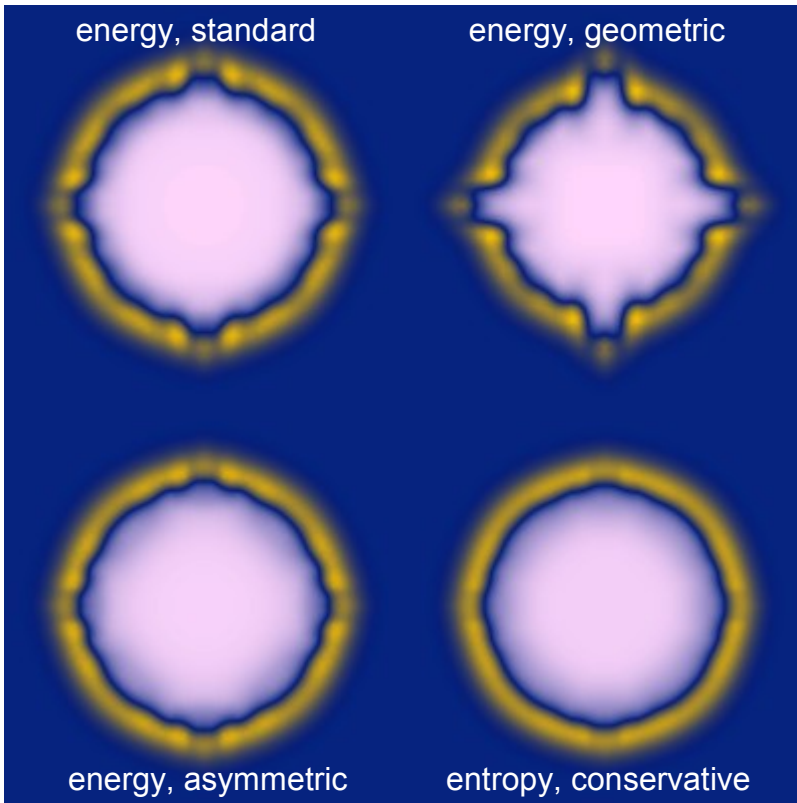
SEDOV-TAYLOR SOLUTIONS FOR **SMOOTHED** EXPLOSION ENERGY

$$R(t) = \beta \left(\frac{Et^2}{\rho} \right)^{1/5}$$



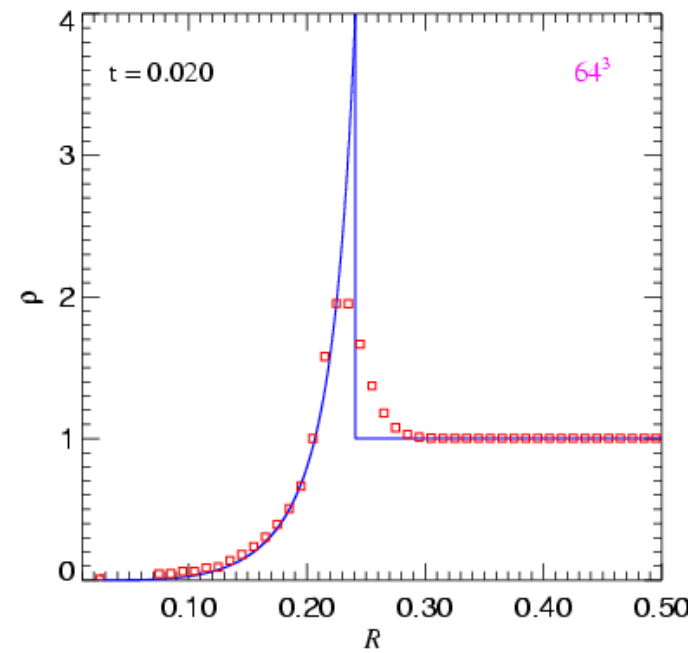
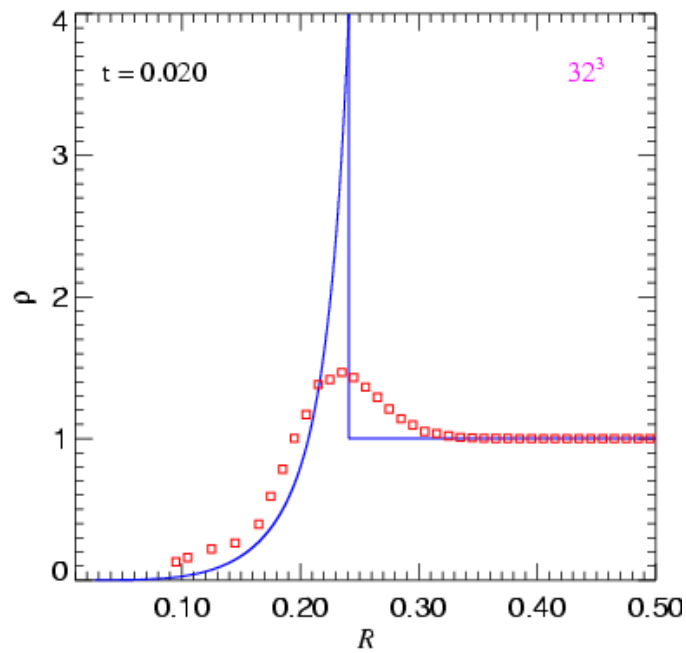
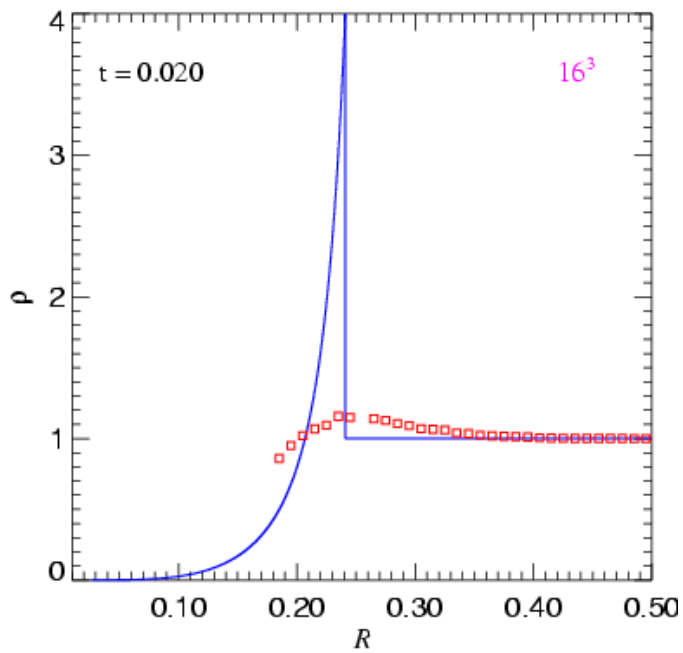
The new conservative formulation gives better results for adiabatic flows

EXPLOSION PROBLEM



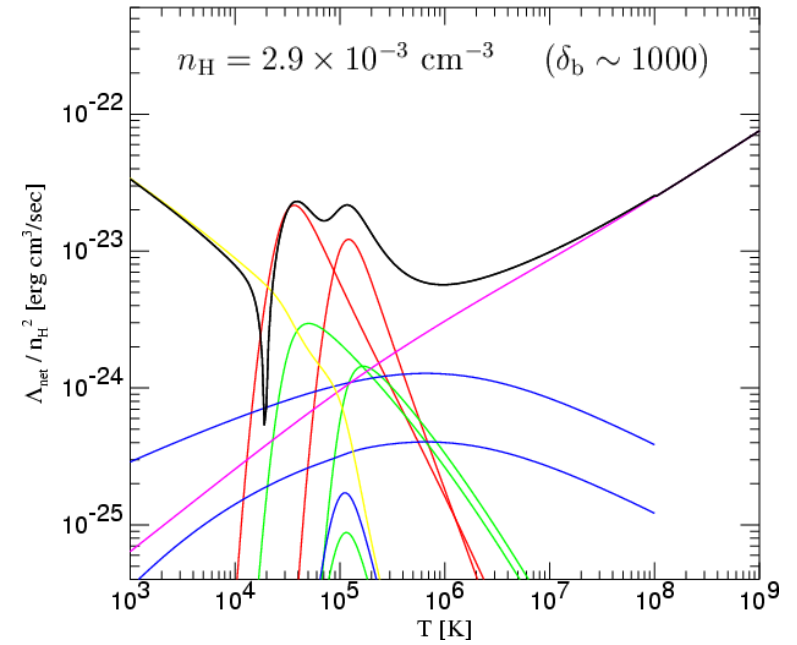
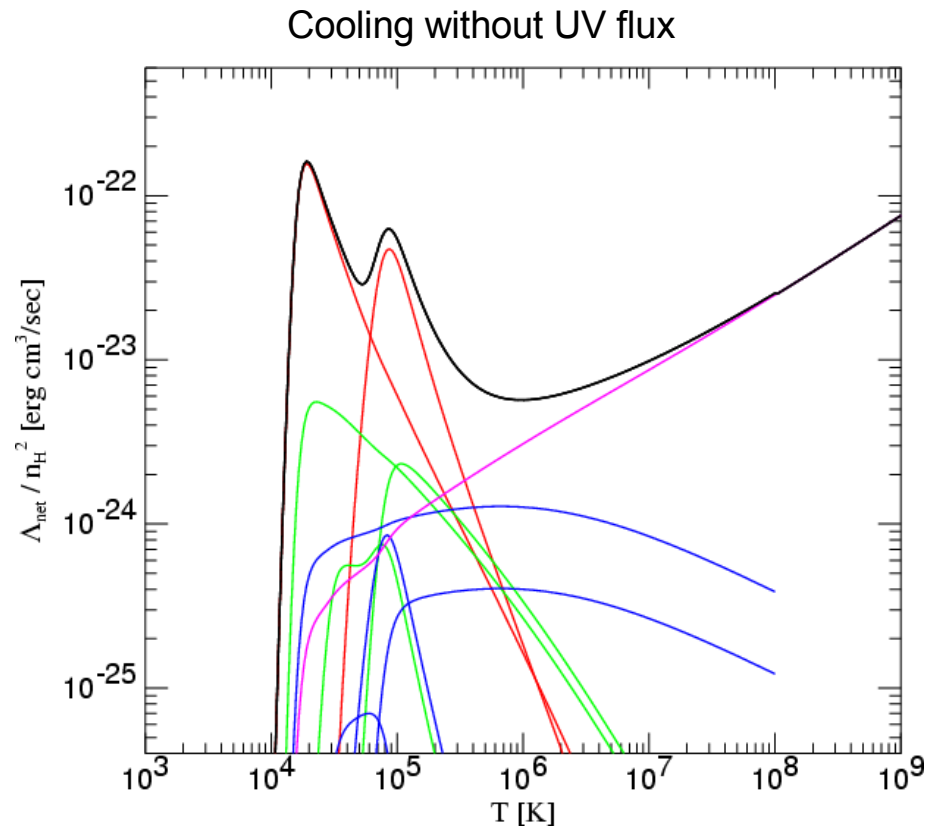
Resolving the narrow blast wave in 3D is numerically challenging

POINT-EXPLOSIONS AT VARYING RESOLUTION

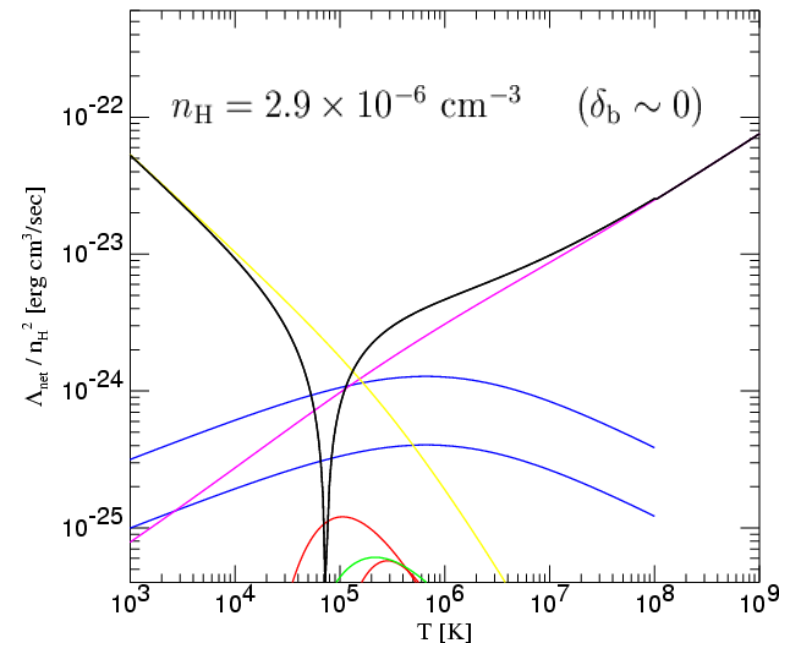


In the presence of an ionizing UV background, the cooling functions depend on density and flux

COOLING FUNCTION



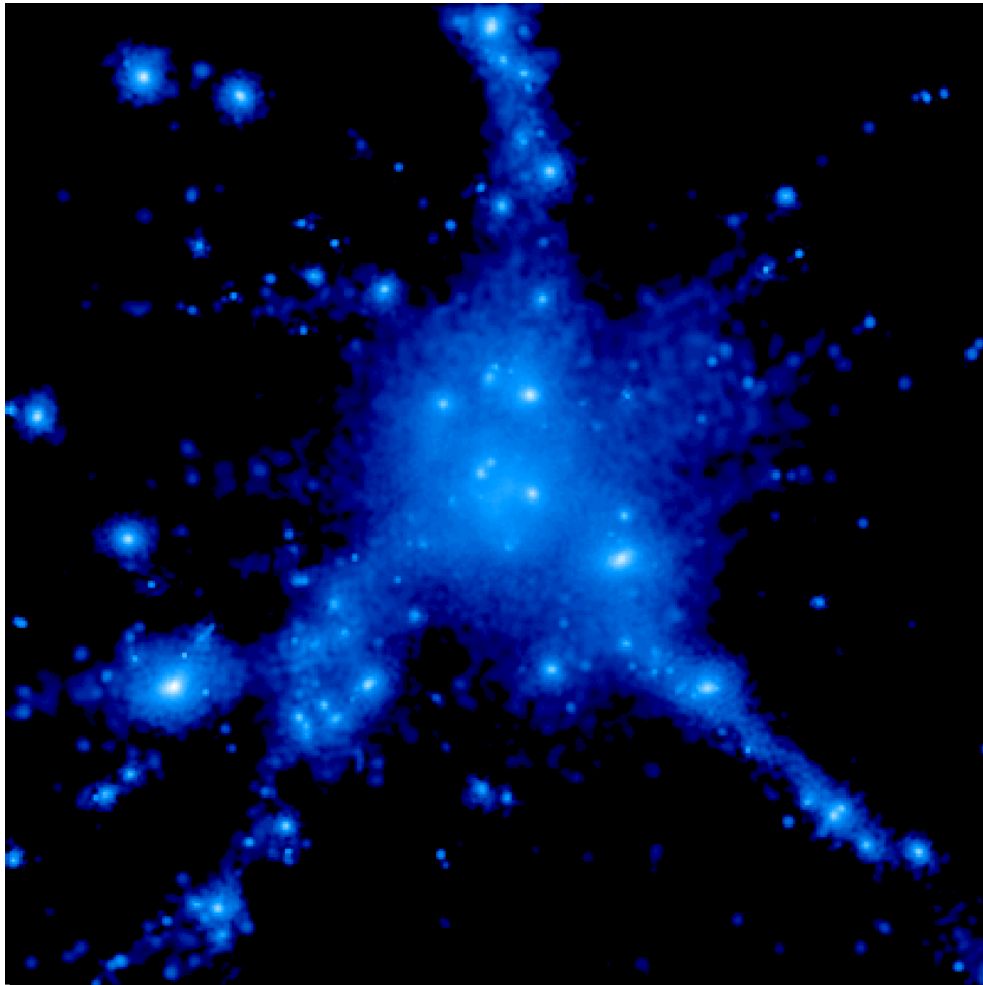
$$J(\nu) = 10^{-22} (\nu_L / \nu) \text{ ergs s}^{-1} \text{ cm}^{-2} \text{ sr}^{-1} \text{ Hz}^{-1} \quad z = 2$$



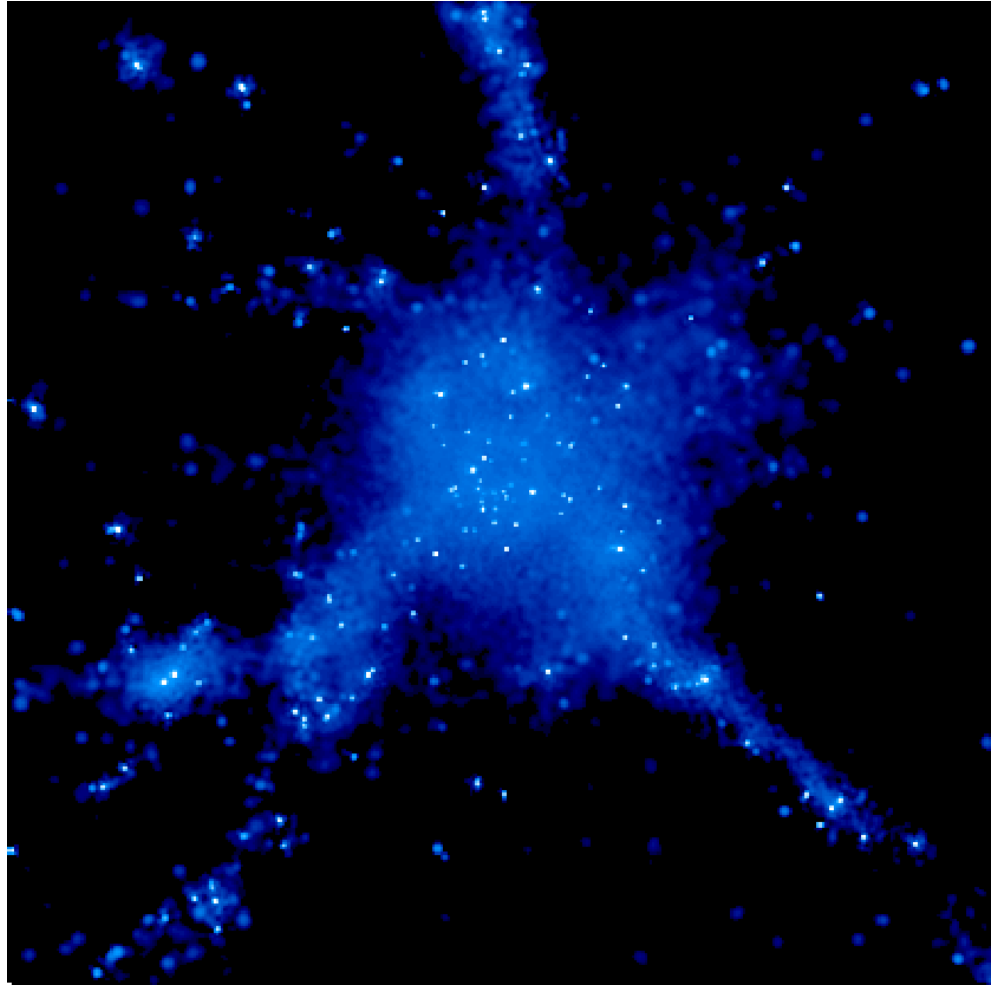
Cooling of gas is extremely efficient in high-resolution simulations of galaxy formation

CLUSTER RUNS WITH AND WITHOUT COOLING

SO_A (adiabatic)



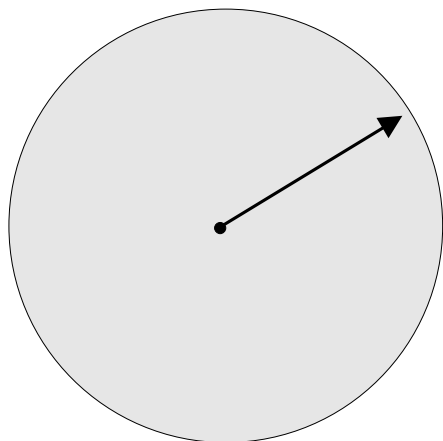
SO_C (cooling only)



A collapsing gas sphere with cooling

MODEL SETUP

Cold gas sphere



$$M = 10^{15} h^{-1} M_{\odot}$$

$$\rho(r) \propto \frac{1}{r}$$

$$R_{\text{init}} = 2 \times R_{\text{vir}}$$

- **collapse under gravity**
- **cooling like a primordial plasma**
- **sink at the center**

Sink

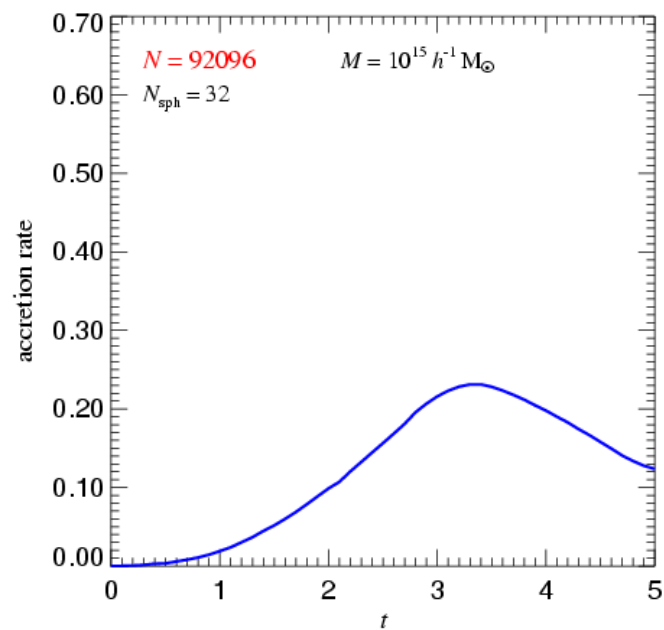
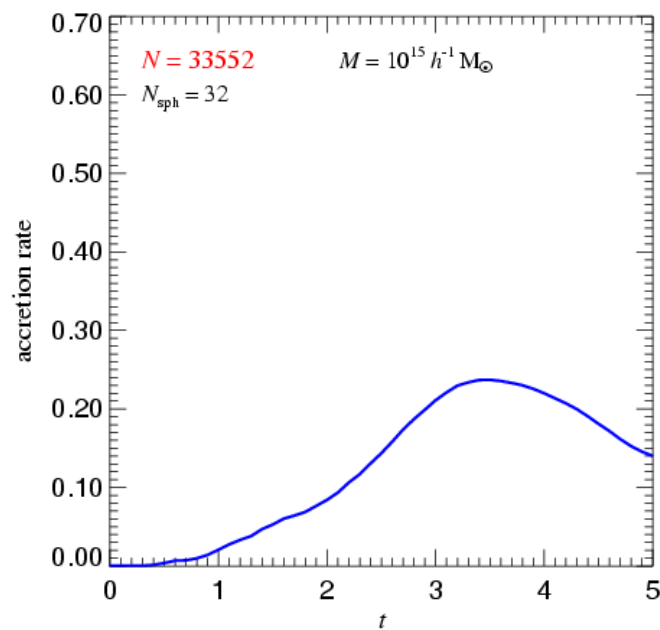
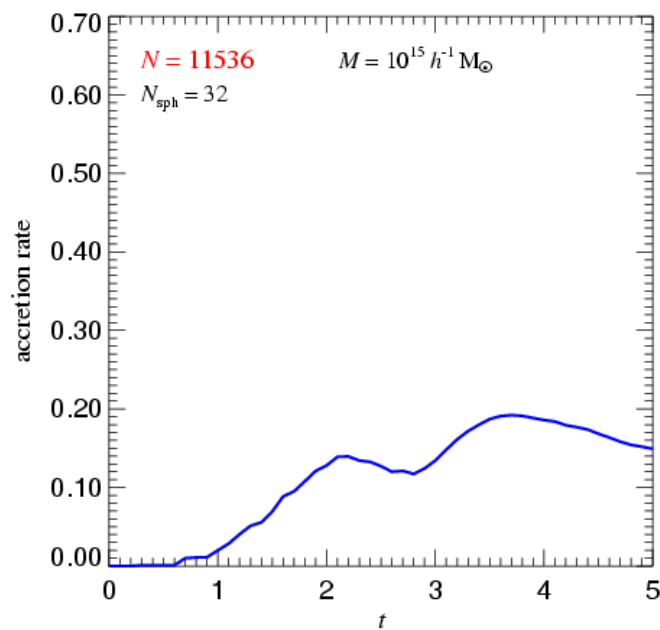
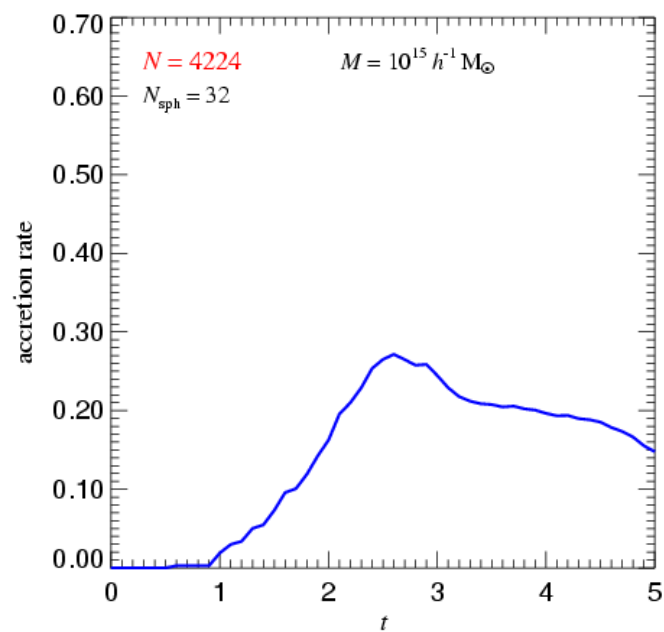
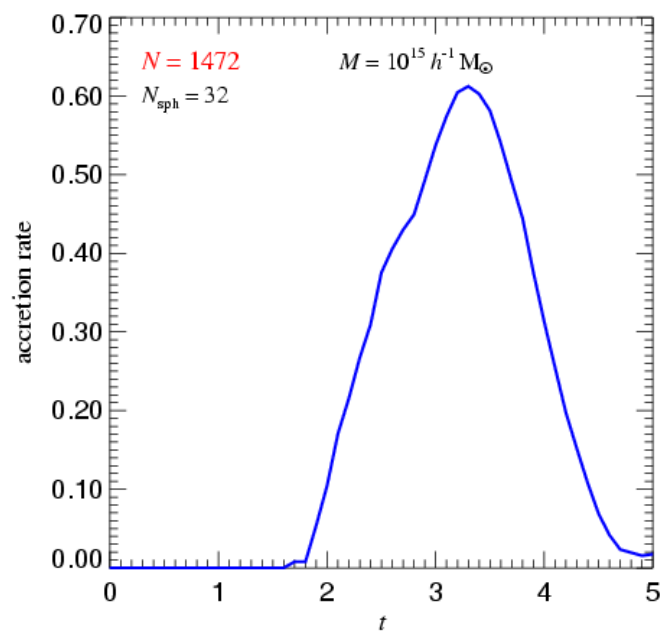
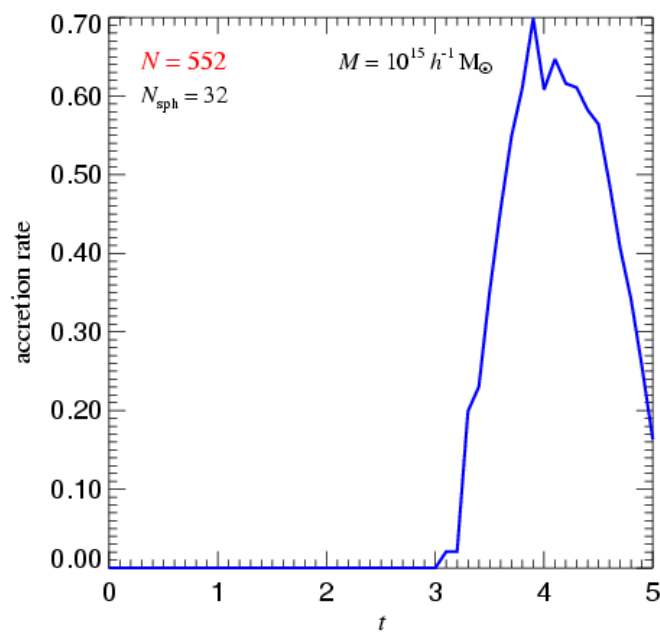
cold gas particles turned into stationary collisionless particles for:

$$\rho > 7.2 \times 10^7 \rho_{\text{crit}}$$

$$r < 0.25 \epsilon$$

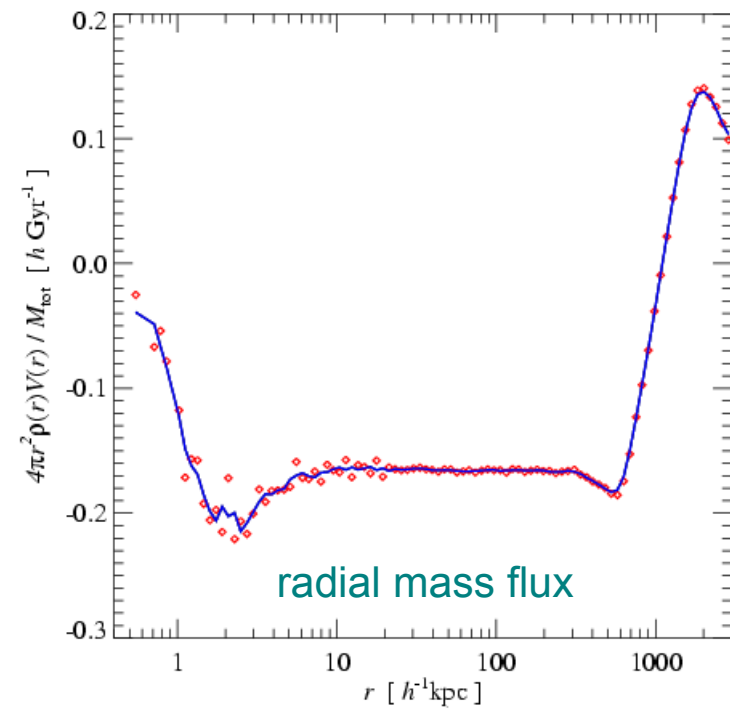
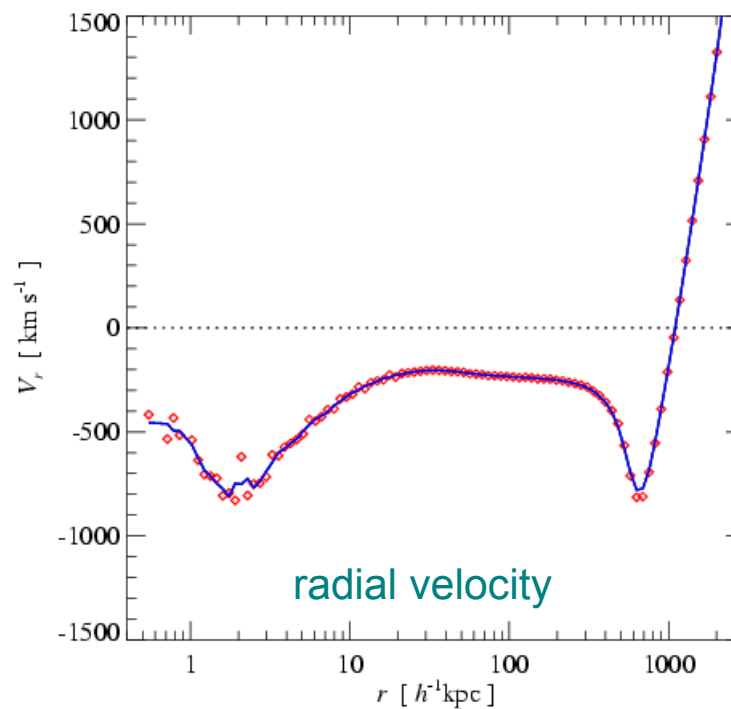
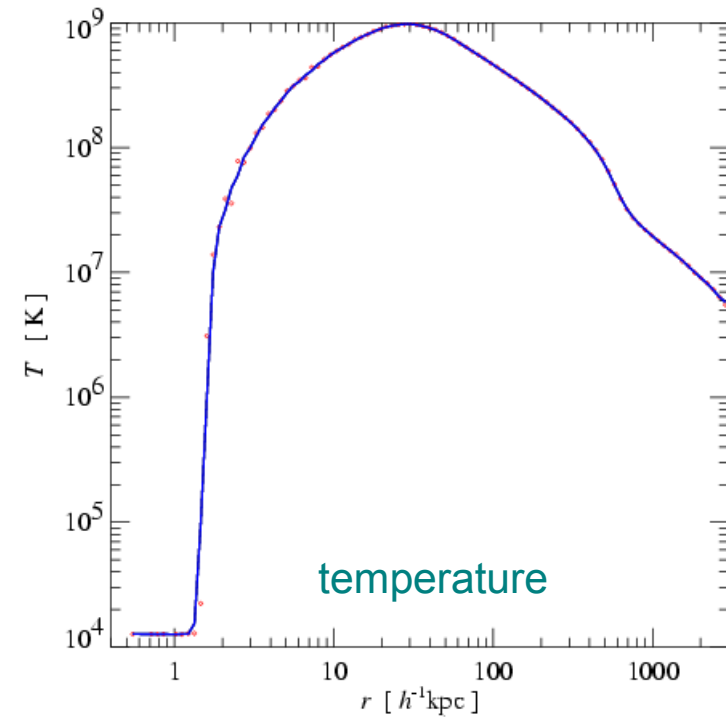
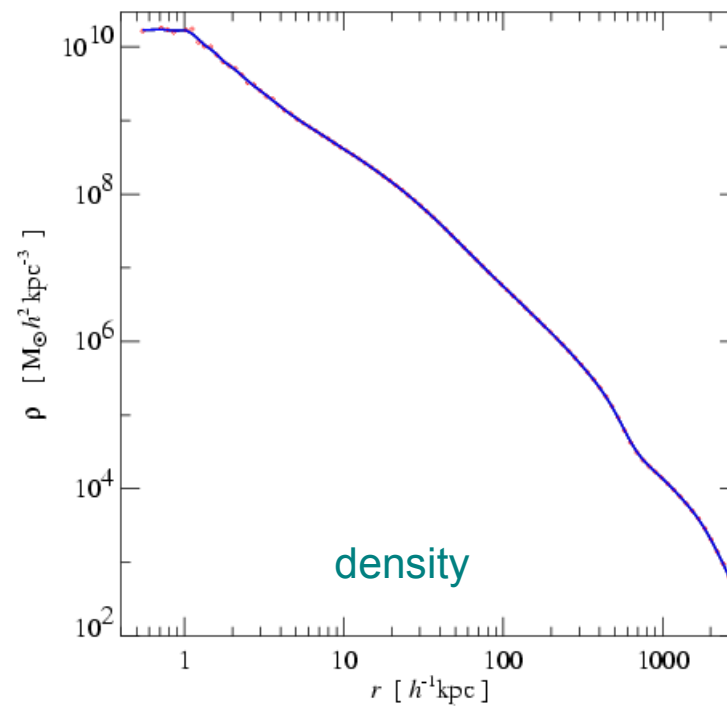
Accretion rate as a function of numerical resolution

GEOMETRIC SYMMETRIZATION METHOD



Before the gas is cooling rapidly close to the center, it is strongly heated by adiabatic compression

NEARLY
STATIONARY
COOLING FLOW

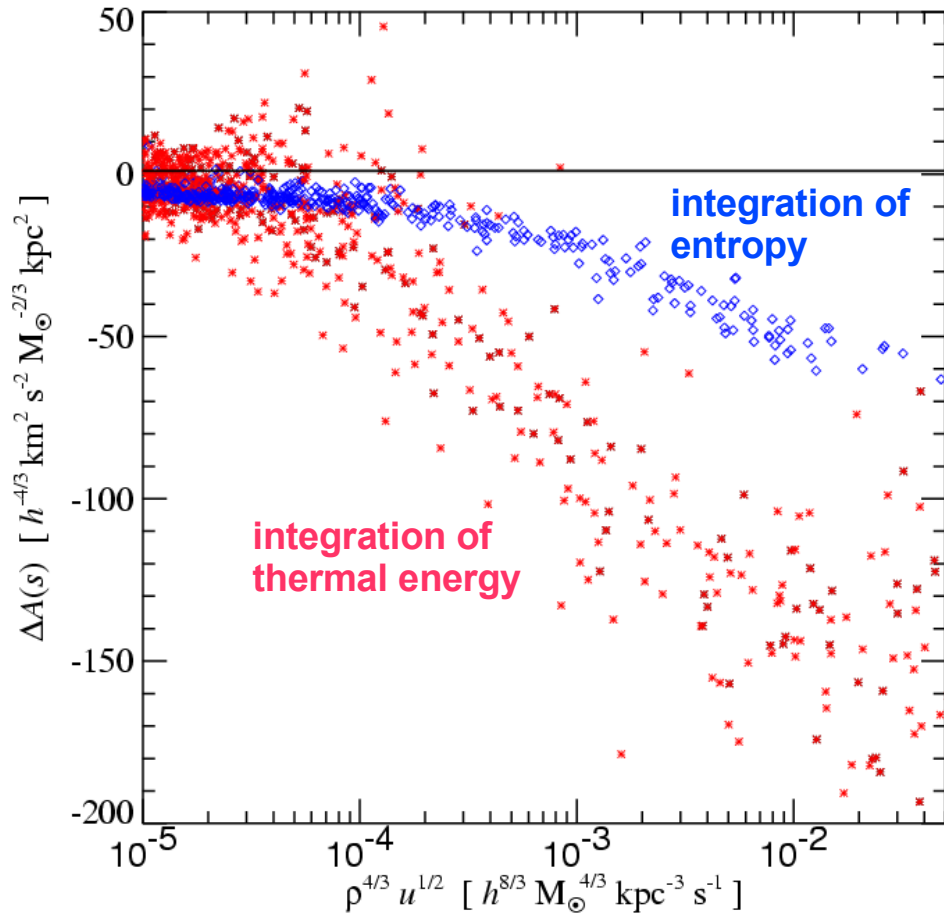


$t = 4.0$

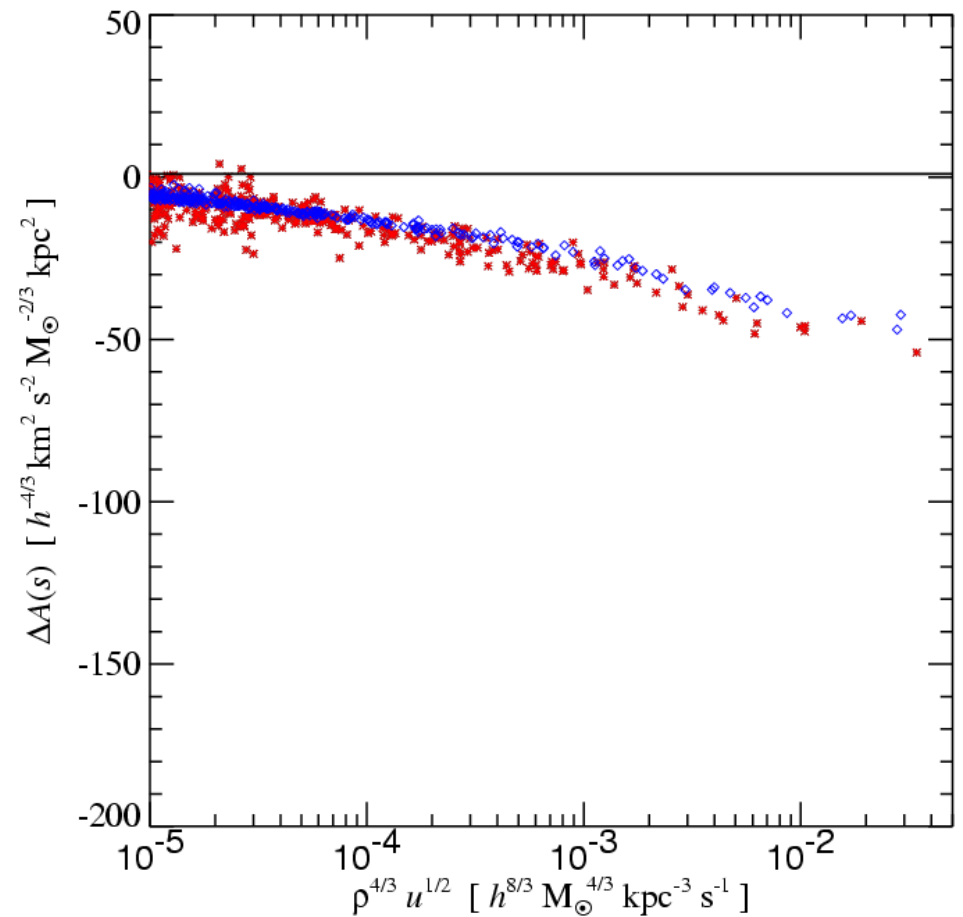
Fluid elements should lose entropy *only* by radiative cooling

DECLINE OF ENTROPY IN COOLING FLOW REGION

low resolution

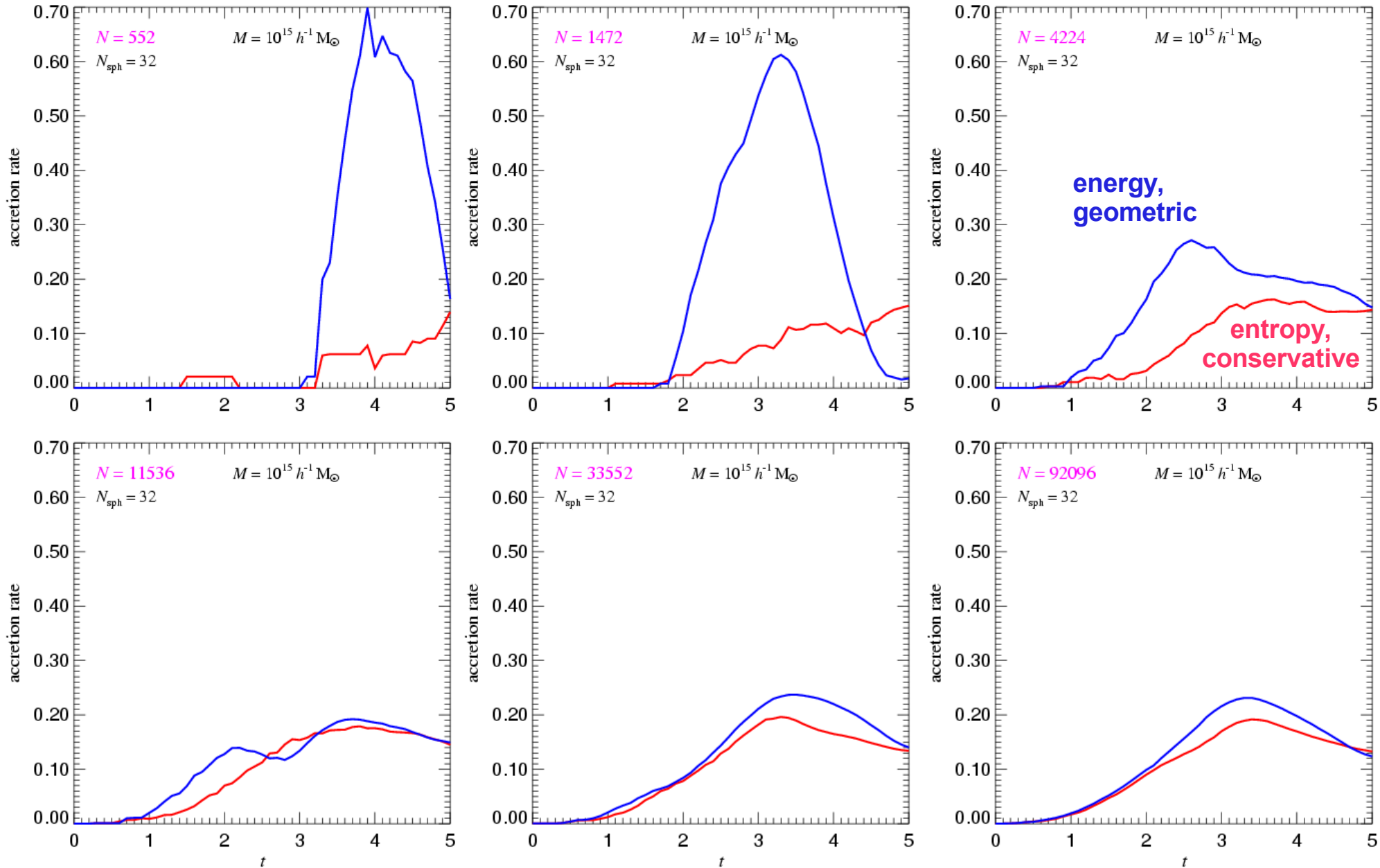


high resolution



The new conservative formulation of SPH is biasing cooling rates slightly low for poor resolution

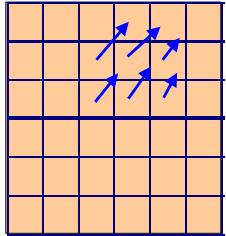
ACCRETION RATES FOR COOLING GAS SPHERES



Differences between SPH and Eulerian hydrodynamics

There are principal differences between SPH and Eulerian schemes

FUNDAMENTAL DIFFERENCE BETWEEN SPH AND MESH-HYDRODYNAMICS



Eulerian

not Galilean invariant

sharp shocks and contact discontinuities
(best schemes resolve fluid discontinuities in one cell)

mixing happens implicitly at the cell level
(can provide closure for turbulence, but will also be a source of spurious mixing entropy from advection errors)

self-gravity of the gas needs to be done on a mesh
(but dark matter must still be represented by particles)

low numerical viscosity

Lagrangian

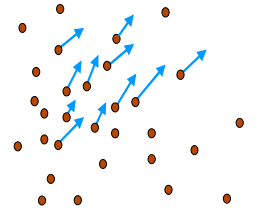
Galilean invariant

shocks broadened over roughly 2-3 smoothing lengths
(post-shock properties are correct though)

mixing entirely suppressed at the particle-level
(no spurious entropy production, but fluid instabilities may be suppressed)

self-gravity of the gas naturally treated with the same accuracy as the dark matter

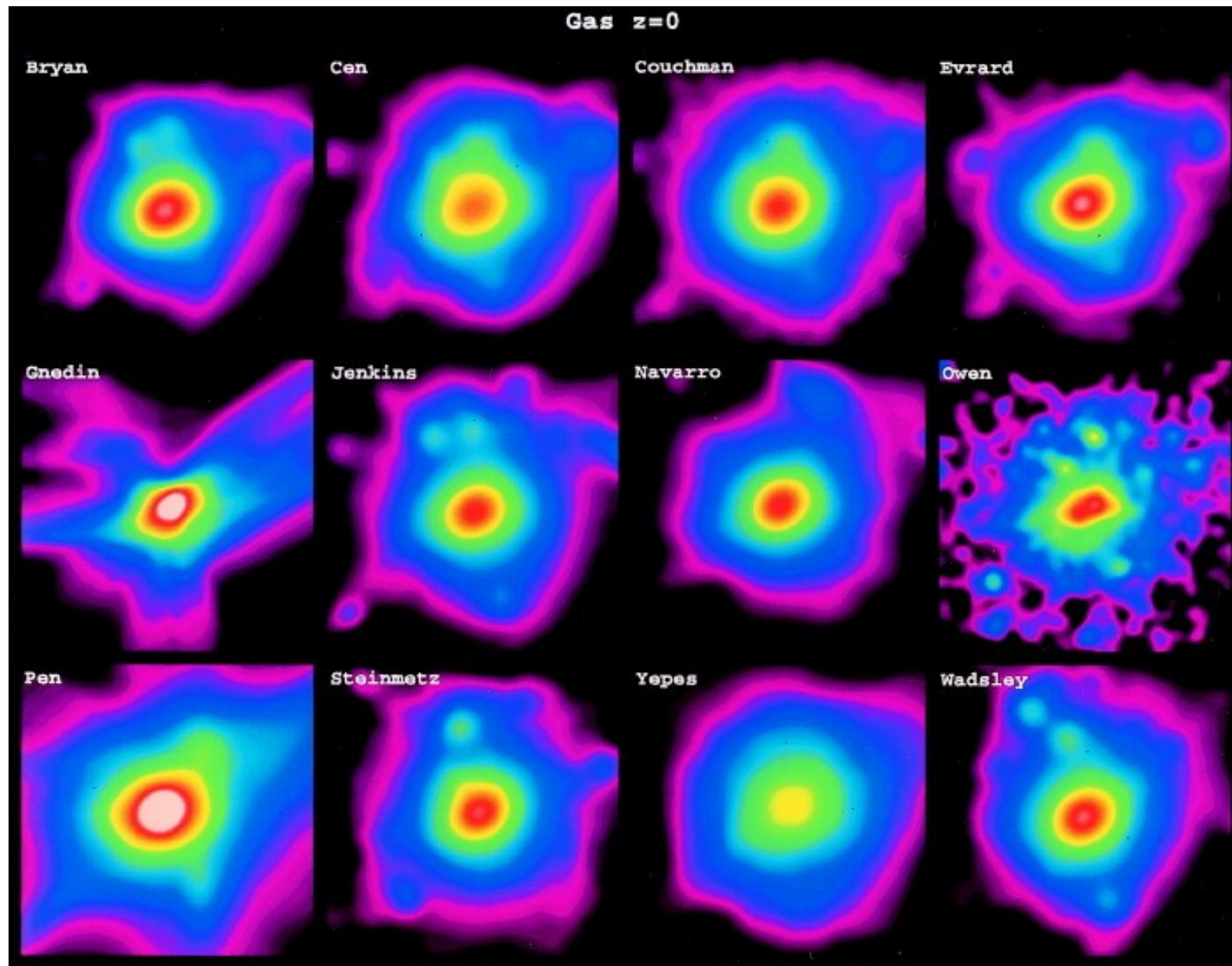
requires artificial viscosity
(lowers Reynolds numbers heavily)



Different hydrodynamical simulation codes are broadly in agreement, albeit with substantial scatter and differences in detail

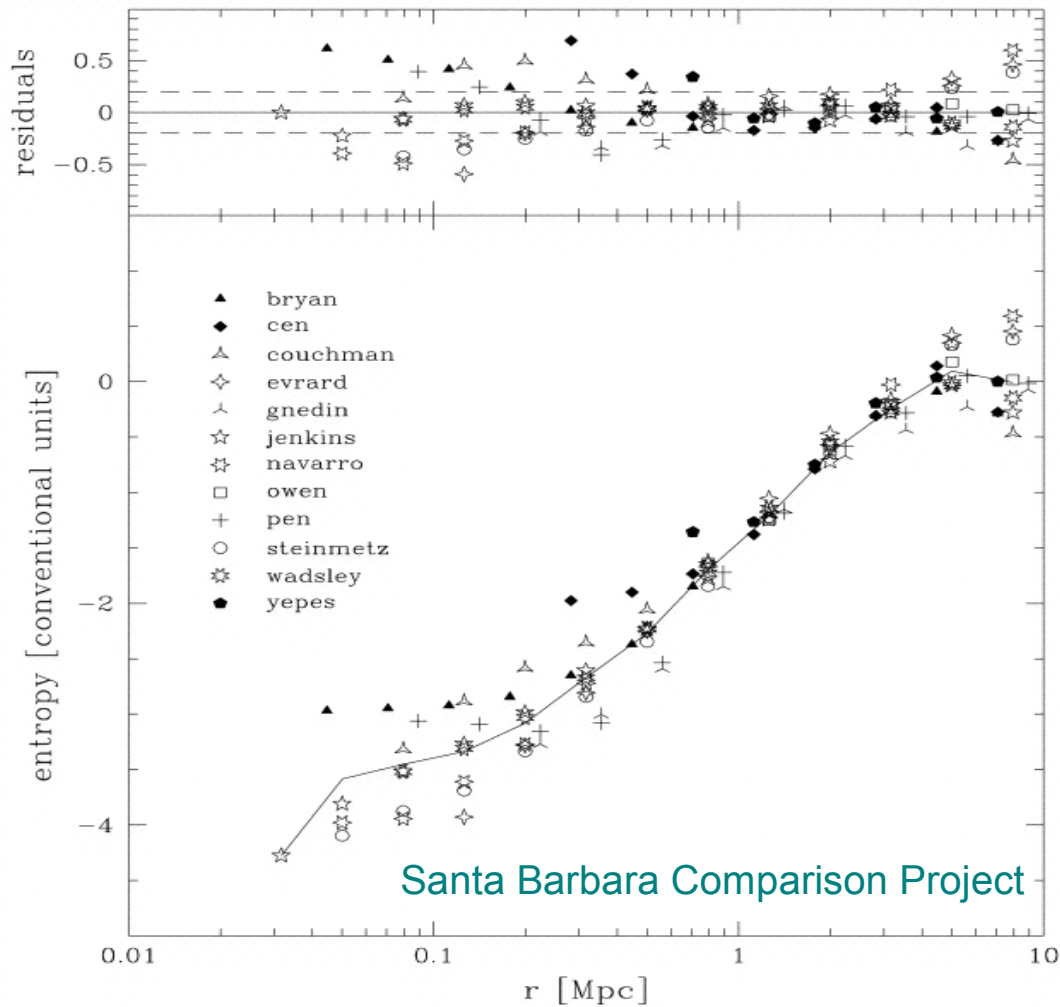
THE SANTA BARBARA CLUSTER COMPARISON PROJECT

Frenk, White & 23 co-authors (1999)



Mesh codes appear to produce higher entropy in the cores of clusters

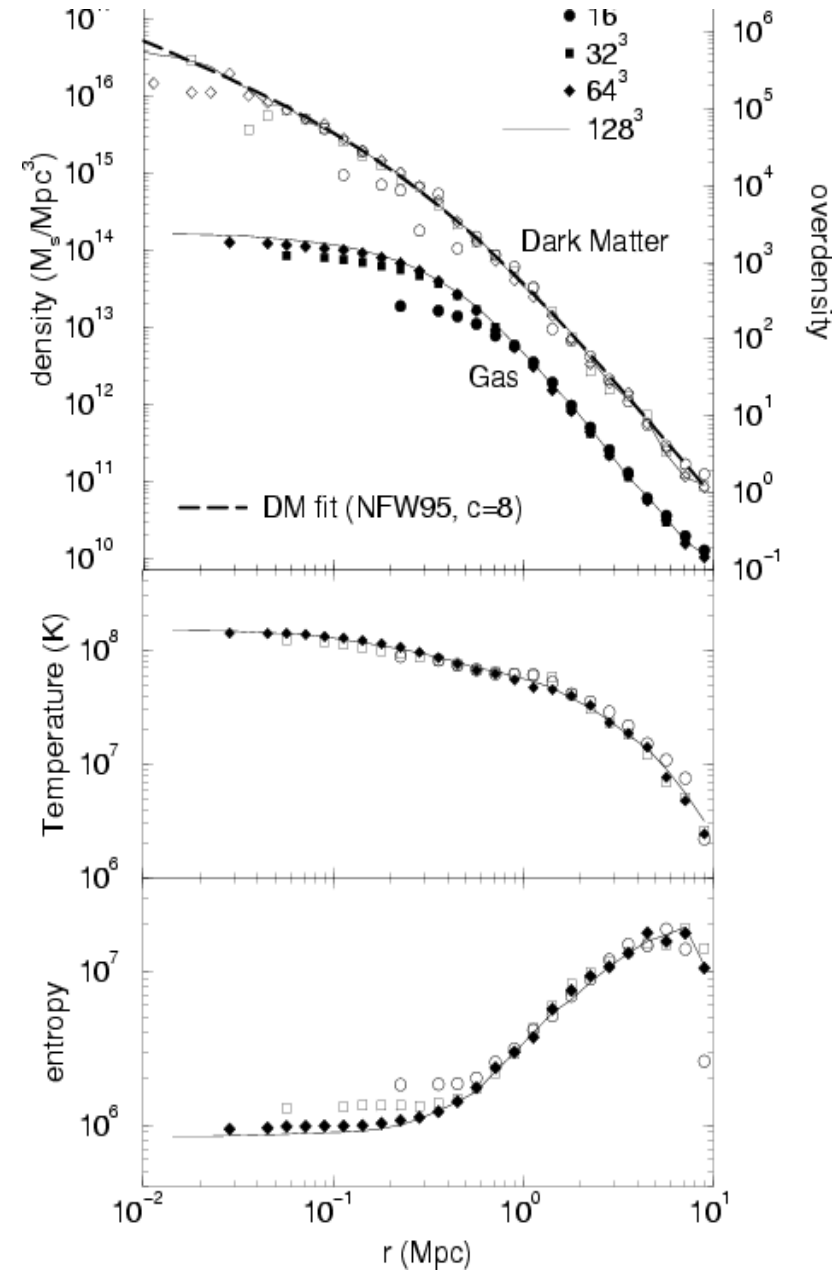
RADIAL ENTROPY PROFILE



Santa Barbara Comparison Project

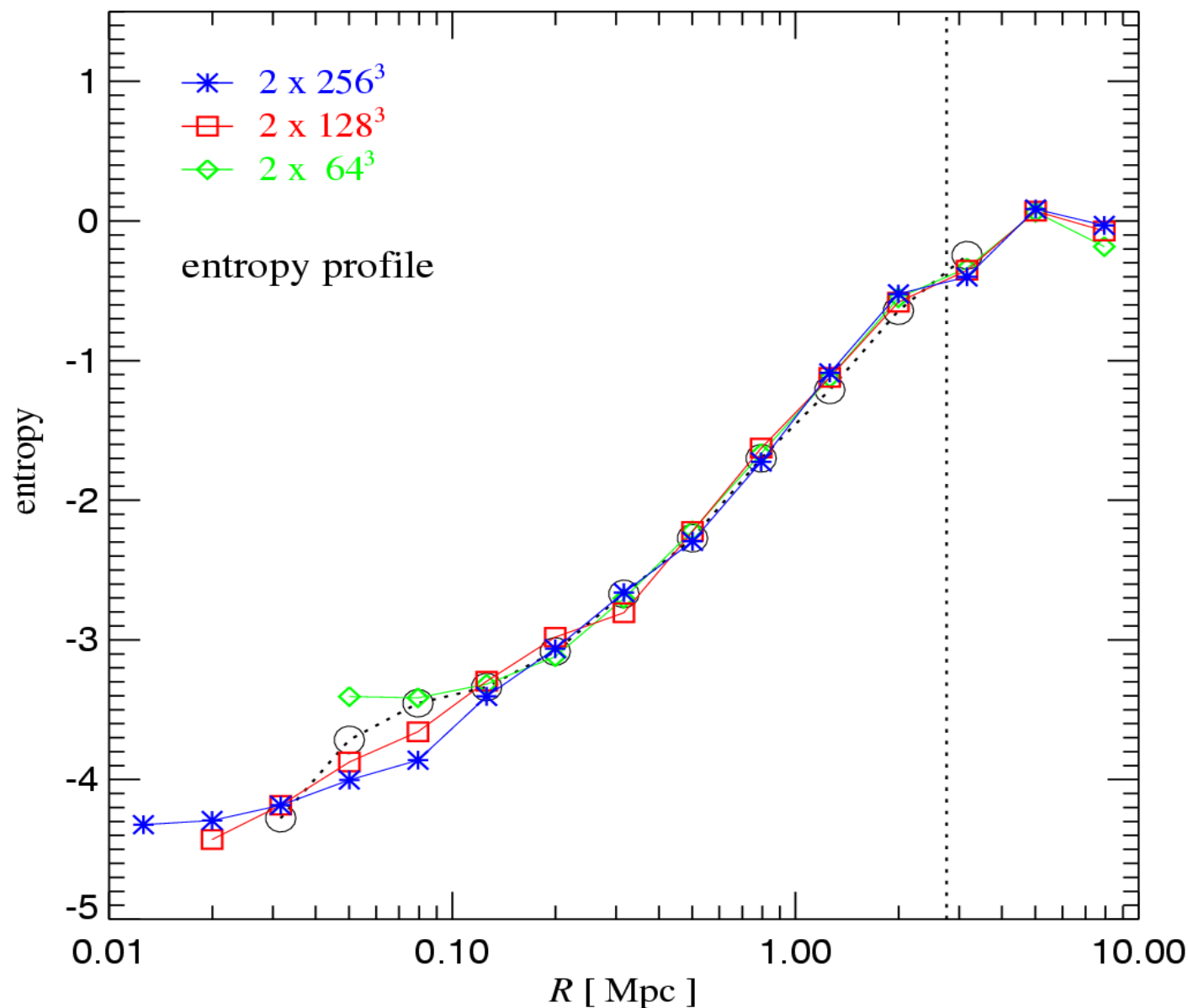
Ascasibar, Yepes, Müller & Gottlöber (2003):
More accurate SPH simulations also seem to develop an entropy core

Bryan & Norman 1997



The entropy profile of the Santa Barbara cluster appears to converge well with SPH, at a lower level than found with mesh codes

ENTROPY PROFILES OBTAINED WITH GADGET2 AT DIFFERENT RESOLUTION



Non-standard physics with SPH: Thermal Conduction

Thermal conduction may partially offset radiative cooling in central cluster regions

THE CONDUCTION IDEA

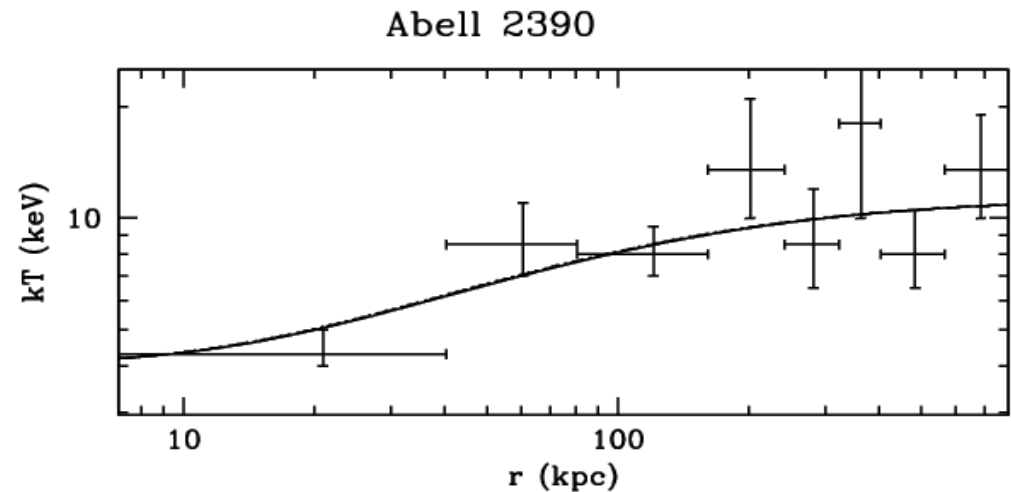
Inner region of clusters (~ 10 -50 kpc) is cooler than the rest of the cluster



Is thermal conduction from the outer hot regions of the cluster the heat source?

Zakamska & Narayan (2003)

- Assume hydrostatic equilibrium with a balance between cooling and conductive heating
- Temperature profiles of five clusters can be well fit, requiring conductivities of the order 30% Spitzer-value



BUT: Magnetic fields are the natural enemy of conduction....

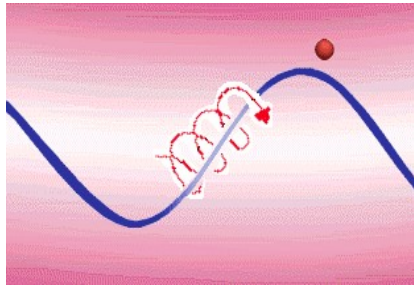
Magnetic fields are the natural enemy of thermal conduction

THE QUEST TO UNDERSTAND THE EFFECTIVE CONDUCTIVITY

Spitzer (1962) Conductivity of unmagnetized plasma:

$$\kappa_{\text{sp}} = 1.31 n_e \lambda_e k \left(\frac{kT_e}{m_e} \right)^{1/2} \quad \lambda_e n_e = \frac{3^{3/2} (kT_e)^2}{4\sqrt{\pi} e^4 \ln \Lambda}$$

→ $\kappa_{\text{sp}} \propto T_e^{5/2}$



If we have an ordered magnetic field:

$$\begin{aligned} \kappa_{\parallel} &\sim \kappa_{\text{sp}}/3 \\ \kappa_{\perp} &\sim (r_L/\lambda)^2 \kappa_{\text{sp}} \end{aligned}$$

In clusters:

$$\begin{aligned} B &\sim 10^{-6} \text{ G} \\ r_L &\sim 10^{-12} \lambda \end{aligned}$$

Rechester & Rosenbluth (1978)
Chandran & Cowley (1998)
Malyskin & Kulsrud (2001)

If the field is **tangled**, the effective conductivity can be heavily suppressed:

$$\kappa_{\text{eff}} \sim \kappa_{\text{sp}}/100$$

Narayan & Medvedev (2001):

If the field is **chaotic on a range of turbulent scales**, conduction may almost reach the Spitzer value:

$$\kappa_{\text{turb}} \sim \kappa_{\text{sp}}/3$$

We have derived a robust and accurate implementation of thermal conduction in SPH

SPH DISCRETIZATION OF CONDUCTION

Conduction equation:

$$\frac{du}{dt} = \frac{1}{\rho} \nabla(\kappa \nabla T) \quad \mathbf{j} = -\kappa \nabla T$$
$$\rho \frac{du}{dt} = -\nabla \mathbf{j}$$

Second-order derivative tends to be noisy...

SPH discretization:

$$\frac{du_i}{dt} = \sum_j \frac{m_j}{\rho_i \rho_j} \frac{(\kappa_j + \kappa_i) (T_j - T_i)}{|\mathbf{x}_{ij}|^2} \mathbf{x}_{ij} \nabla_i W_{ij}$$

Brookshaw (1985)

Problems encountered in practice:

- Explicit time integration can easily lead to instabilities
- Individual timestepping may easily lead to errors in energy conservation (conductivity depends strongly on temperature)

—————▶ After some painful experiences, we have arrived at a manifestly conservative, accurate and robust solution

In our SPH code, we use an explicitly conservative scheme for conduction when adaptive timesteps are used

SPH DISCRETIZATION OF CONDUCTION

$$A = (\gamma - 1) \frac{u}{\rho^{\gamma-1}}$$

Pairwise rate of energy exchange

$$E_{ij} \equiv \frac{2\mu}{k_B} \frac{m_i m_j \kappa_{ij}}{\rho_i \rho_j} \left(\frac{A_j}{\rho_j^{\gamma-1}} - \frac{A_i}{\rho_i^{\gamma-1}} \right) \frac{\mathbf{x}_{ij} \cdot \nabla_i W_{ij}}{|\mathbf{x}_{ij}|^2}$$

Entropy change due to conduction in one system step

$$A'_i = A_i + \frac{(\gamma - 1)}{2m_i \rho_i^{\gamma-1}} \sum_{jk} \Delta t_j (\delta_{ij} - \delta_{ik}) E_{jk}$$

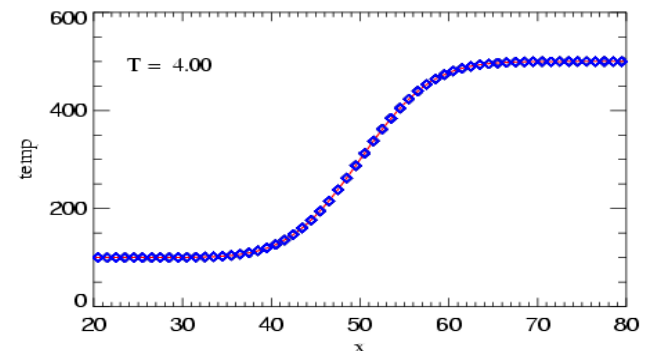
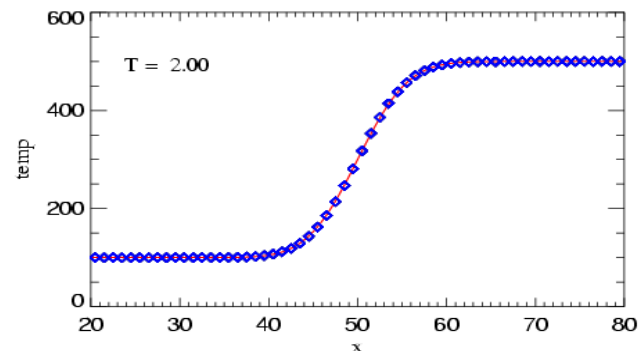
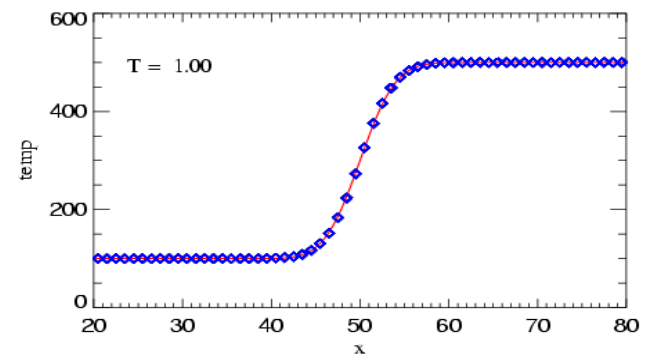
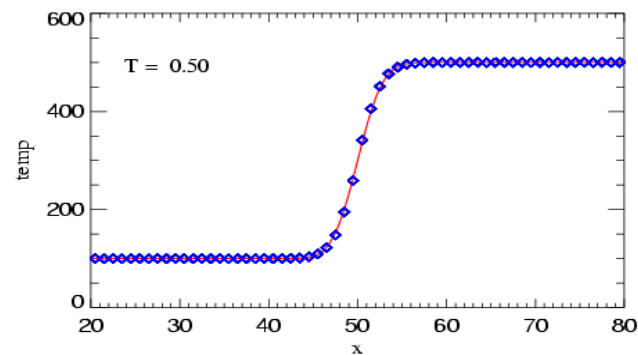
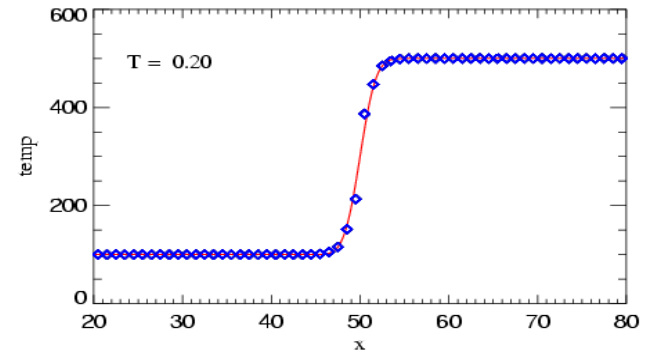
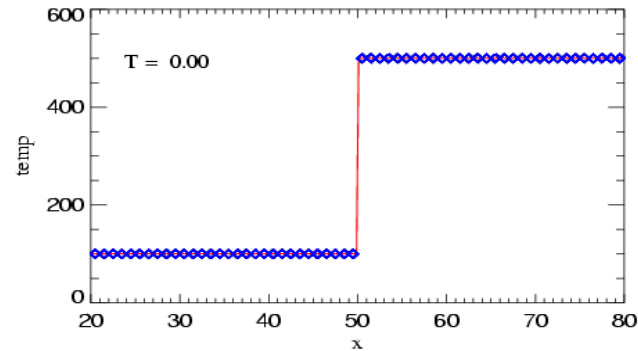
Symmetrization of conductivities

$$\kappa_{ij} = \frac{\kappa_i \kappa_j}{\kappa_i + \kappa_j}$$

Simple conduction problems are reproduced accurately by the 3D code

THERMAL CONDUCTION IN A SLAB

A simple test problem of conduction across a temperature jump



Jubelgas, Springel,
Dolag & White (2003)

The SPH-discretization of
conduction is:

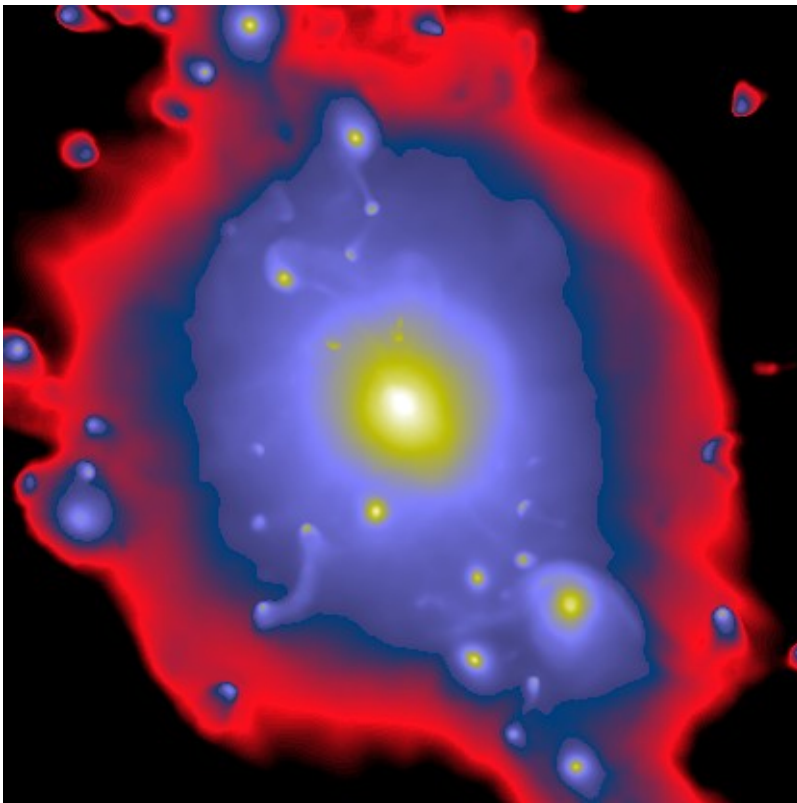
- manifestly conservative
- accurate
- robust against particle noise

Self-consistent cosmological simulations of cluster formation are used to study the impact of conduction on the ICM

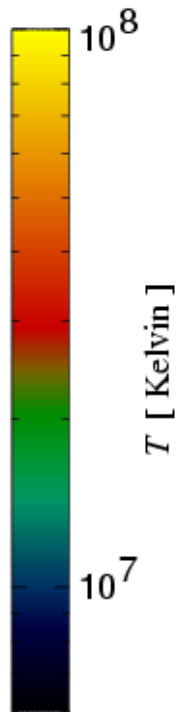
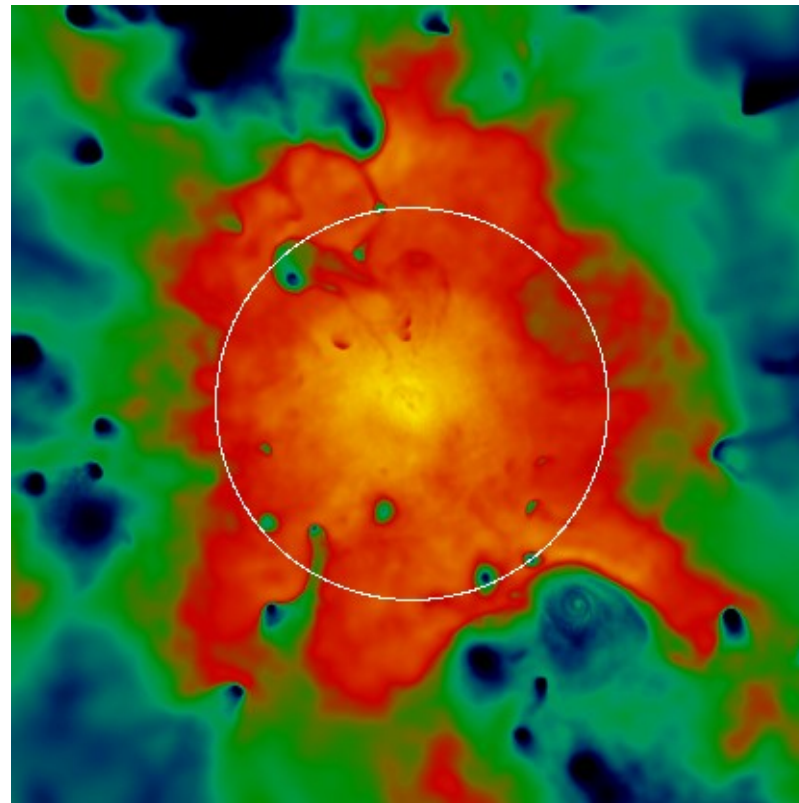
X-RAY AND TEMPERATURE MAPS

Coma-sized cluster, $M_{\text{vir}} \sim 10^{15} M_{\odot}$, adiabatic hydrodynamics

Gas density (X-rays)



Mass-weighted temperature

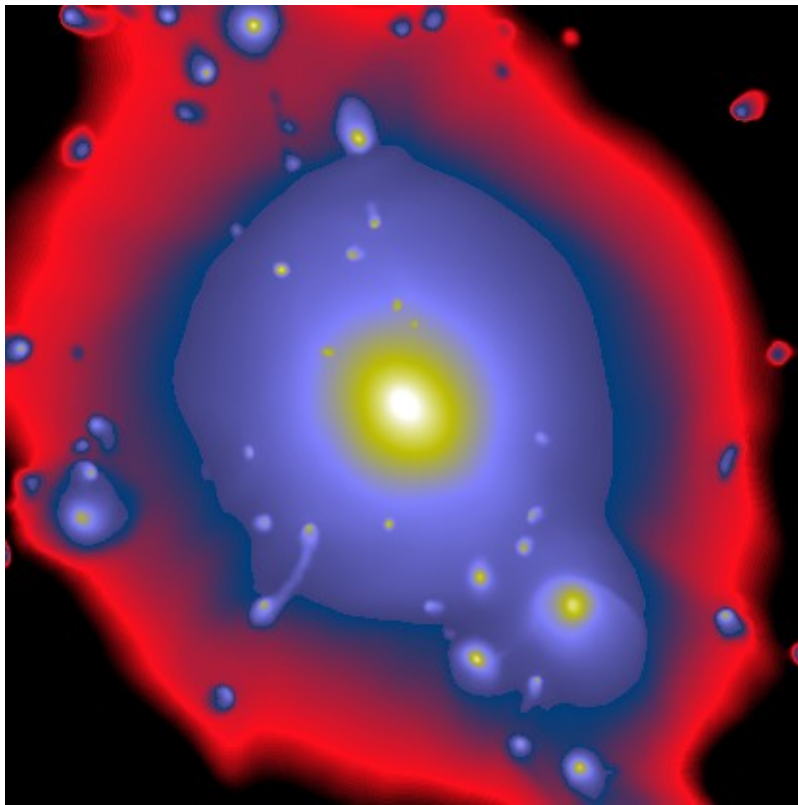


Thermal conduction near the Spitzer value strongly affects rich clusters of galaxies

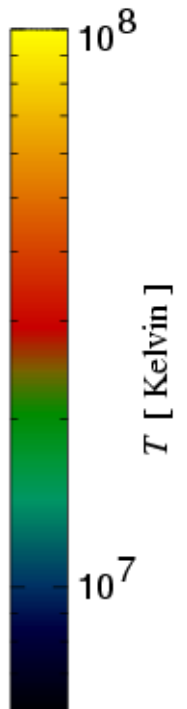
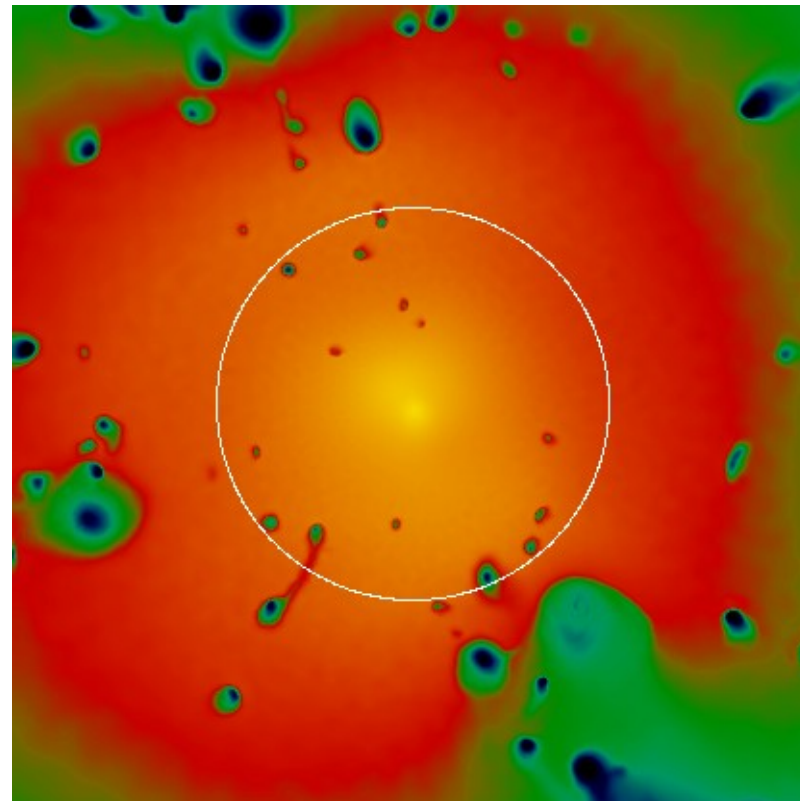
X-RAY AND TEMPERATURE MAPS

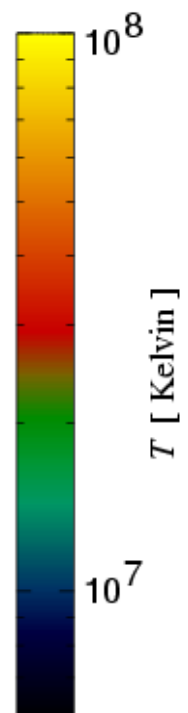
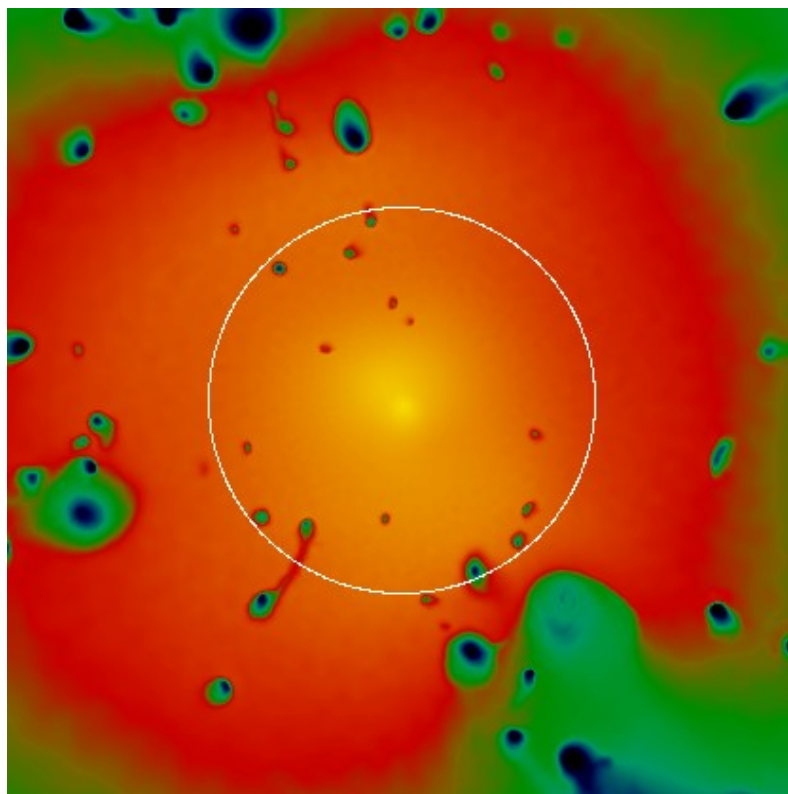
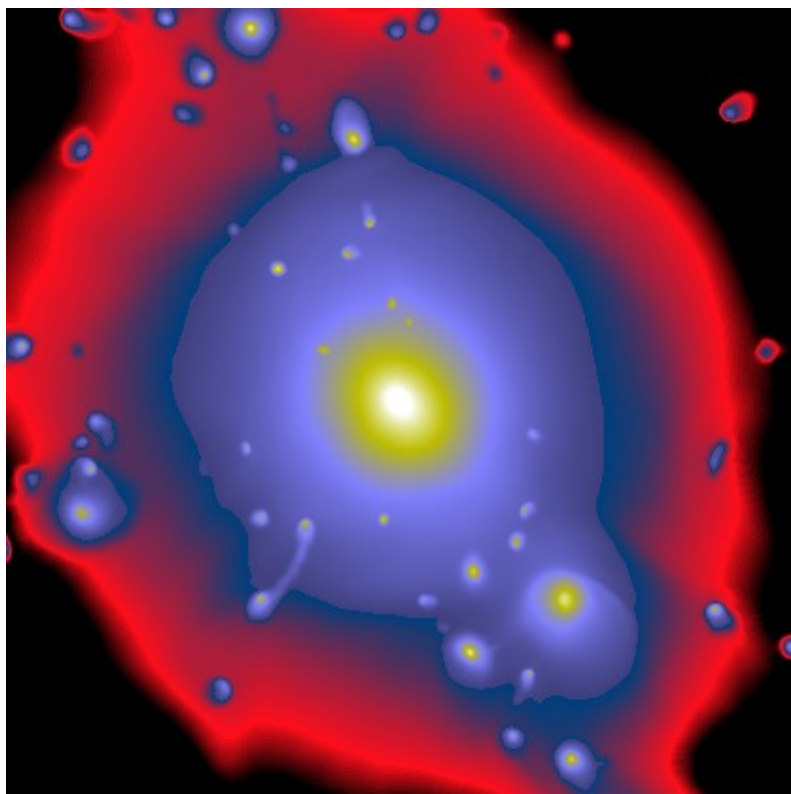
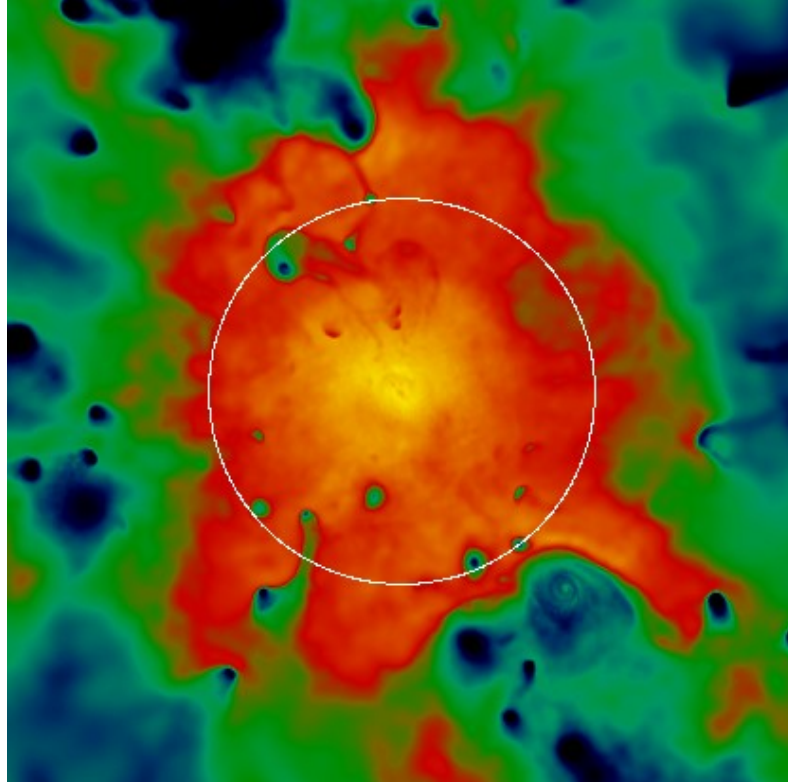
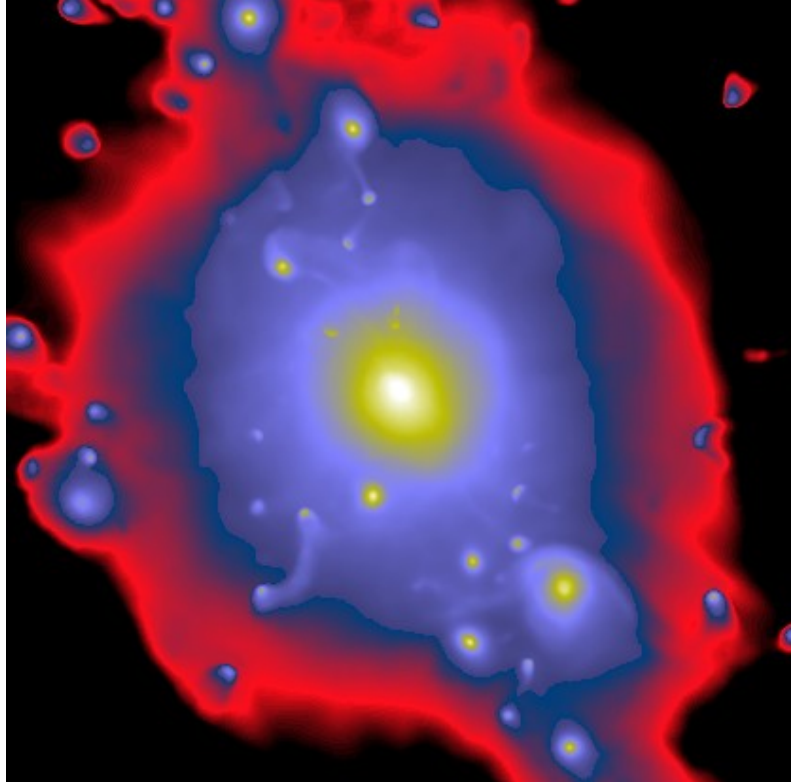
Coma-sized cluster, $M_{\text{vir}} \sim 10^{15} M_{\odot}$,
adiabatic hydrodynamics, **thermal conduction with $\kappa = \kappa_{\text{sp}}$**

Gas density (X-rays)



Mass-weighted temperature



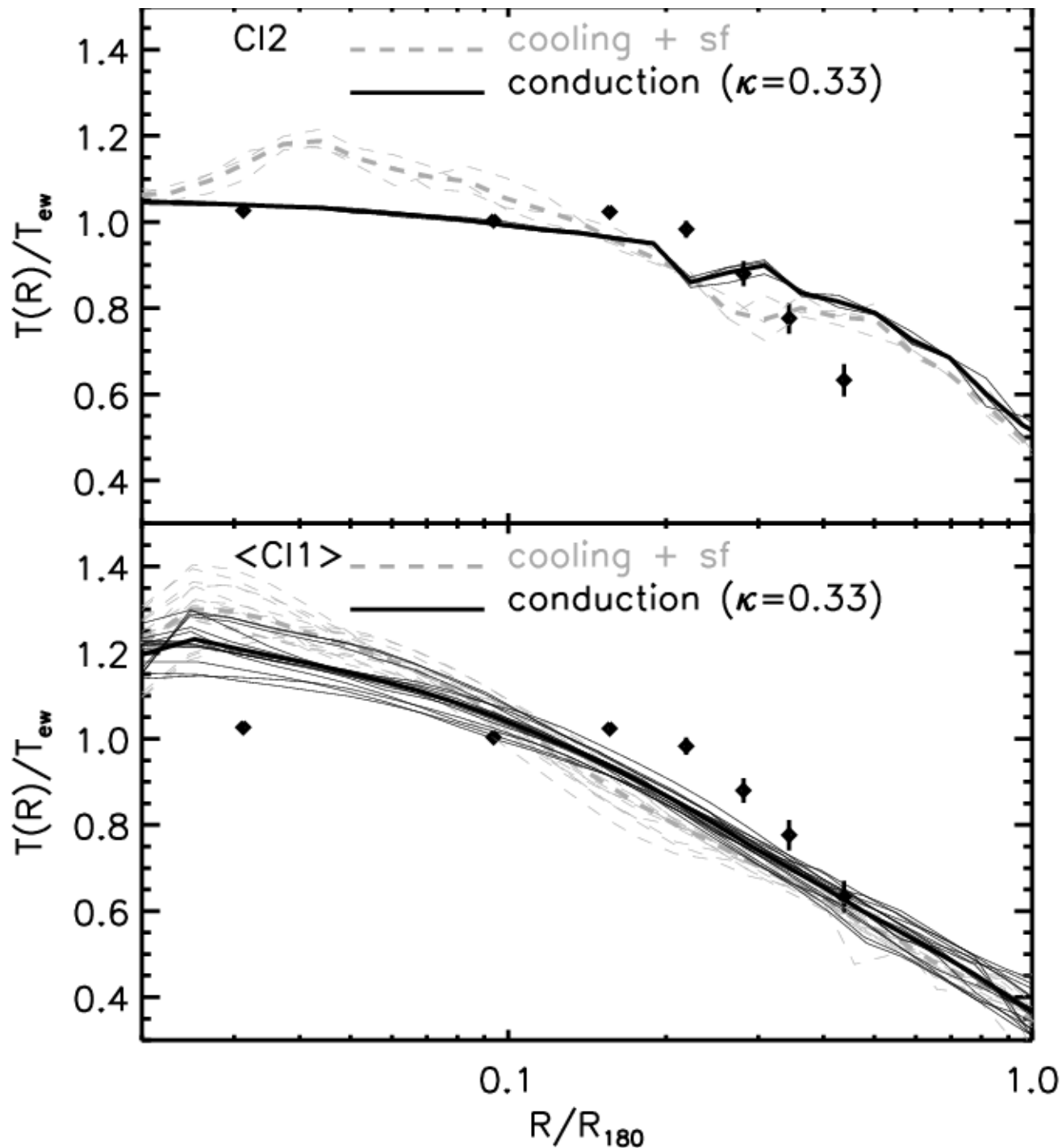


Due to its sensitive temperature dependence, conduction changes the radial temperature profile of hot systems strongly, but leaves poor systems unaffected

RADIAL TEMPERATURE PROFILES

$$\kappa \propto T^{5/2}$$

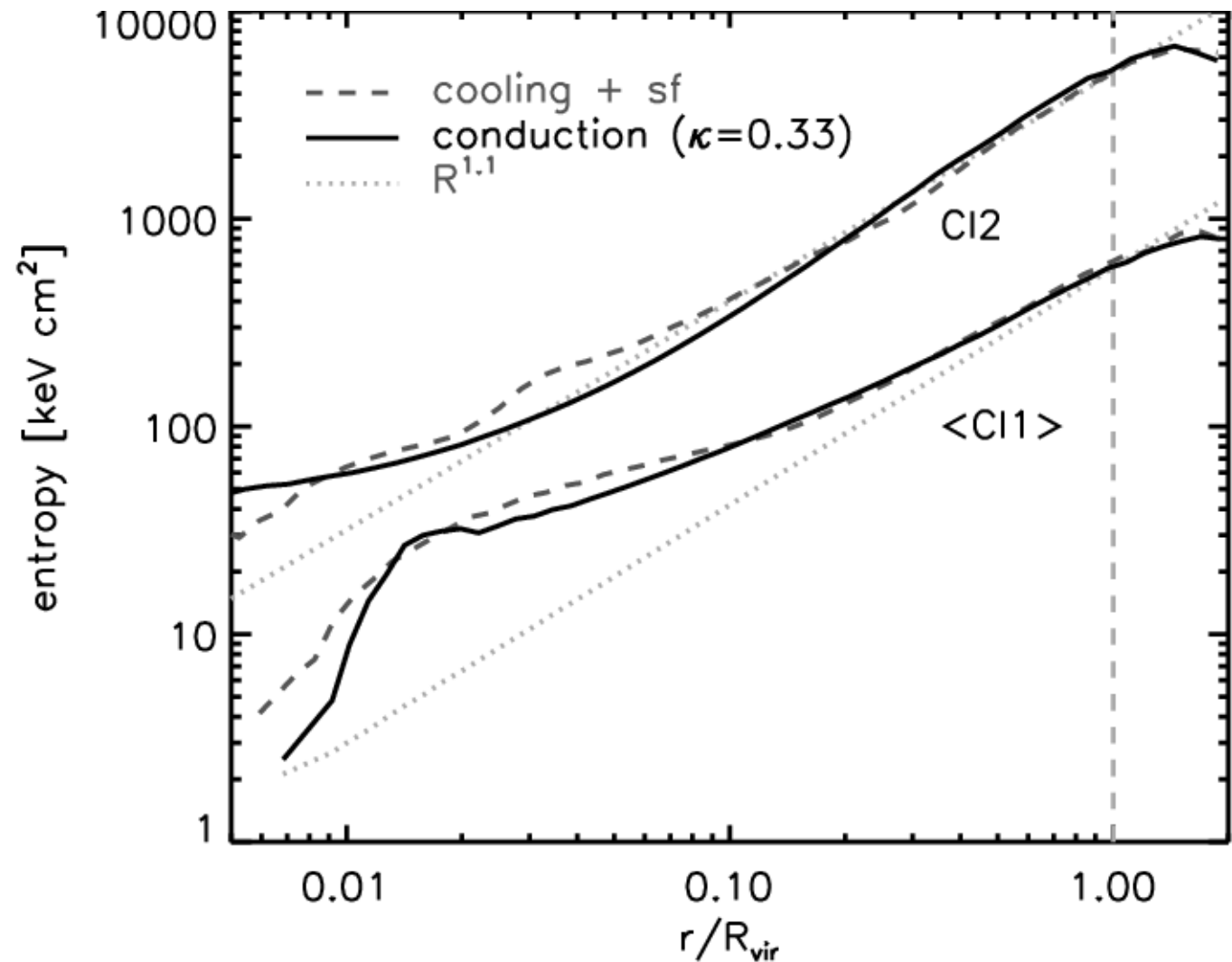
The clusters with conduction still cool out large amounts of gas!



The entropy profiles are only mildly affected by conduction, even for massive systems

RADIAL ENTROPY PROFILES

Dolag et al. (2003)

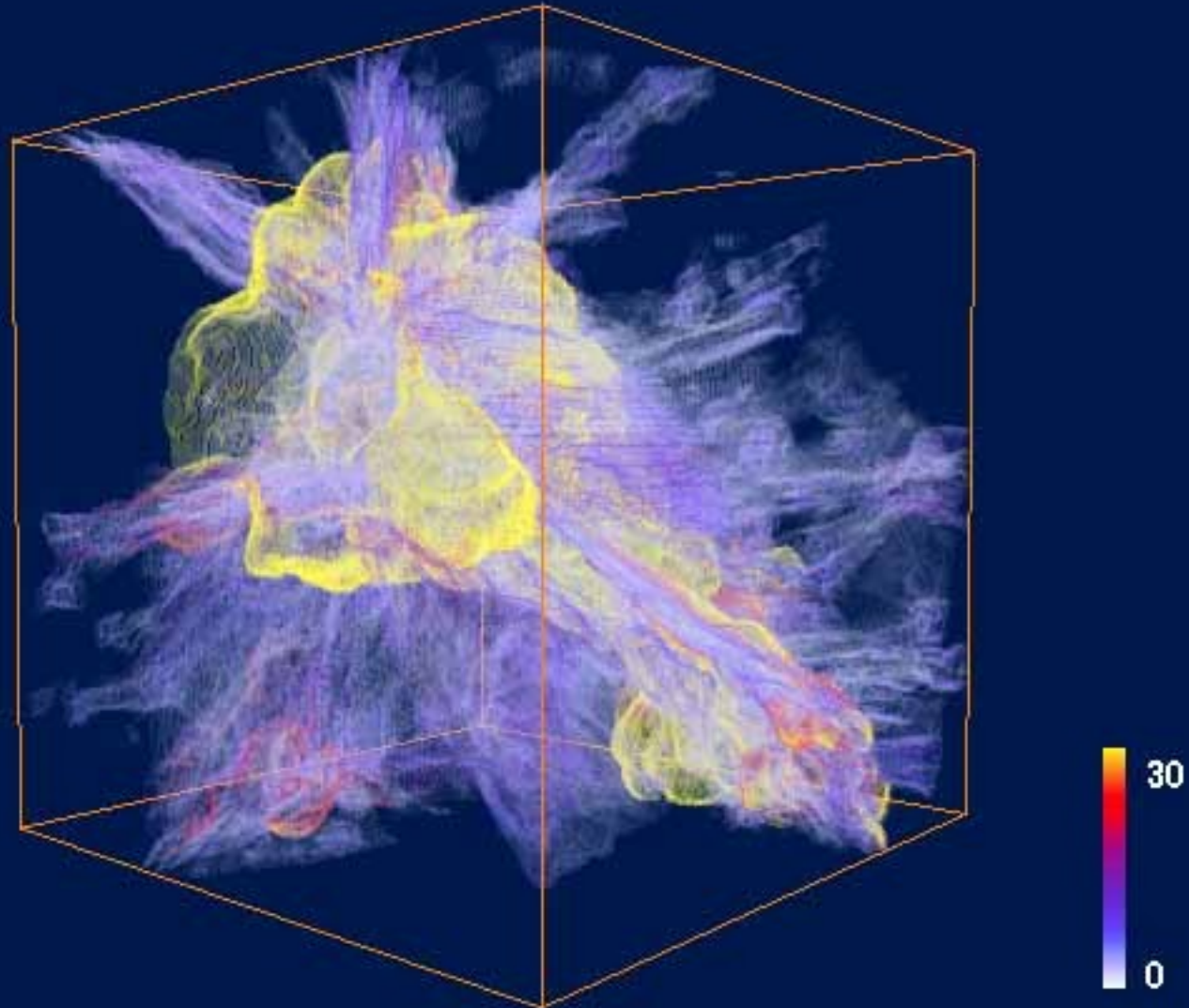


Non-standard physics with SPH: Cosmic Rays

Clusters are surrounded and filled with a complex pattern of shock waves

SHOCKS OF DIFFERENT MACH NUMBER AROUND A CLUSTER

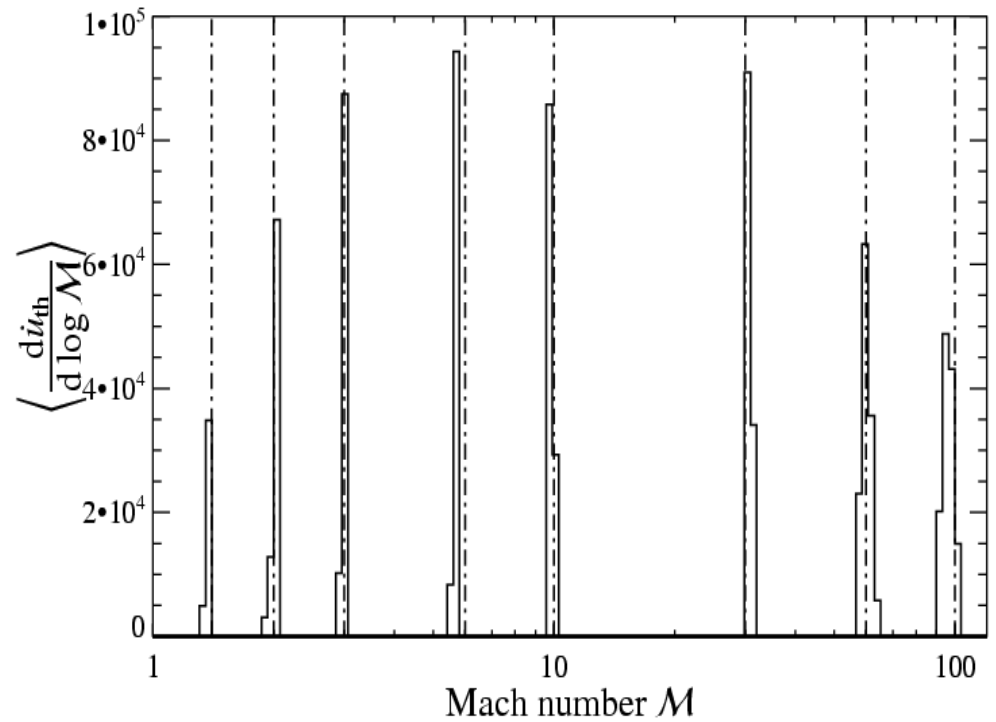
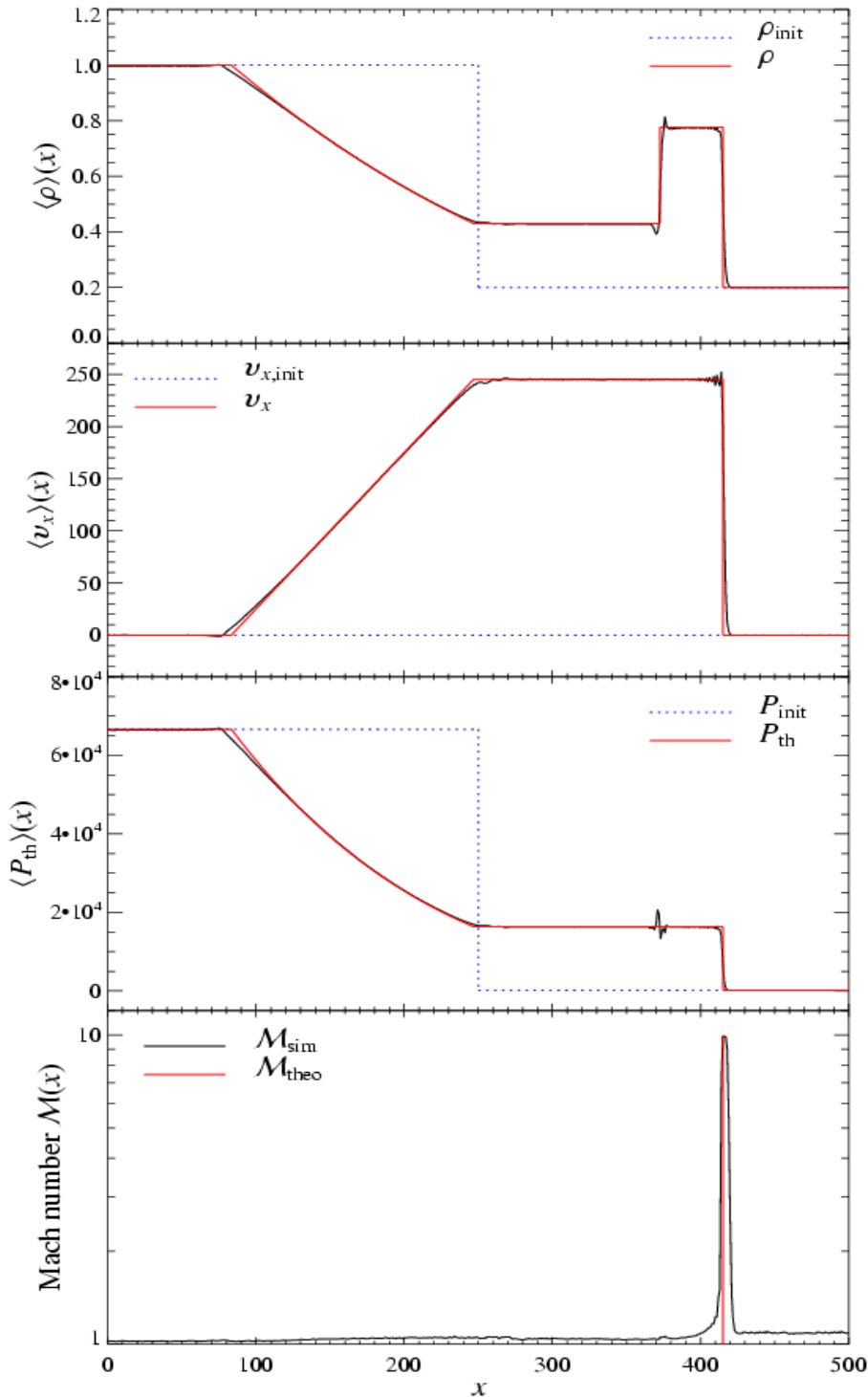
Ryu, Kang, Hallman & Jones (2003)



A new methods allows an on-the-fly detection of shocks in SPH calculations and an estimation of their Mach number

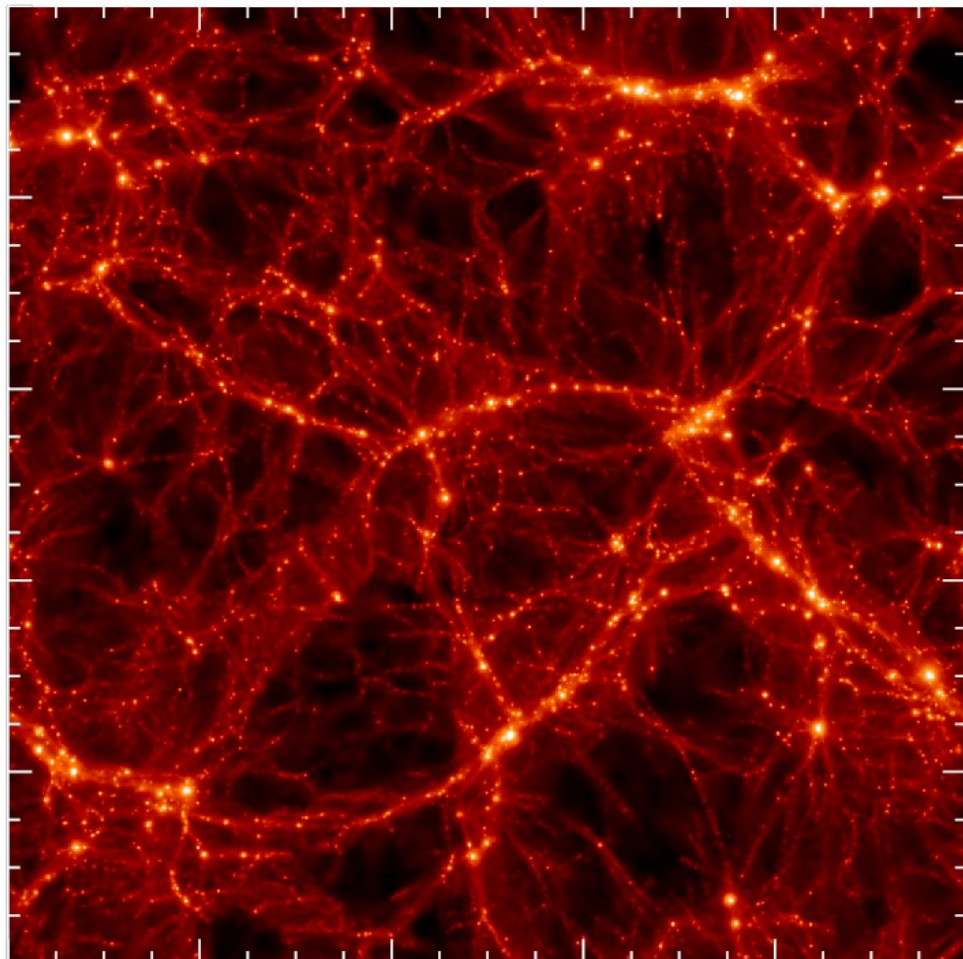
AN SPH SHOCK FINDER

Pfrommer, Springel, Enßlin & Jubelgas (2005)

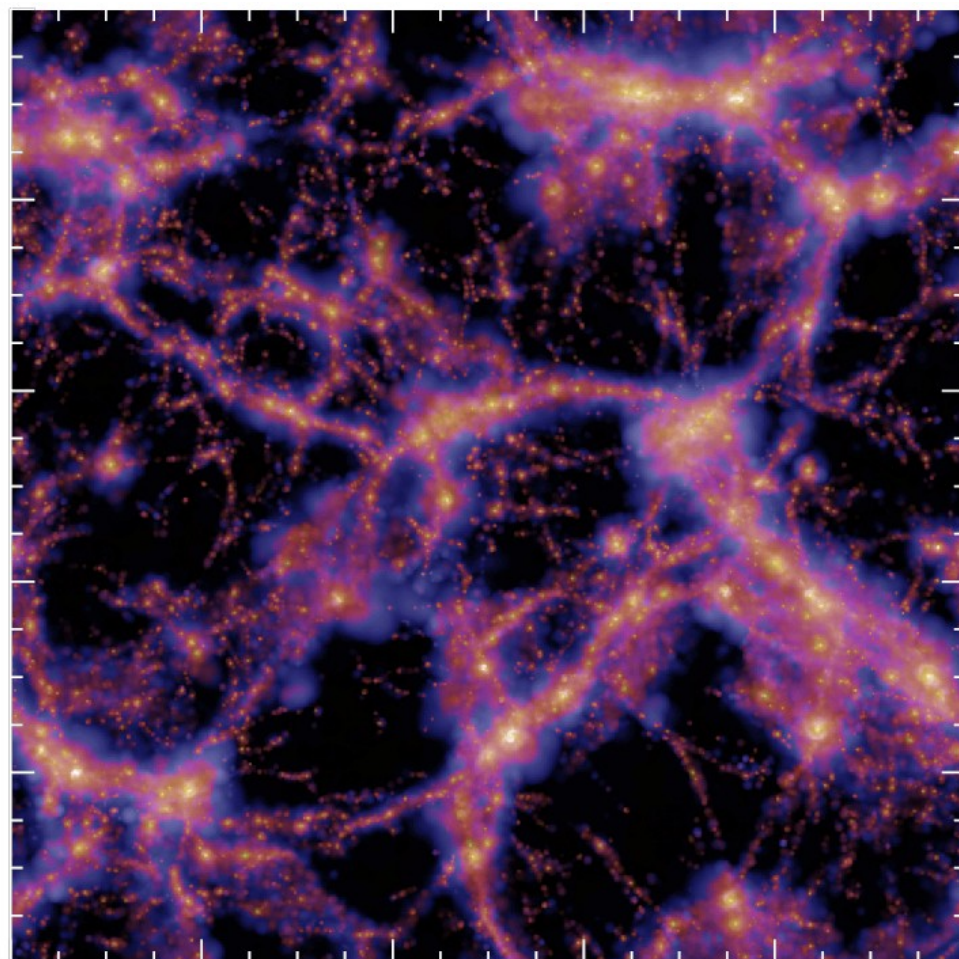
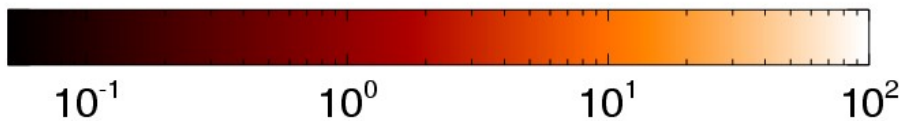


Structure formation shocks can be studied in situ in SPH

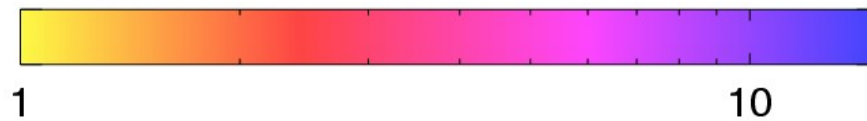
SHOCK STRENGTH DISTRIBUTION, WEIGHTED BY DISSIPATION RATE



$$\langle 1 + \delta_{\text{gas}} \rangle_{\text{los}}$$

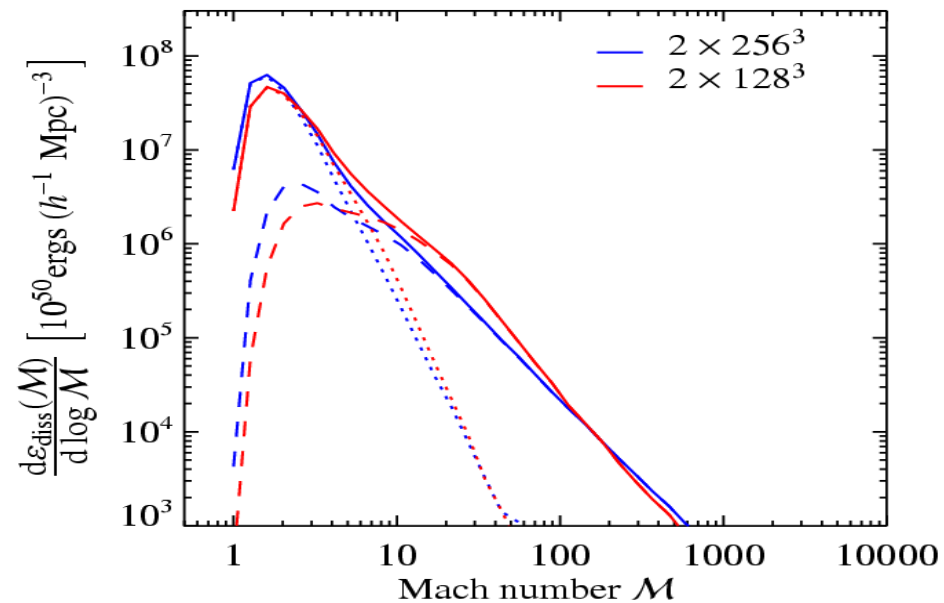


$$\frac{\langle \mathcal{M} d\epsilon_{\text{diss}} / (d \log a) \rangle_{\text{los}}}{\langle d\epsilon_{\text{diss}} / (d \log a) \rangle_{\text{los}}}$$

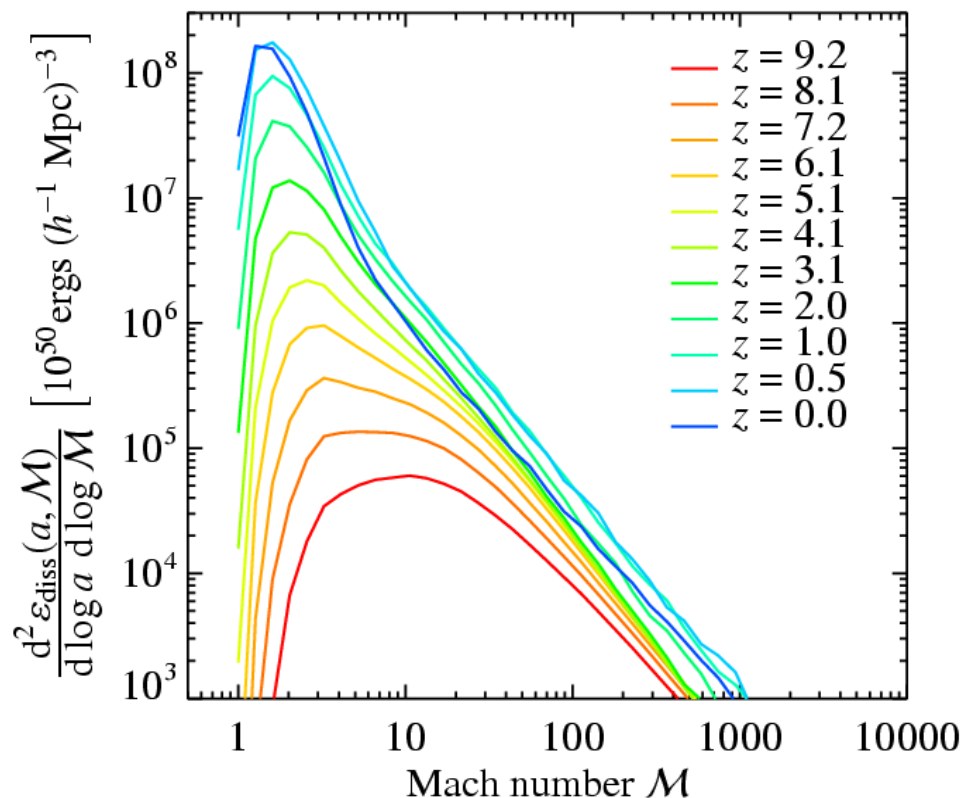
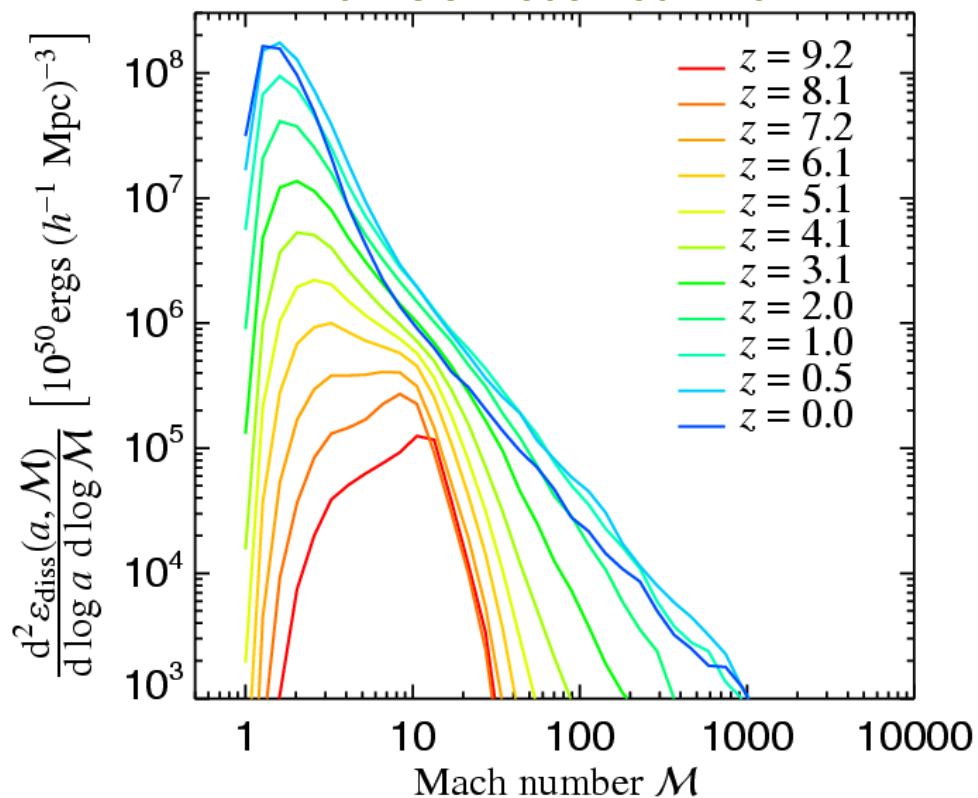


As time progresses, the characteristic shock mach number declines

THE COSMIC MACH NUMBER DISTRIBUTION AT DIFFERENT EPOCHS



with 'reionization' at $z=10$



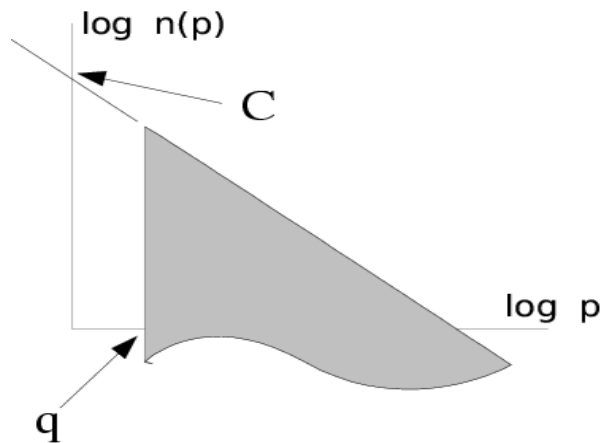
Part of the shock energy is used to accelerate protons and inject a relativistic power-law cosmic ray component

A SIMPLIFIED FORMALISM FOR COSMIC RAYS

Enßlin, Pfrommer, Jubelgas & Springel (2006)

cosmic ray momentum spectrum

$$f(p) = \frac{dN}{dp dV} = C p^{-\alpha} \theta(p - q)$$



cosmic ray pressure

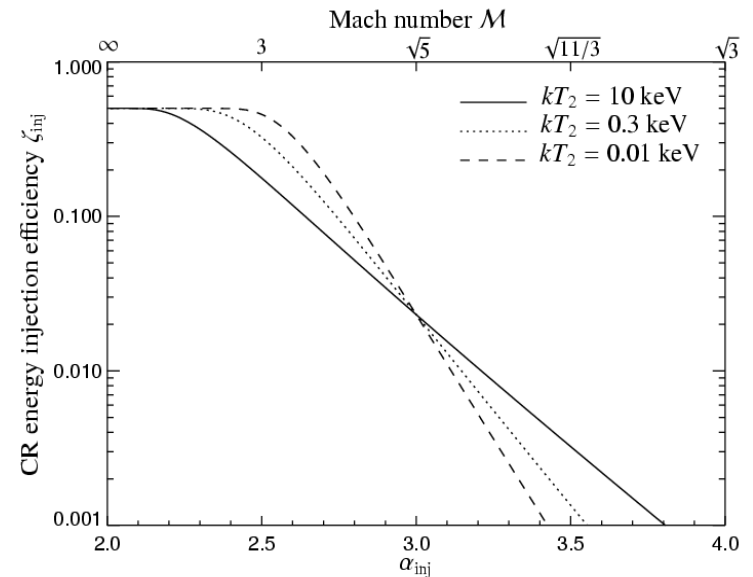
$$P_{\text{CR}} = \frac{C m_p c_{\text{light}}^2}{6} \mathcal{B}_{\frac{1}{1+q^2}} \left(\frac{\alpha - 2}{2}, \frac{3 - \alpha}{2} \right)$$

adiabatic evolution

$$q(\rho) = (\rho/\rho_0)^{\frac{1}{3}} q_0 \quad C(\rho) = (\rho/\rho_0)^{\frac{\alpha+2}{3}} C_0$$

injection mechanism

- Supernovae injection
- Diffuse shock acceleration at structure formation shocks



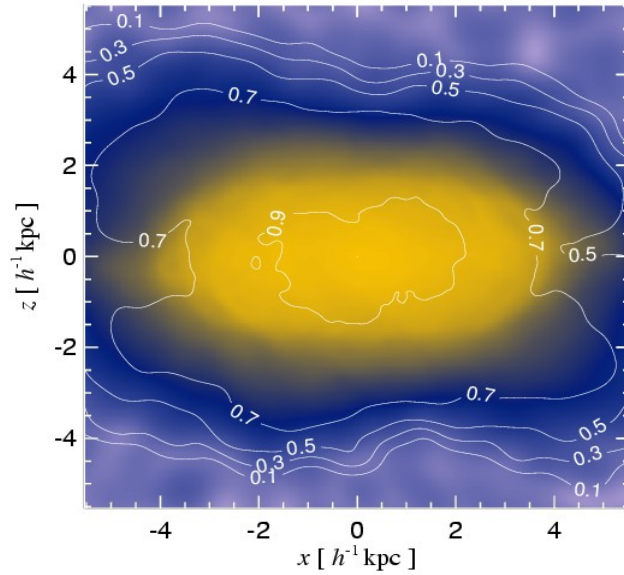
loss processes

- Coulomb losses
- Cosmic ray diffusion
- Hadronic interactions, mostly pion production (catastrophic losses)
- Bremsstrahlung (negligible for protons)

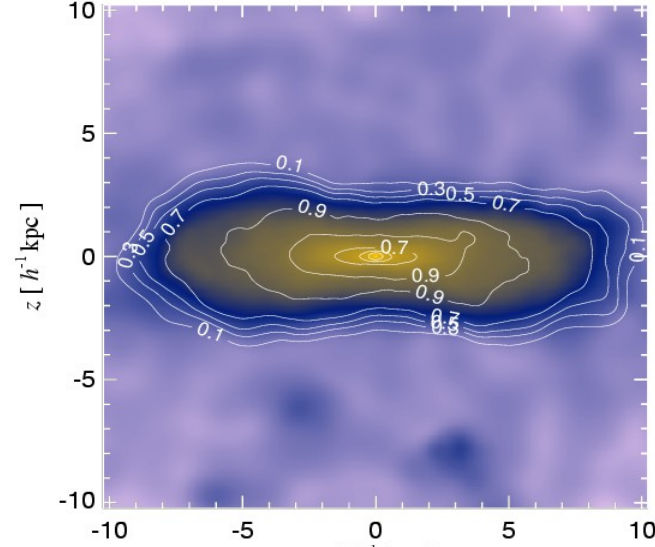
Cosmic rays injected by supernovae affect star-forming dwarf galaxies

EDGE-ON GAS AND PRESSURE MAPS AND STELLAR PROFILES

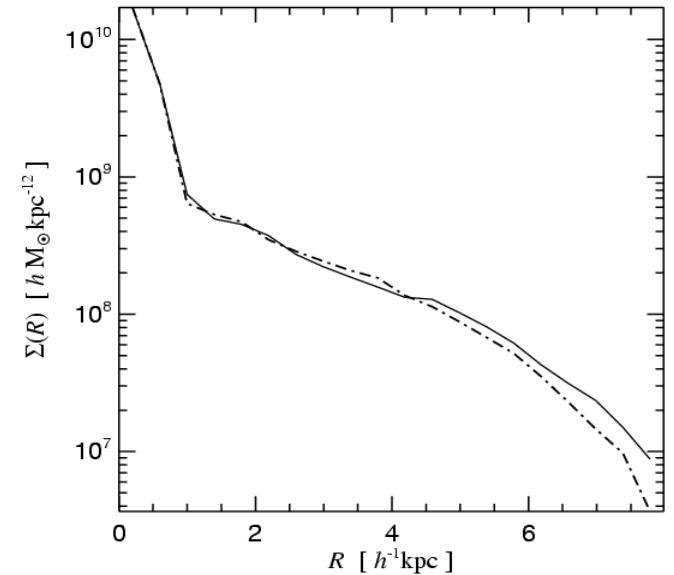
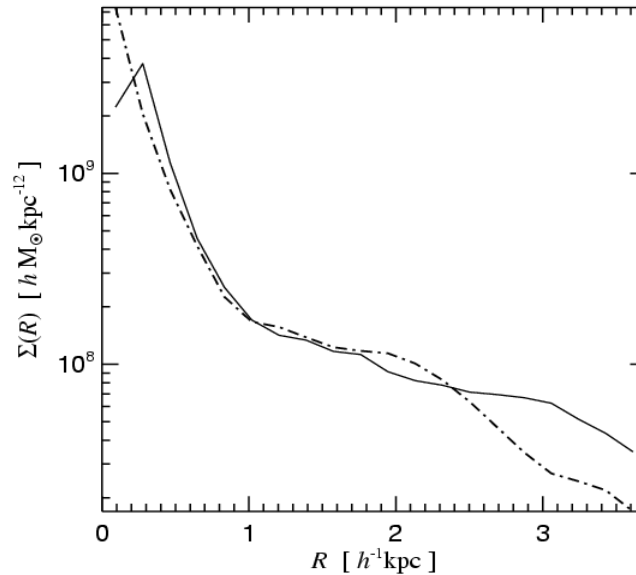
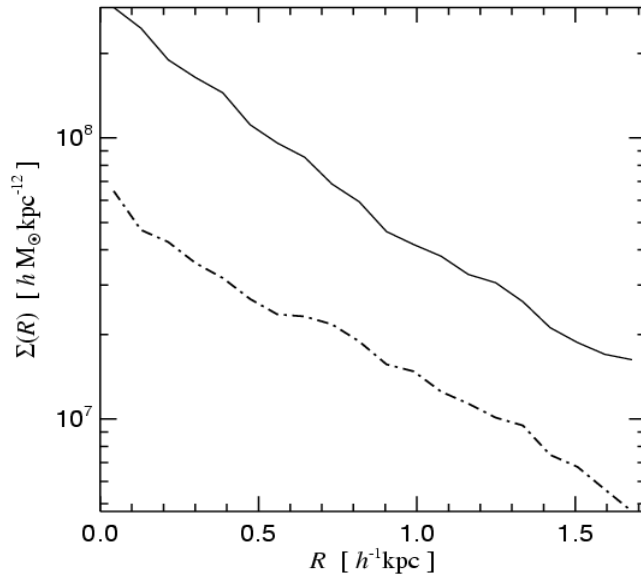
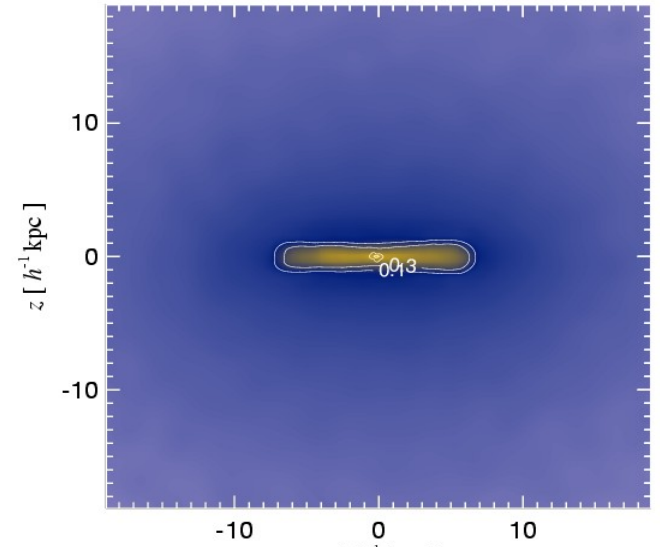
$M = 10^{10} M_{\odot}/h$



$M = 10^{11} M_{\odot}/h$

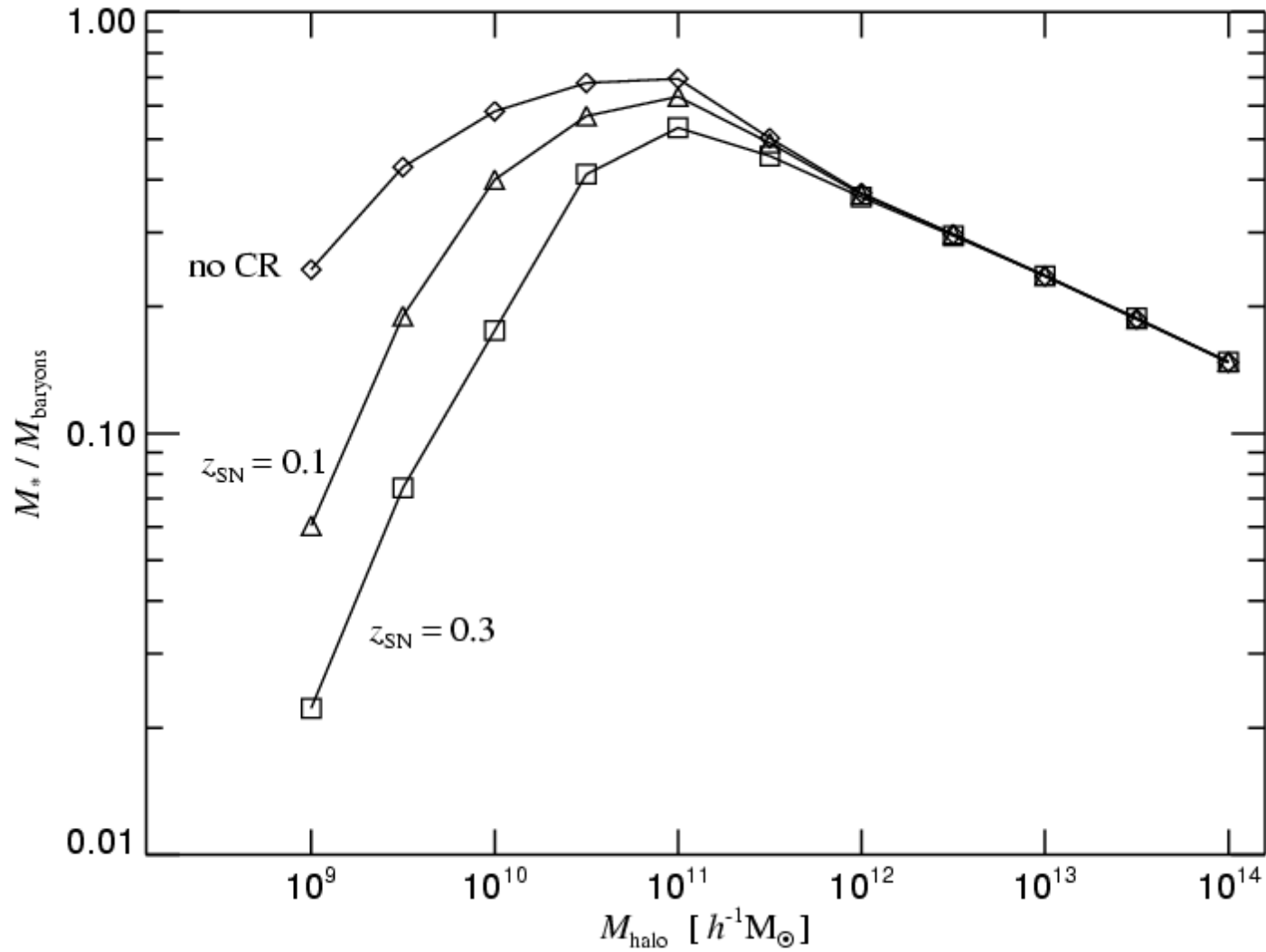


$M = 10^{12} M_{\odot}/h$



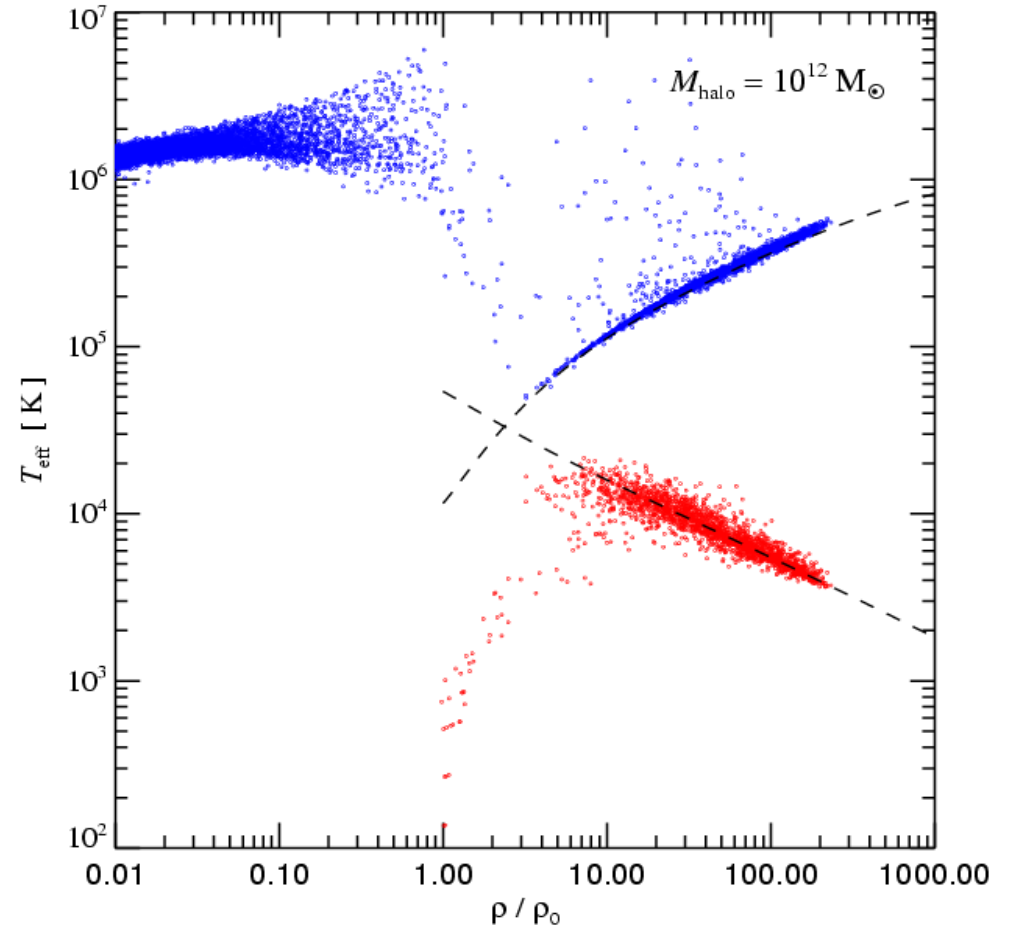
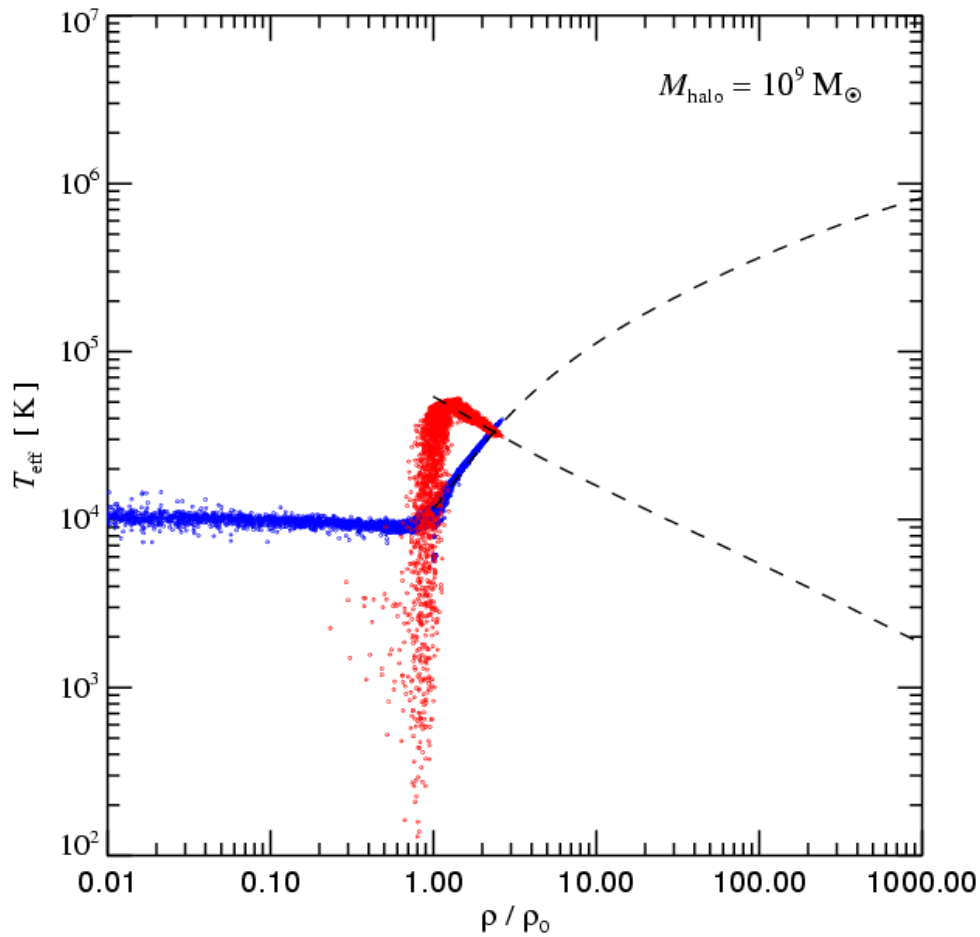
Cosmic rays injected by supernovae suppress star formation in small galaxies

EFFECTS OF COSMIC RAYS AS A FUNCTION OF MASS



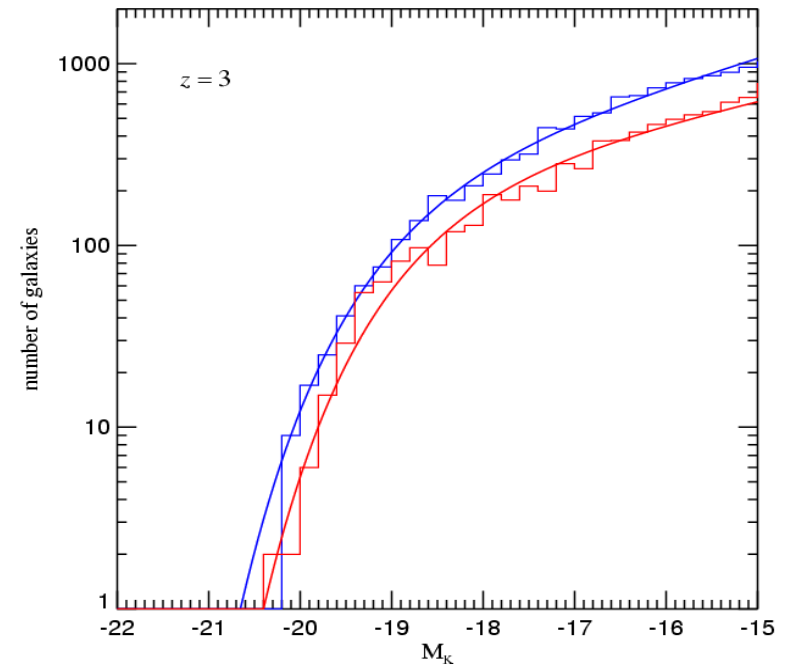
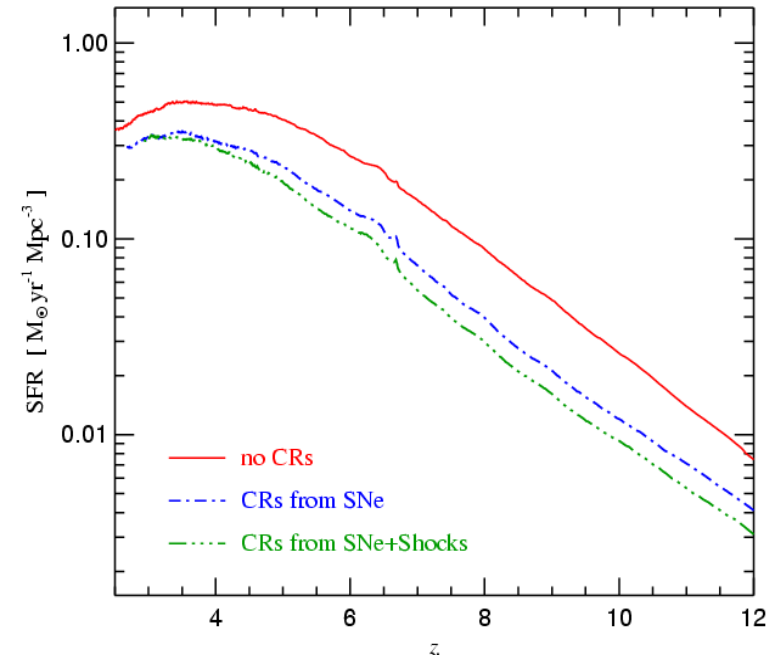
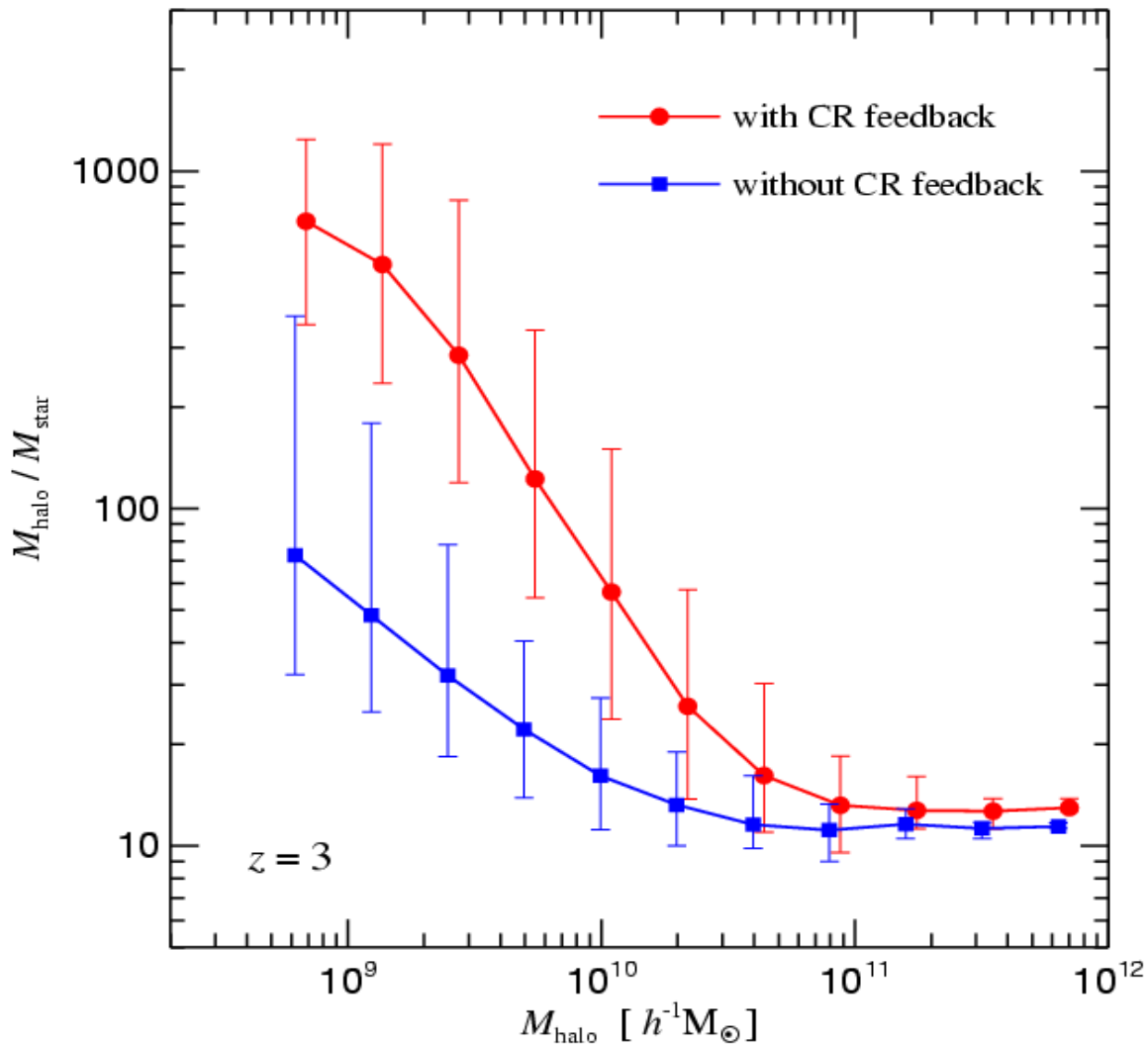
Only in small galaxies can the cosmic ray pressure exceed the effective thermal pressure of the star-forming ISM

PHASE-SPACE DIAGRAMS



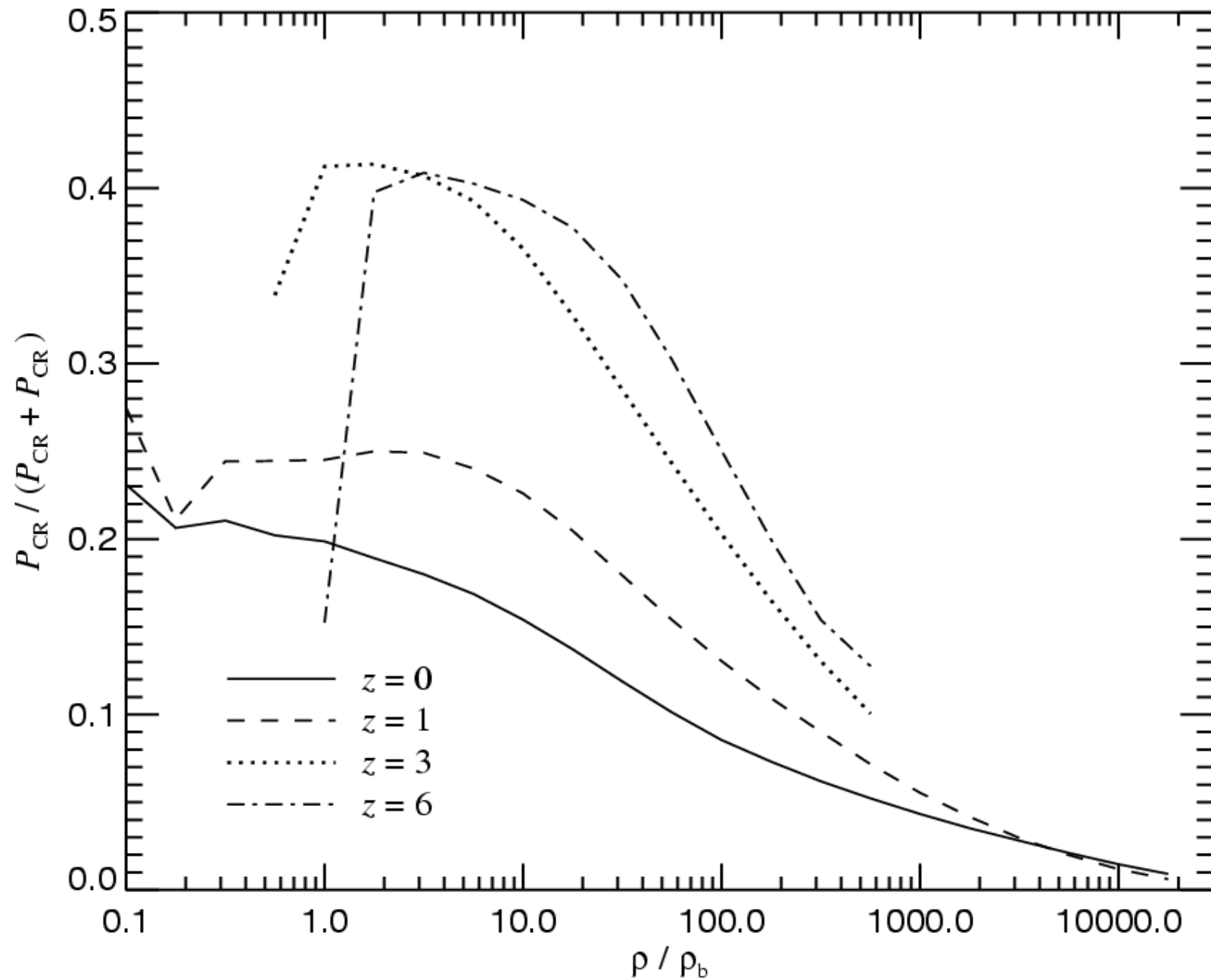
Cosmic rays affect star formation history and the faint-end of the galaxy luminosity function

MASS-TO-LIGHT RATIO OF HIGH-REDSHIFT GALAXIES



High Mach-number structure formation shock waves produce cosmic rays

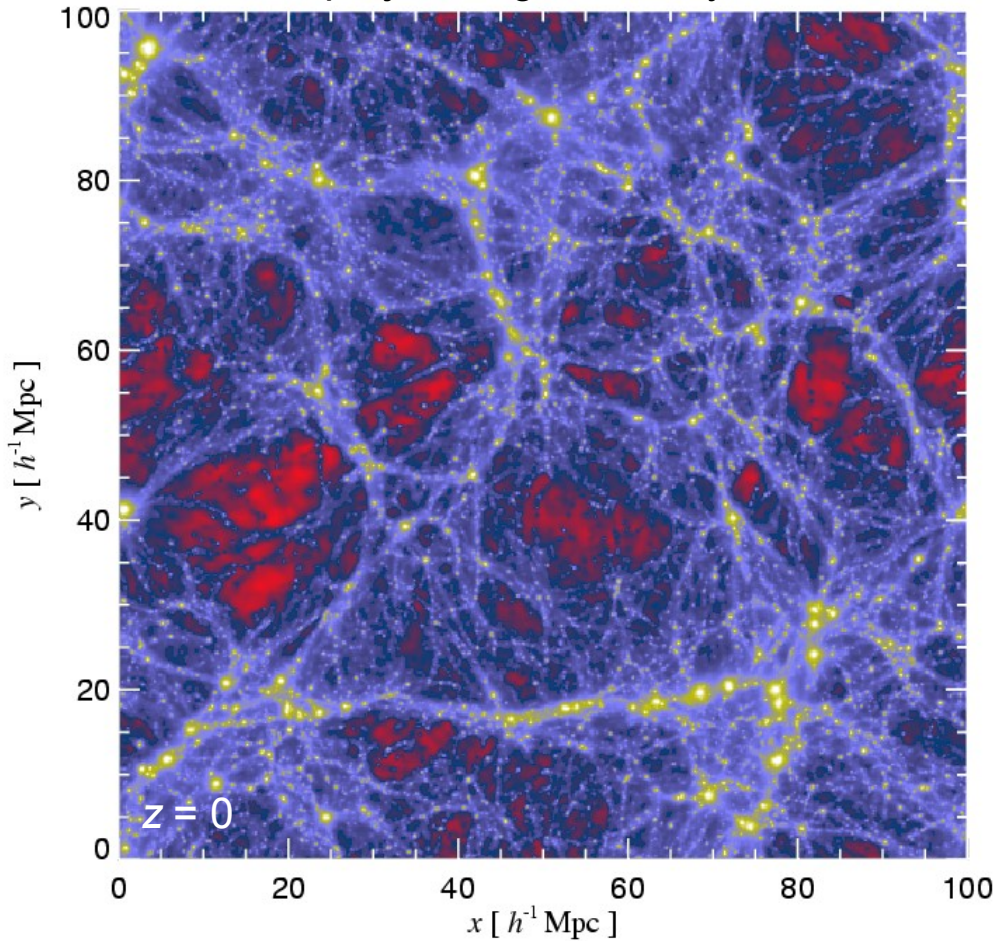
RELATIVE COSMIC RAY PRESSURE CONTRIBUTION AS A FUNCTION OF DENSITY AND EPOCH



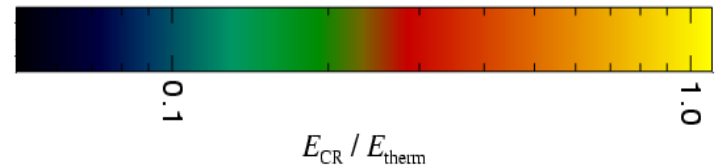
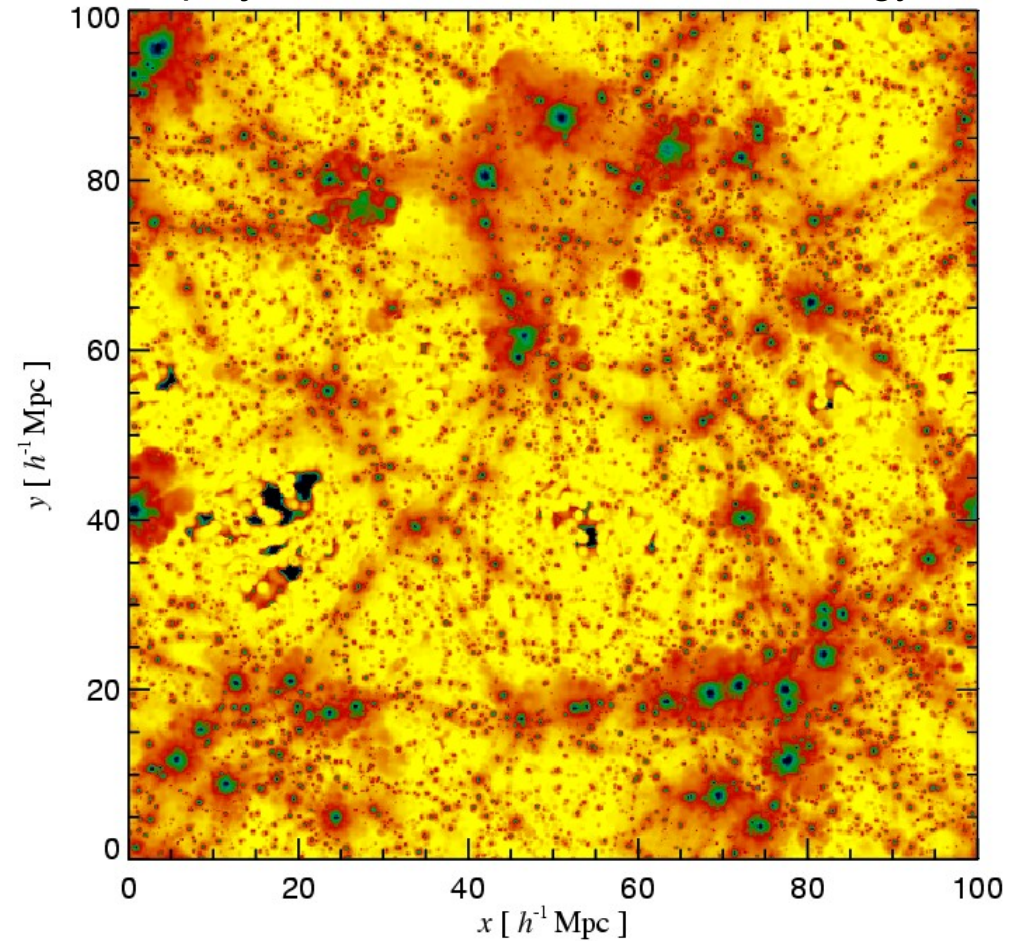
Cosmic rays can contribute substantially to the energy density in low density regions but are less important within virialized structures

RELATIVE COSMIC RAY PRESSURE CONTRIBUTION AS A FUNCTION OF DENSITY AND EPOCH

projected gas density

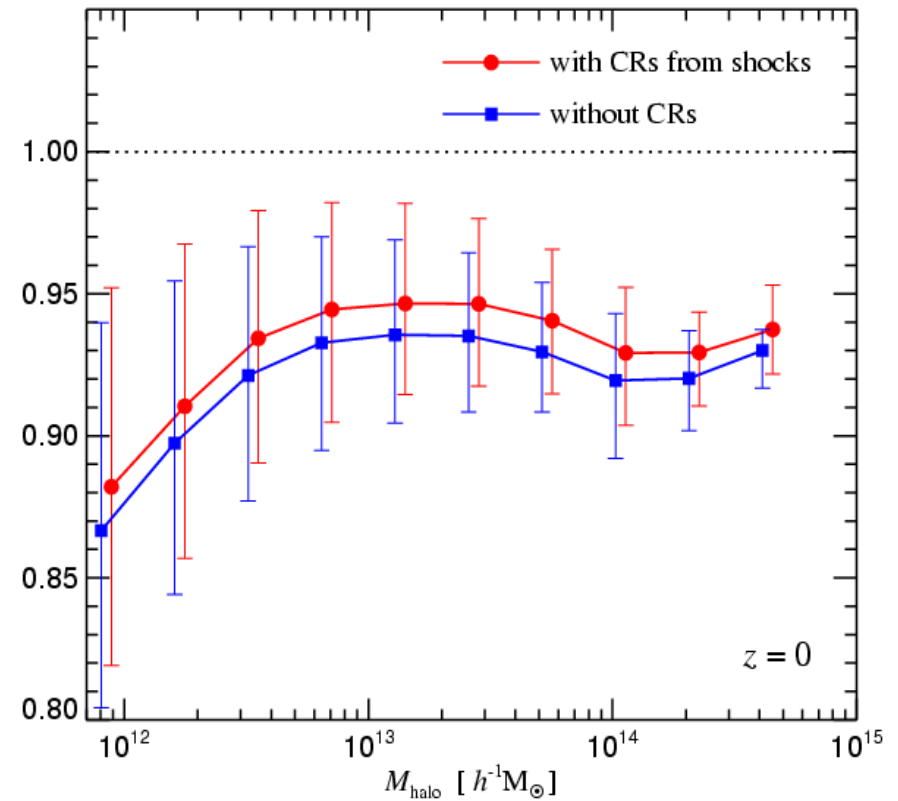
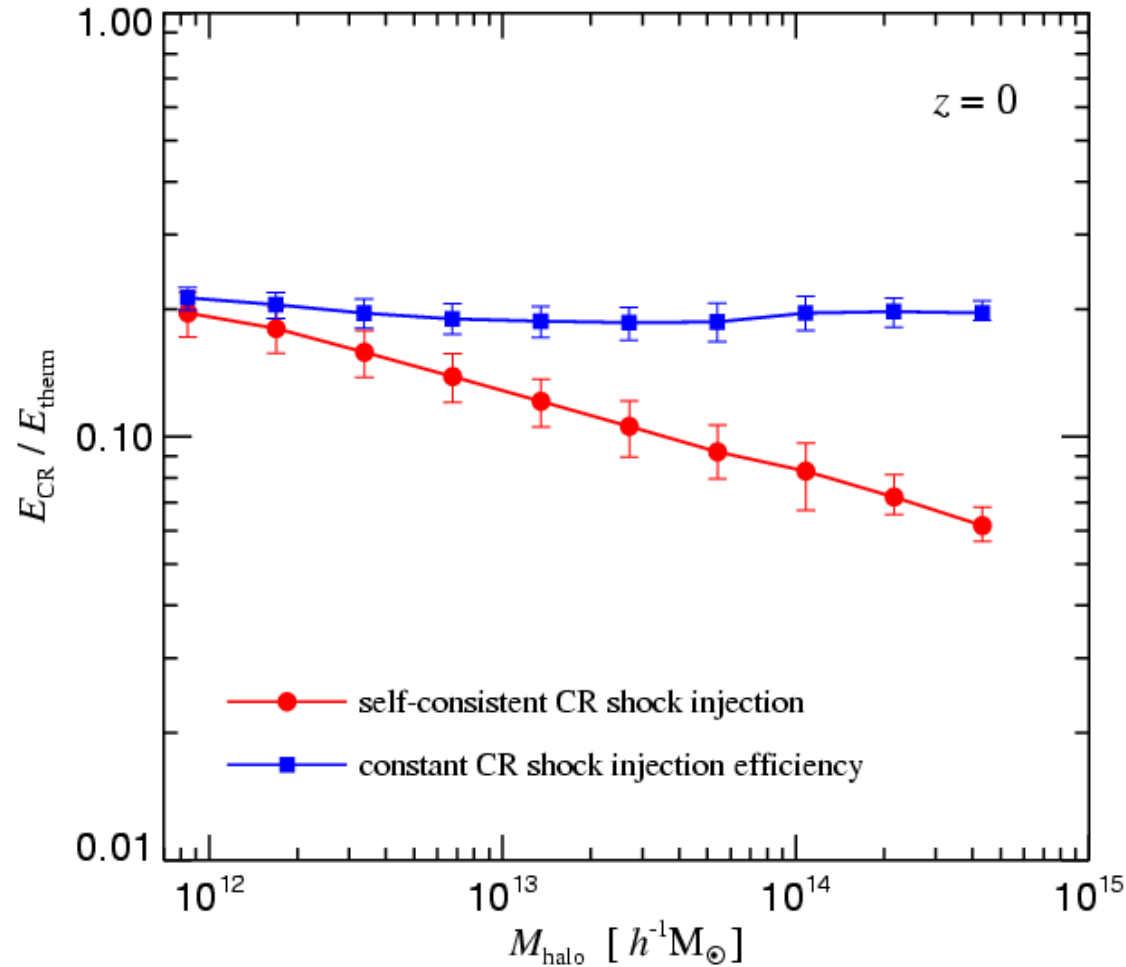


projected ratio of CR to thermal energy



The effective equation of state of the gas in halos becomes softer by cosmic rays, which increases its central concentration

ENERGY FRACTION IN COSMIC RAYS AND BARYON FRACTION IN VIRIALIZED HALOS



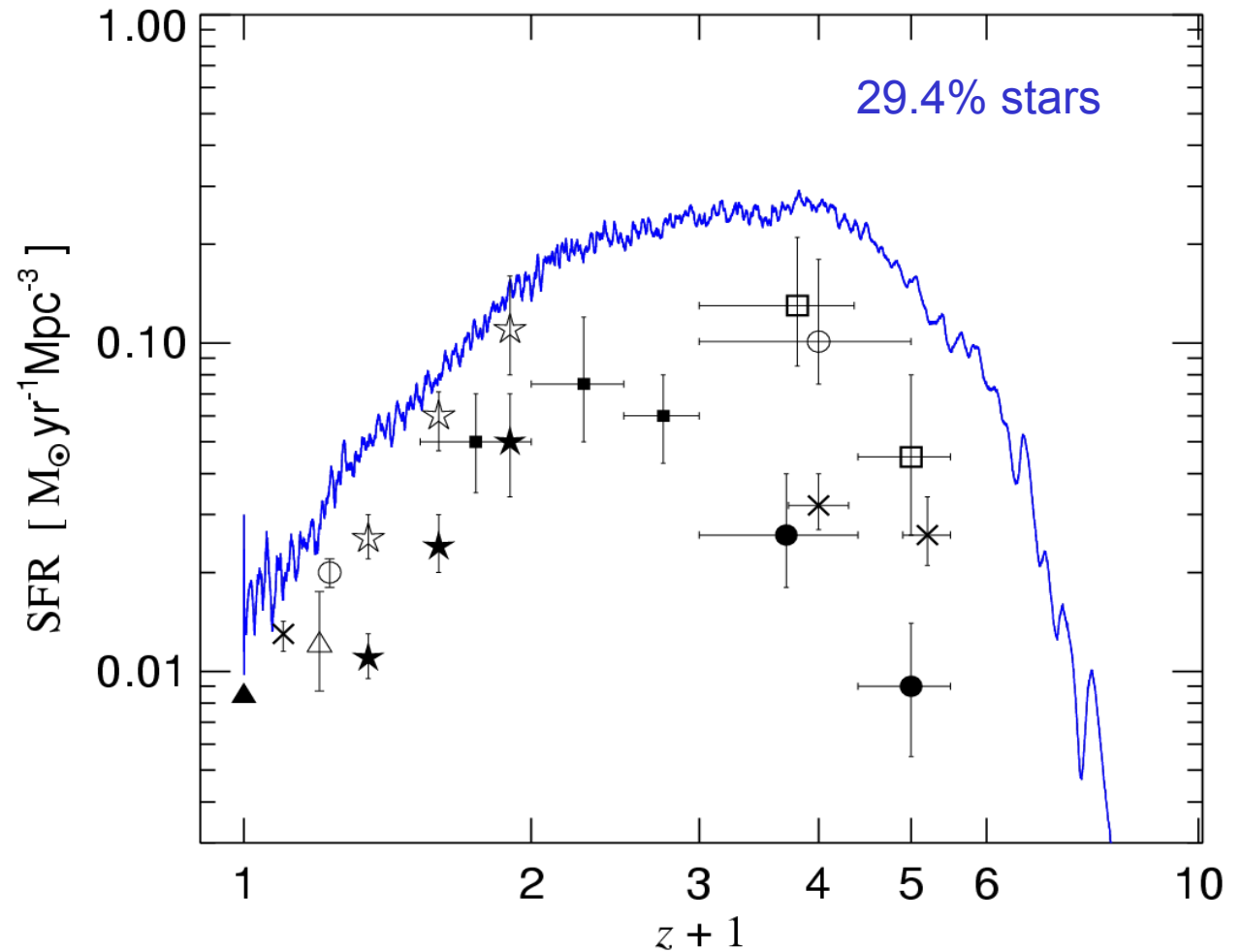
Non-standard physics in SPH:
The need for subresolution
modelling of star formation and
feedback

"Standard" simulations with only thermal feedback tend to overpredict the cosmic star formation history

COOLING, STAR FORMATION & THERMAL FEEDBACK

Data points by:

- Gallego et al. (1996, filled triangles)
- Gronwall (1999, diagonal crosses)
- Tryer et al. (1998, open triangle)
- Tresse & Maddox (1998, empty circle)
- Lilly et al. (1996, filled stars)
- Conolly et al. (1997, filled squares)
- Madau et al. (1996, filled circles)
- Pettini et al. (1998 empty squares)
- Flores et al. (1999, empty stars)



Run: T50_C

Modeling of star formation and feedback in cosmological simulations has proven to be difficult

THE CASE FOR MULTI-PHASE MODELS

- Phenomenological single-phase models largely fail, except perhaps if:
 - Cooling of reheated gas is artificially delayed
 - strong kinetic feedback is invoked

on the other hand:

- Stars form in GMC's
- Strongly cooling gas is subject to instabilities
- The real structure of the ISM is known to be multi-phase
- Galactic winds and outflows are observed

→ *Do multi-phase models allow the difficulties of the current generation of cosmological simulations to be overcome?*

Modeling true multi-phase ISM in cosmological volumes is currently not feasible

THE COMPUTATIONAL CHALLENGE

Giant molecular clouds

$$M_{\text{cl}} \sim 5 \times 10^5 M_{\odot}$$

$$R_{\text{cl}} \sim 30 \text{ pc}$$

$$\bar{n} \sim 200 \text{ cm}^{-3}$$

$$\delta \sim 10^9$$

$$t_{\text{cl}} \sim 4 \times 10^6 \text{ yr}$$

Currently achievable resolution

for $L \geq 50 h^{-1} \text{ Mpc}$:

$$M_{\text{sph}} \sim 10^7 M_{\odot}$$

$$\epsilon \sim 1 \text{ kpc}$$

$$\delta \sim 10^7$$

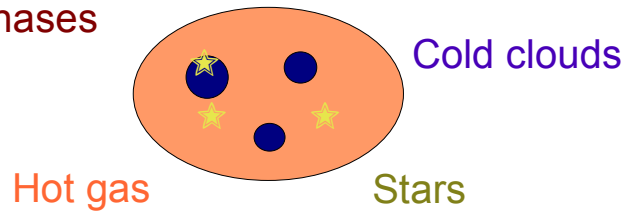
huge dynamic range + difficult/unclear physics !

→ *Need to develop effective subgrid-models that are motivated by physical models of the ISM*

A multi-phase model for cosmological simulations

MODEL EQUATIONS

Subresolution phases
of the ISM:



Yepes, Kates, Khokhlov & Klypin (1997)
Hultman & Pharasyn (1999)

Star formation:

$$\frac{d\rho_{\star}}{dt} = (1 - \beta) \frac{\rho_c}{t_{\star}}$$

supernova mass fraction

star formation timescale

Cloud evaporation:

$$\left. \frac{d\rho_h}{dt} \right|_{\text{evap}} = A\beta \frac{\rho_c}{t_{\star}}$$

cloud evaporation parameter

Growth of clouds:

$$\left. \frac{d\rho_c}{dt} \right|_{\text{TI}} = - \left. \frac{d\rho_h}{dt} \right|_{\text{TI}} = \frac{\Lambda_{\text{net}}(\rho_h, u_h)}{u_h - u_c}$$

radiative losses cool material from the hot phase to the cold clouds

Thermal energy budget:

supernova 'temperature' ~ 10⁸ K

$$\frac{d}{dt} (\rho_h u_h + \rho_c u_c) = -\Lambda_{\text{net}}(\rho_h, u_h) + \beta \frac{\rho_c}{t_\star} u_{\text{SN}} - (1 - \beta) \frac{\rho_c}{t_\star} u_c,$$

Total energy
Cooling
Feedback
Loss to stars

cold clouds:

$$\frac{d}{dt} (\rho_c u_c) = -\frac{\rho_c}{t_\star} u_c - A\beta \frac{\rho_c}{t_\star} u_c + \frac{(1-f)u_c}{u_h - u_c} \Lambda_{\text{net}}$$

$$f = \begin{cases} 1 & \text{normal cooling} \\ 0 & \text{thermal instability} \end{cases}$$

hot phase:

$$\frac{d}{dt} (\rho_h u_h) = \beta \frac{\rho_c}{t_\star} (u_{\text{SN}} + u_c) + A\beta \frac{\rho_c}{t_\star} u_c - \frac{u_h - f u_c}{u_h - u_c} \Lambda_{\text{net}}$$

Mass transfer budget:

cold clouds:

$$\frac{d\rho_c}{dt} = -\frac{\rho_c}{t_\star} - A\beta \frac{\rho_c}{t_\star} + \frac{(1-f)}{u_h - u_c} \Lambda_{\text{net}}$$

Star formation
Evaporation
Cloud Growth

hot phase:

$$\frac{d\rho_h}{dt} = \beta \frac{\rho_c}{t_\star} + A\beta \frac{\rho_c}{t_\star} - \frac{(1-f)}{u_h - u_c} \Lambda_{\text{net}}$$

Supernovas

Temperature evolution:

hot phase:

$$\rho_h \frac{du_h}{dt} = [u_{\text{SN}} - (A + 1)(u_h - u_c)] \beta \frac{\rho_c}{t_\star} - f \Lambda_{\text{net}}$$

cold clouds: temperature assumed to be constant at $\sim 10^4$ K

equilibrium temperature for star formation
+ thermal instability



$$u_h = \frac{u_{\text{SN}}}{A + 1} + u_c$$

Evaporation efficiency:

$$A(\rho) = A_0 \left(\frac{\rho}{\rho_{\text{th}}} \right)^{-4/5}$$

McKee & Ostriker (1977)

Star formation timescale:

$$t_\star(\rho) = t_\star^0 \left(\frac{\rho}{\rho_{\text{th}}} \right)^{-1/2}$$

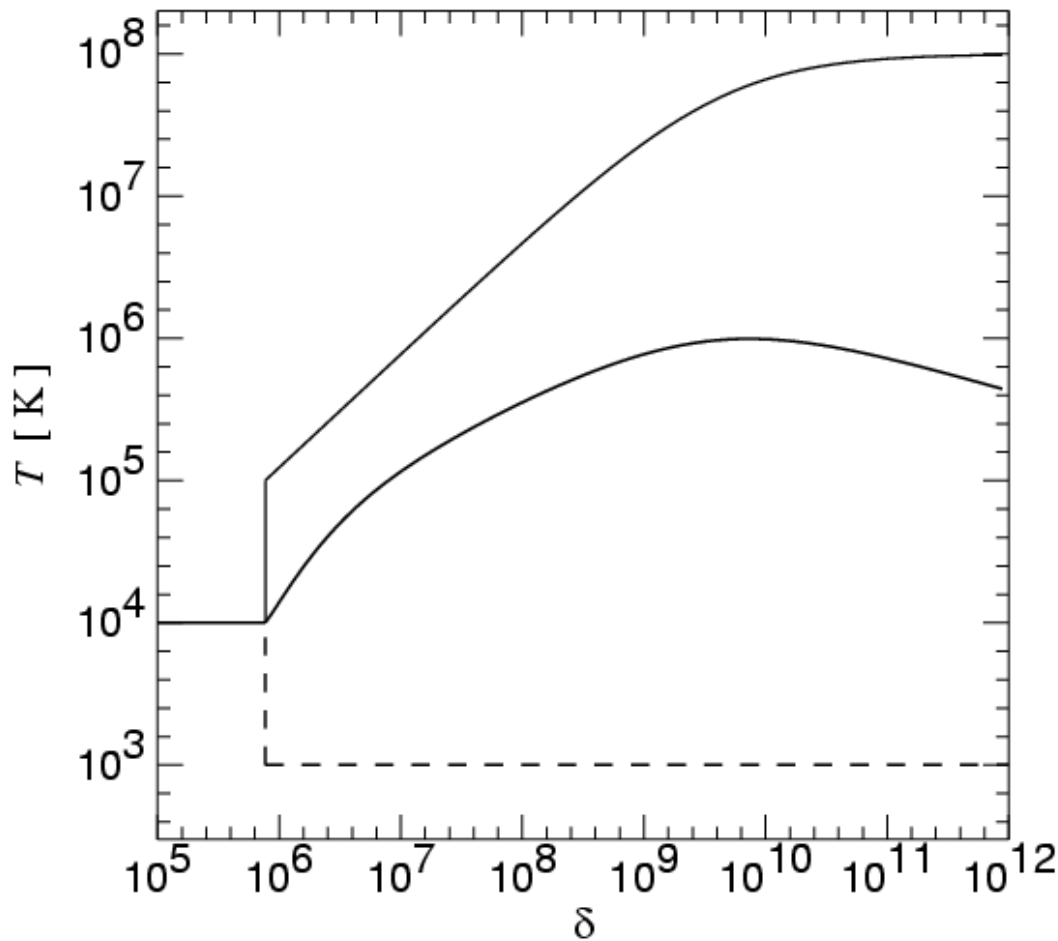
ρ_{th} and A_0 are constraint by
plausible temperature range of the ISM



star formation timescale t_\star^0
is adjustable parameter of model

The ISM is pressurized by star formation in the region of coexistence between a hot medium and embedded cold clouds

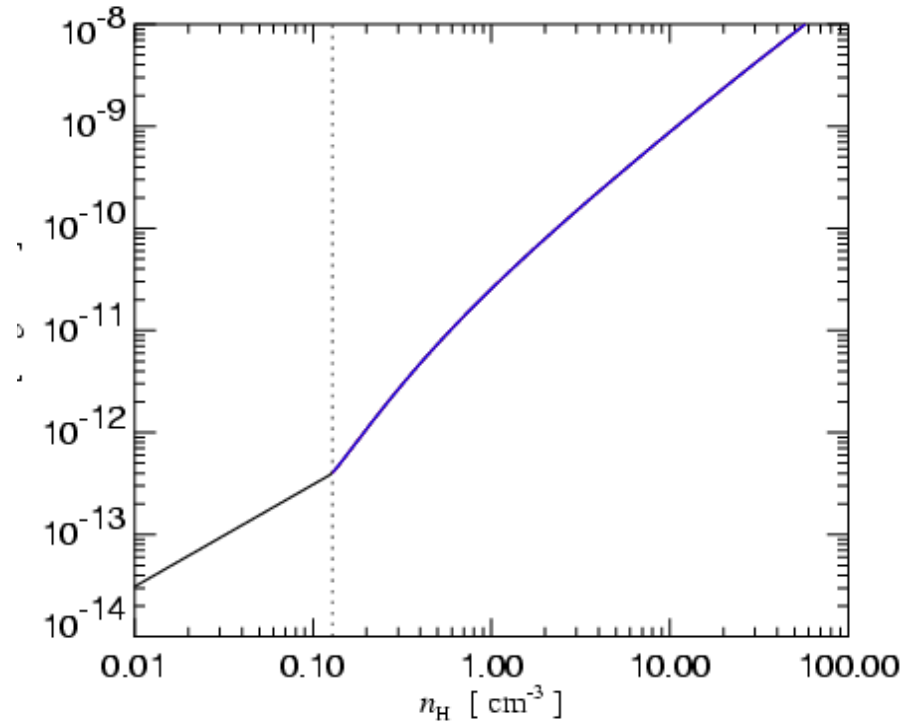
EFFECTIVE EQUATION OF STATE



Effective Pressure:

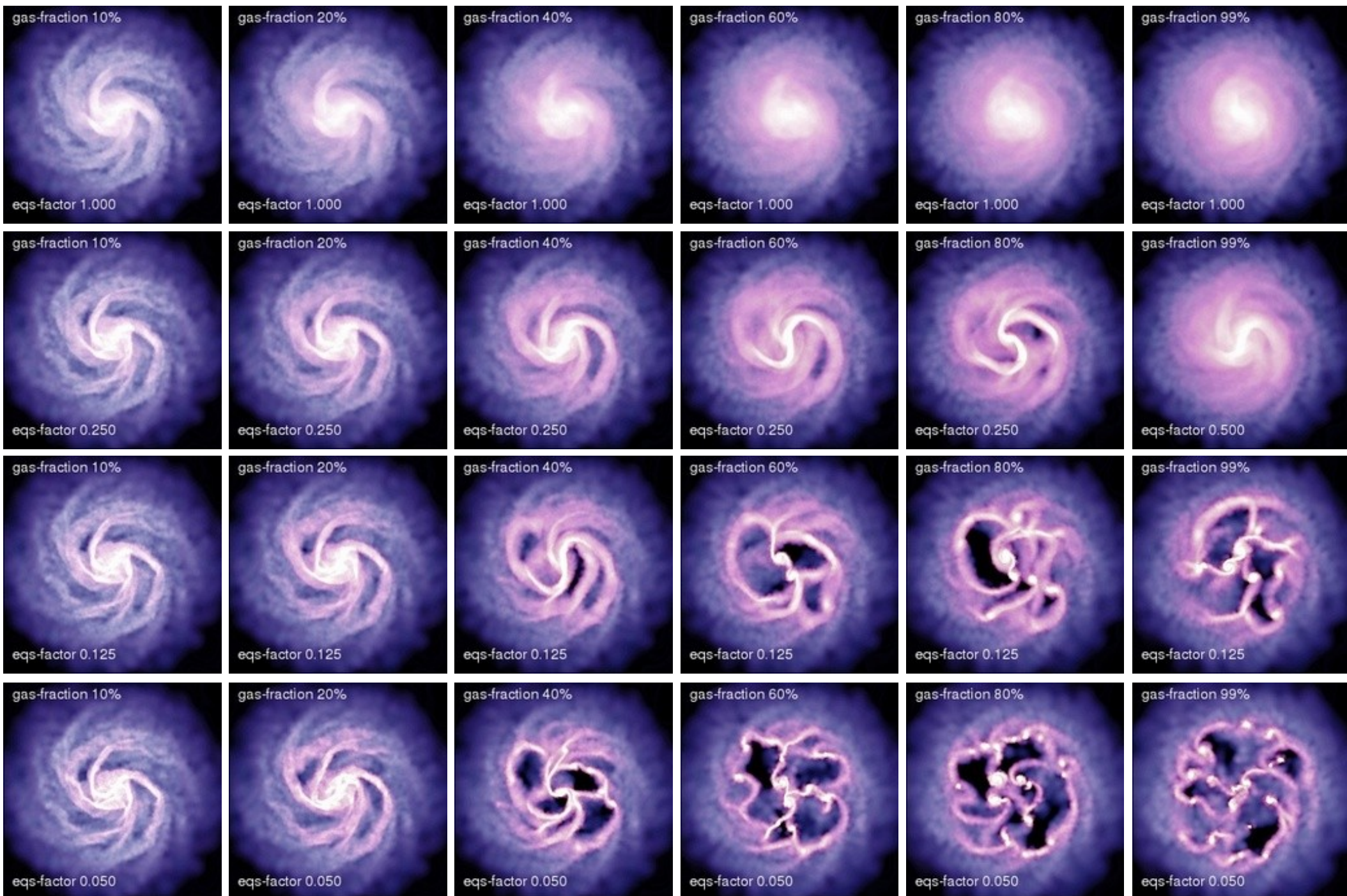
$$P_{\text{eff}} \equiv (\gamma - 1)(\rho_h u_h + \rho_c u_c)$$

$$T_{\text{eff}} \equiv \frac{\mu P_{\text{eff}}}{k \rho}$$



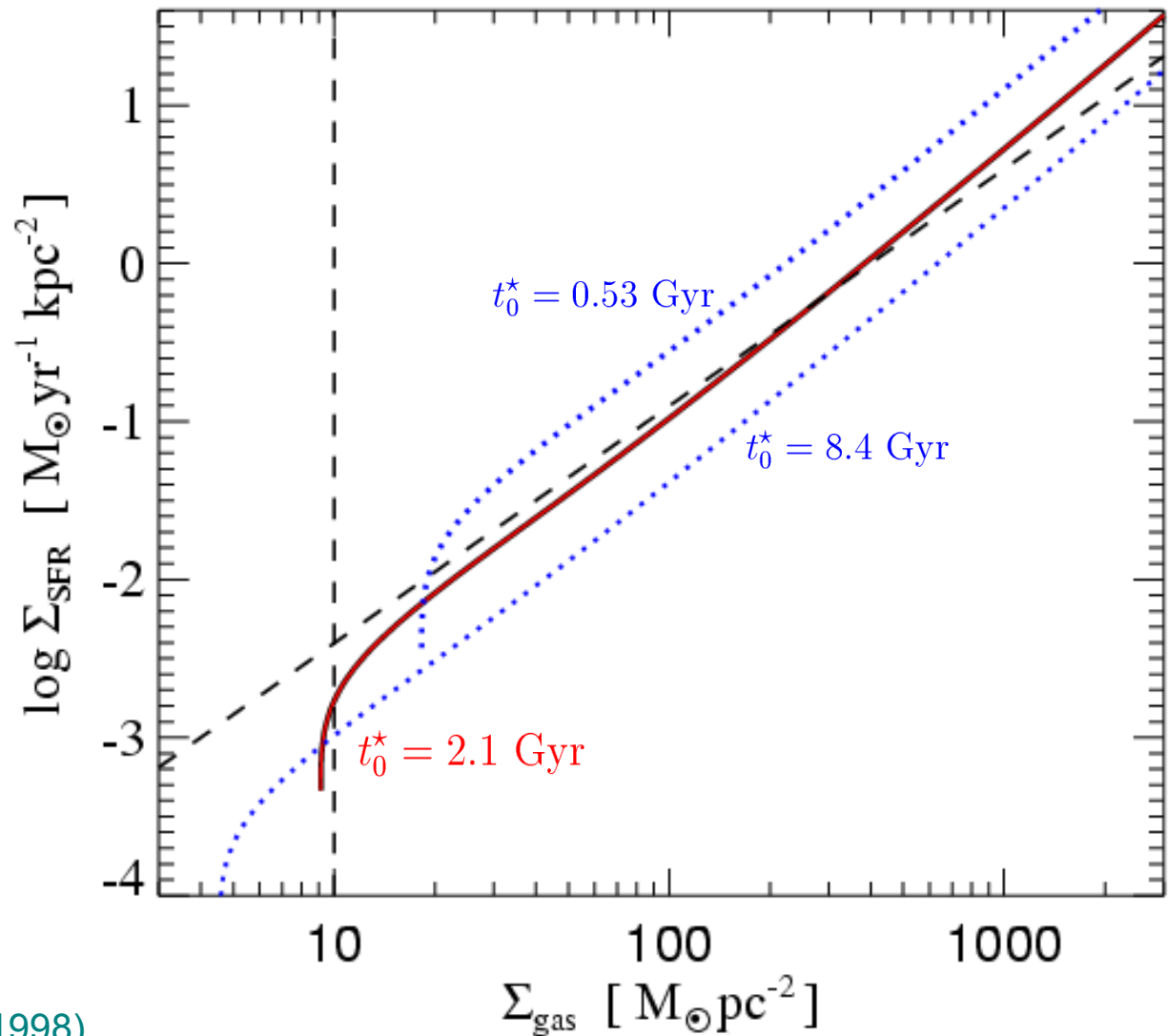
The multiphase-model allows stable disk galaxies even for very high gas surface densities

STABILITY OF DISKS AS A FUNCTION OF GAS FRACTION AND EQUATION OF STATE



Self-gravitating sheets of gas are used to normalize the multi-phase model

KENNICUTT LAW

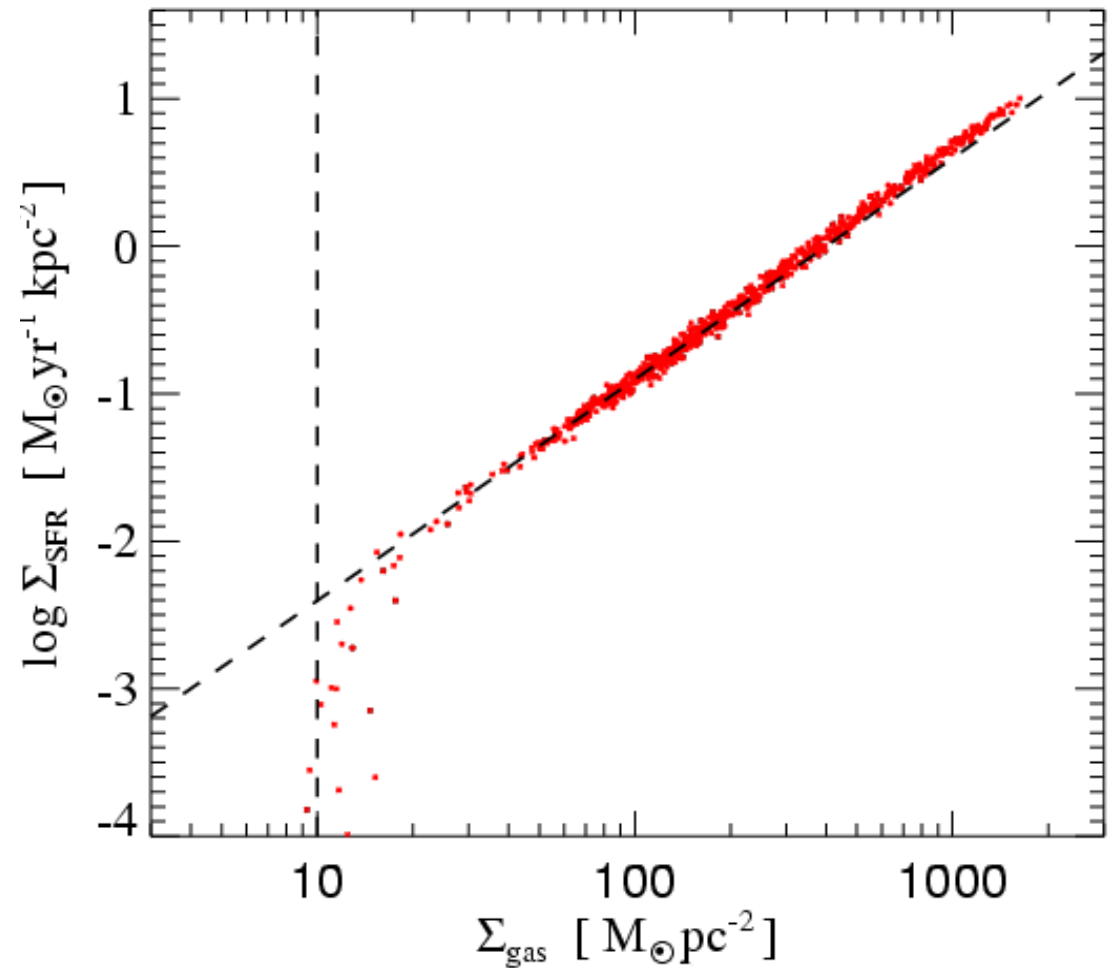
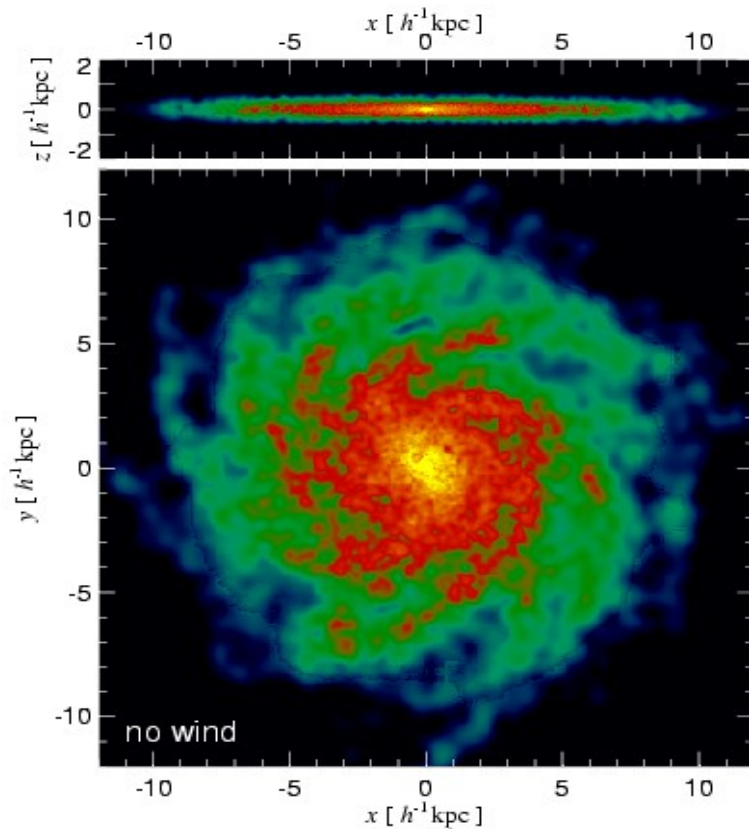


Global "Kennicutt-law" (Kennicutt 1998)

$$\Sigma_{\text{SFR}} = (2.5 \pm 0.7) \times 10^{-4} \left(\frac{\Sigma_{\text{gas}}}{\text{M}_{\odot} \text{pc}^{-2}} \right)^{1.4 \pm 0.15} \frac{\text{M}_{\odot}}{\text{yr kpc}^2}$$

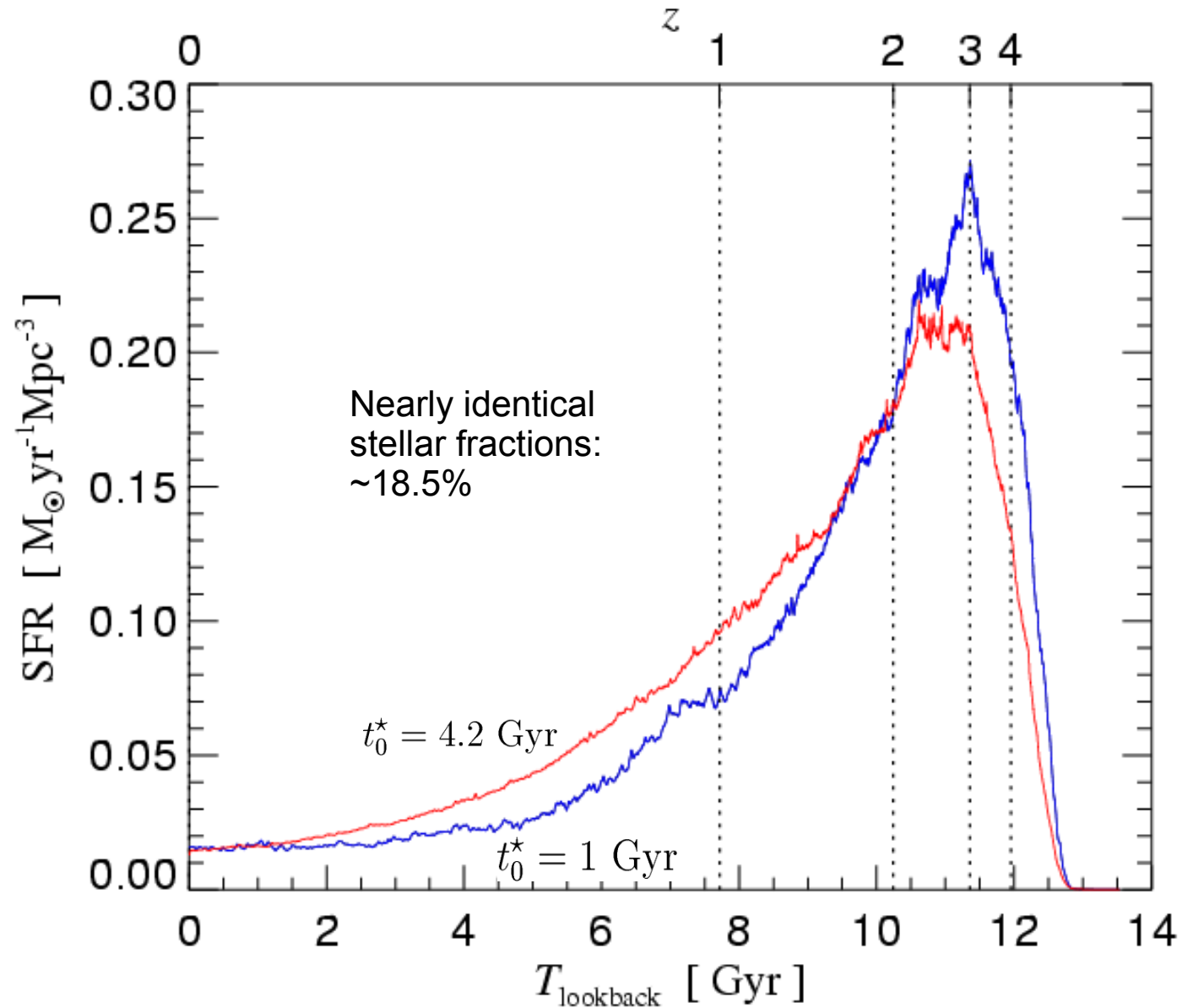
Simulations of isolated disk galaxies are used to check the normalization of the multi-phase model

MEASURED KENNICUTT LAW



The quiescent model of star formation does hardly affect the total amount of baryons locked up in stars

COSMIC STAR FORMATION HISTORY



Galactic winds associated with star formation transport metals and provide strong feedback

A PHENOMENOLOGICAL WIND MODEL

- Observations suggest disk-mass loss rates of order the star-formation rate or higher

(e.g. Martin 1998,1999)

$$\dot{M}_w = \eta \dot{M}_\star$$

- Parameterize the energy in the wind as a fraction χ of the supernova energy

$$\frac{1}{2} \dot{M}_w v_w^2 = \chi \epsilon_{\text{SN}} \dot{M}_\star$$

for : $\eta = 2, \chi = 0.25$

$$v_w = 242 \text{ km s}^{-1}$$

Galactic winds provide strong feedback in halos of small mass, leading to metal enrichment of the halo and the IGM

A WIND IN A $10^{10} M_{\odot}/h$ HALO

$$M_{\text{tot}} = 10^{10} h^{-1} M_{\odot}$$

$$R_{\text{vir}} = 35 h^{-1} \text{ kpc}$$

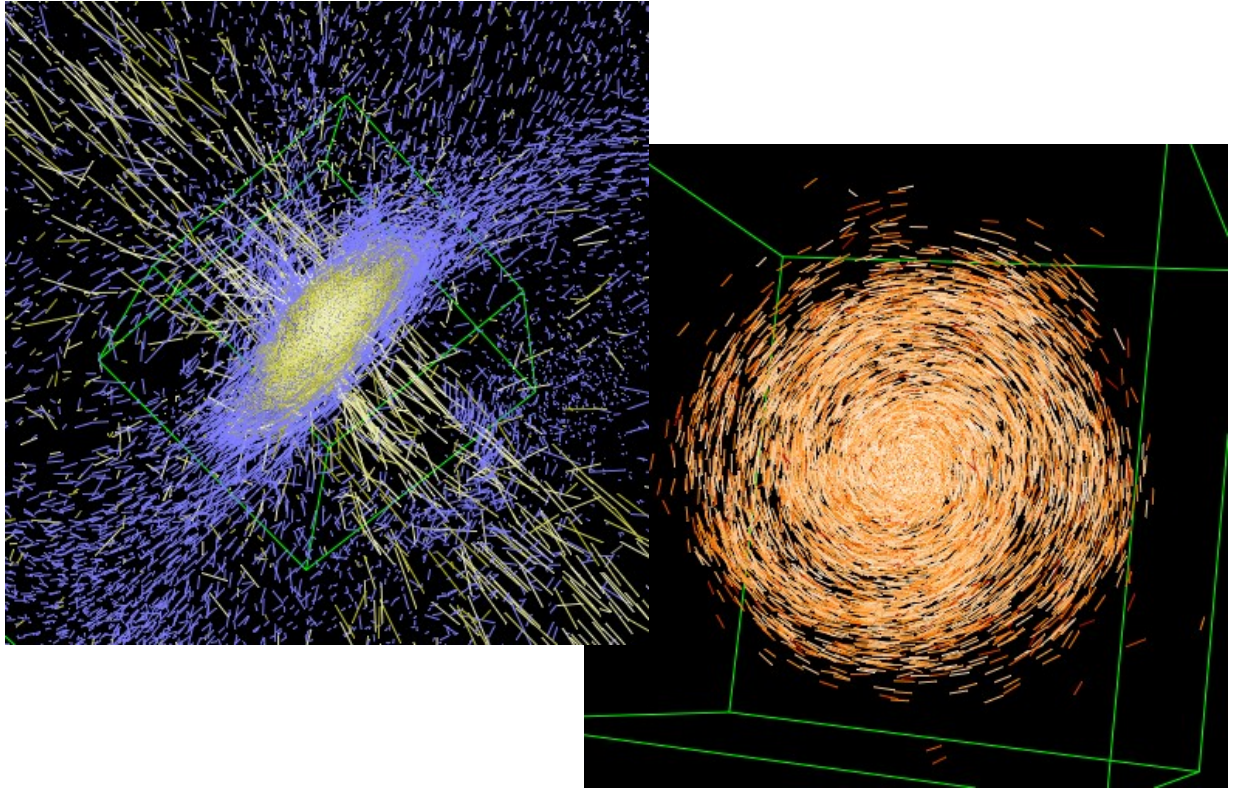
$$c = 15$$

$$\lambda = 0.1$$

$$f_{\text{gas}} = 10\%$$

$$v_{\text{esc}} \simeq 130 \text{ km s}^{-1}$$

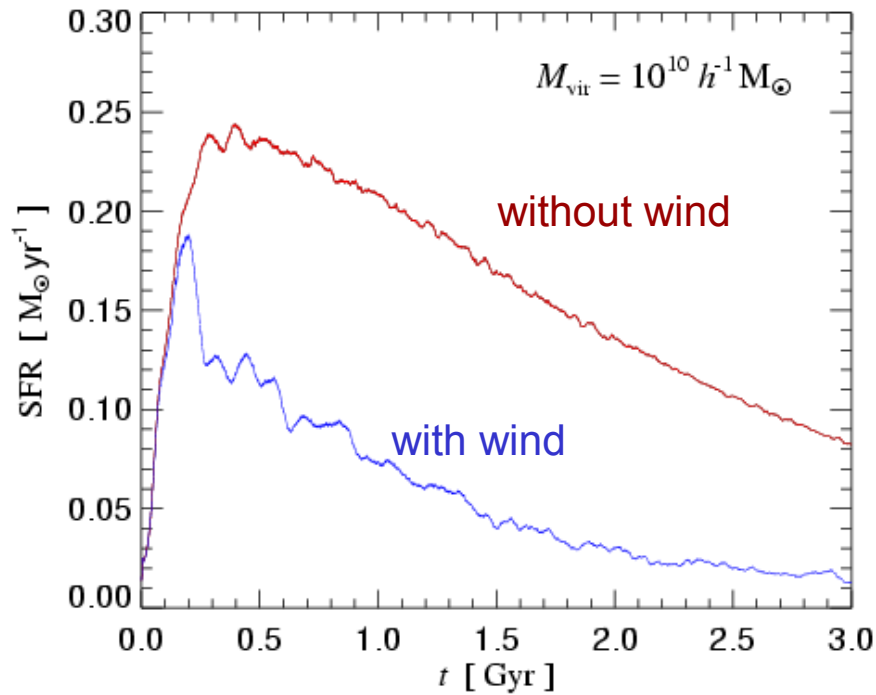
$$v_{\text{w}} = 242 \text{ km s}^{-1}$$



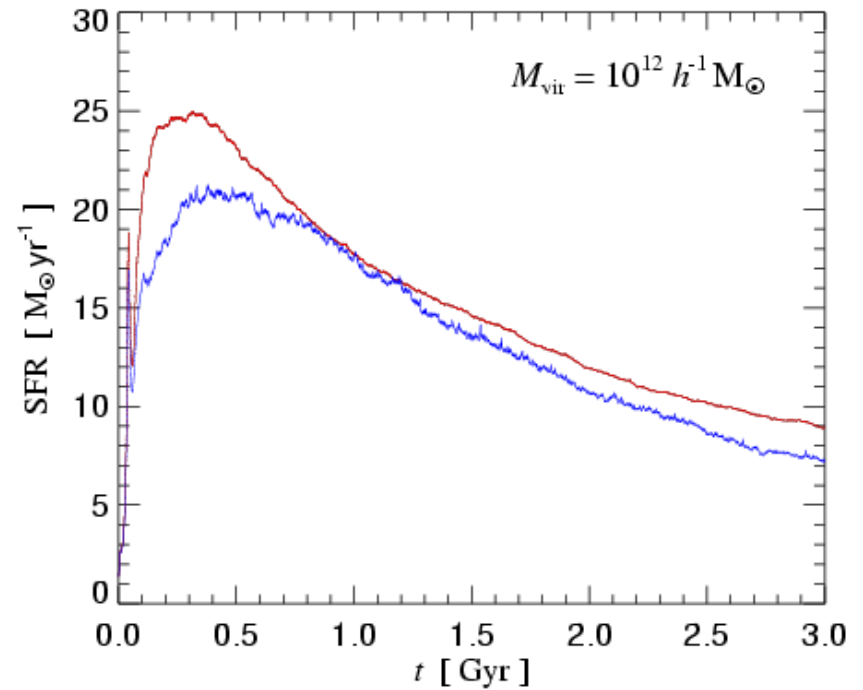
A galactic wind can strongly reduce the star formation rate in a halo if the wind can (nearly) escape from the halo

STAR FORMATION RATES IN HALOS

$10^{10} M_{\odot}/h$

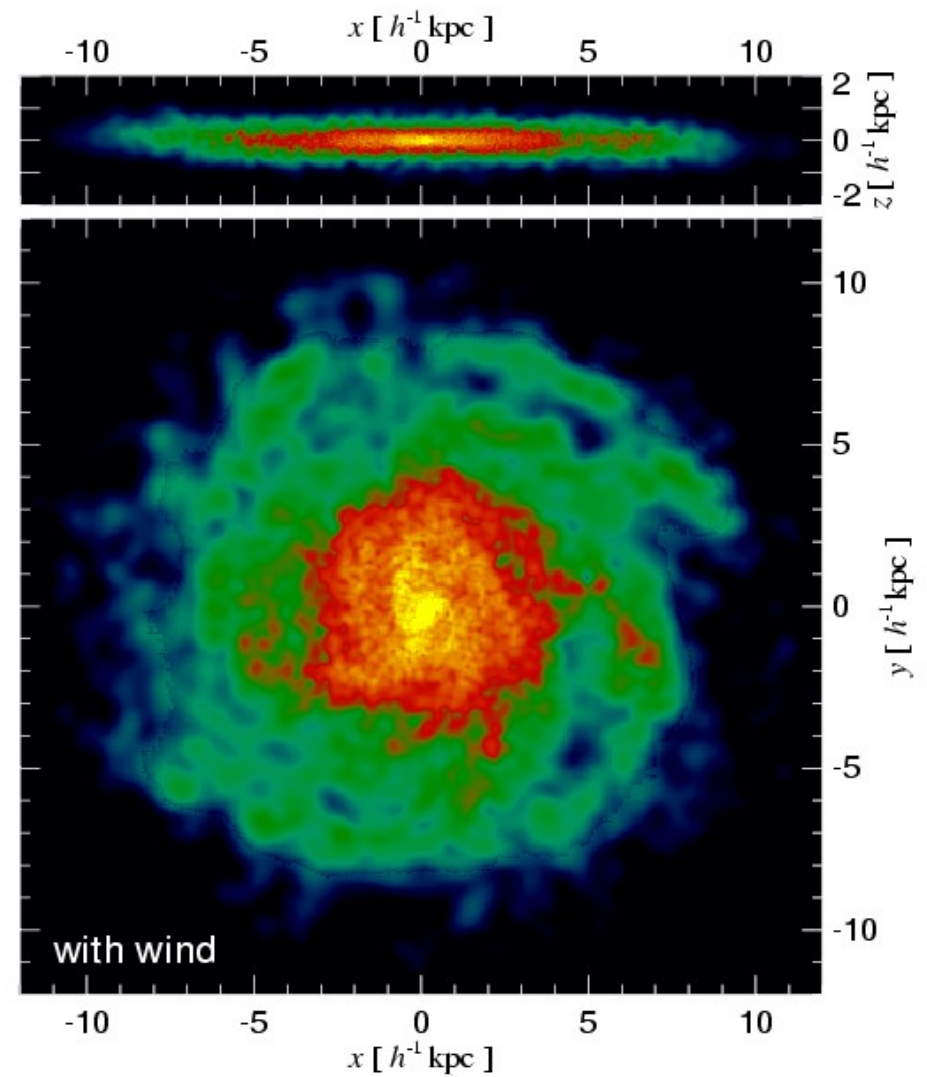
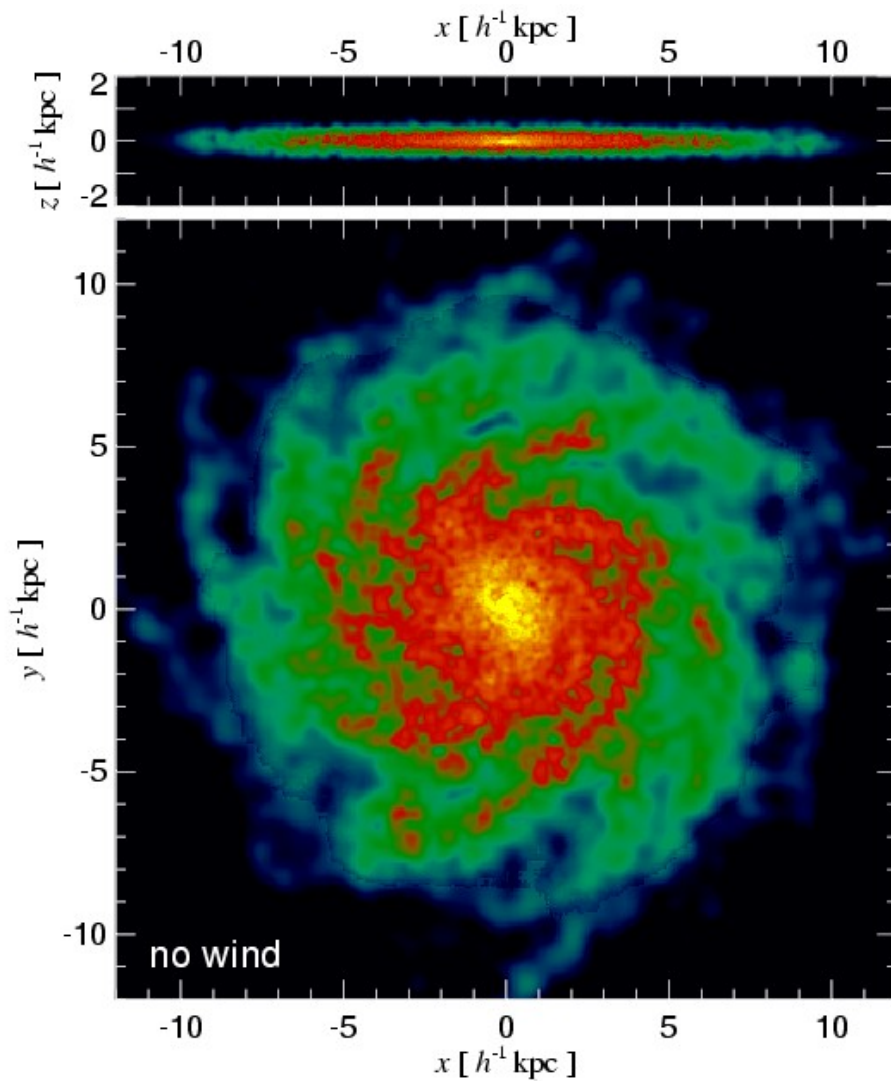


$10^{12} M_{\odot}/h$



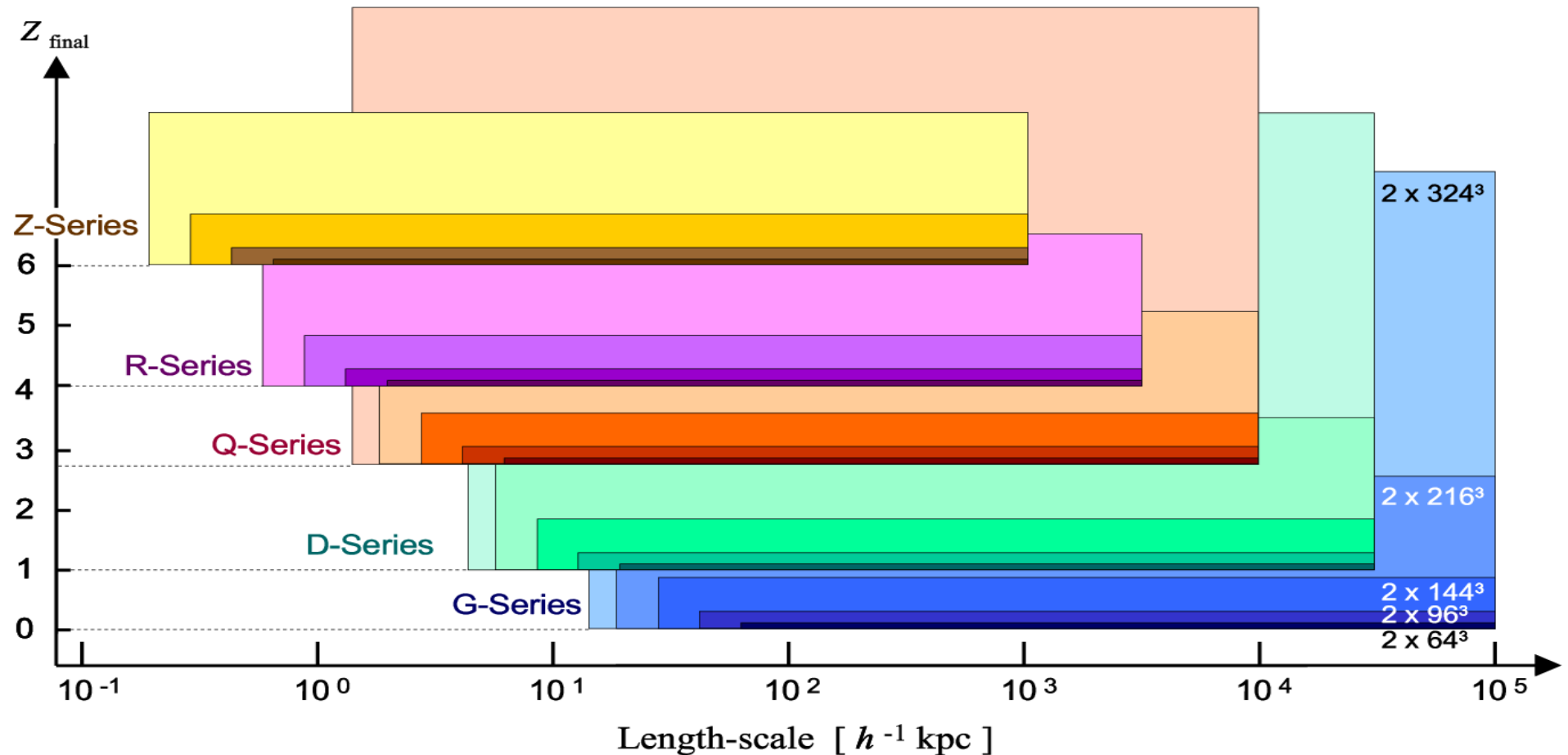
The winds hardly affect the morphology of the forming stellar disks

STELLAR DISK IN A $10^{12} M_{\odot}/h$ HALO



We have run a program of simulations on a set of interlocking scales and resolutions

SIMULATION PROGRAM



Beowulf-class computer

Configuration:

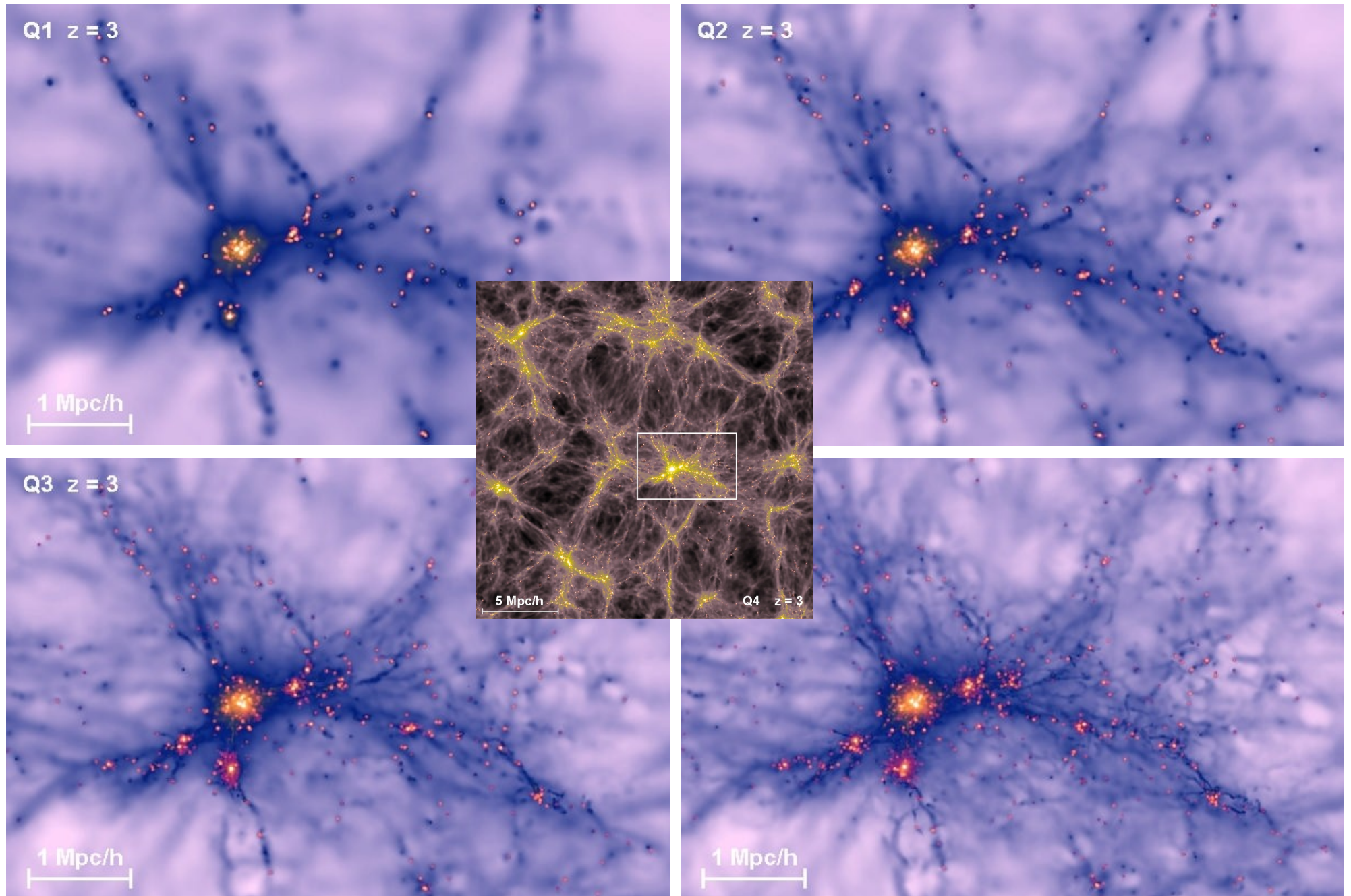
256 Athlon MP (1.6 GHz) arranged in 128 double-processor SMP nodes with 1 GB RAM each, 100 Base-T switched Ethernet, Linux Separate Frontend and 2 big Fileservers

A large set of simulations on interlocking scales has been run

TABLE OF SIMULATIONS

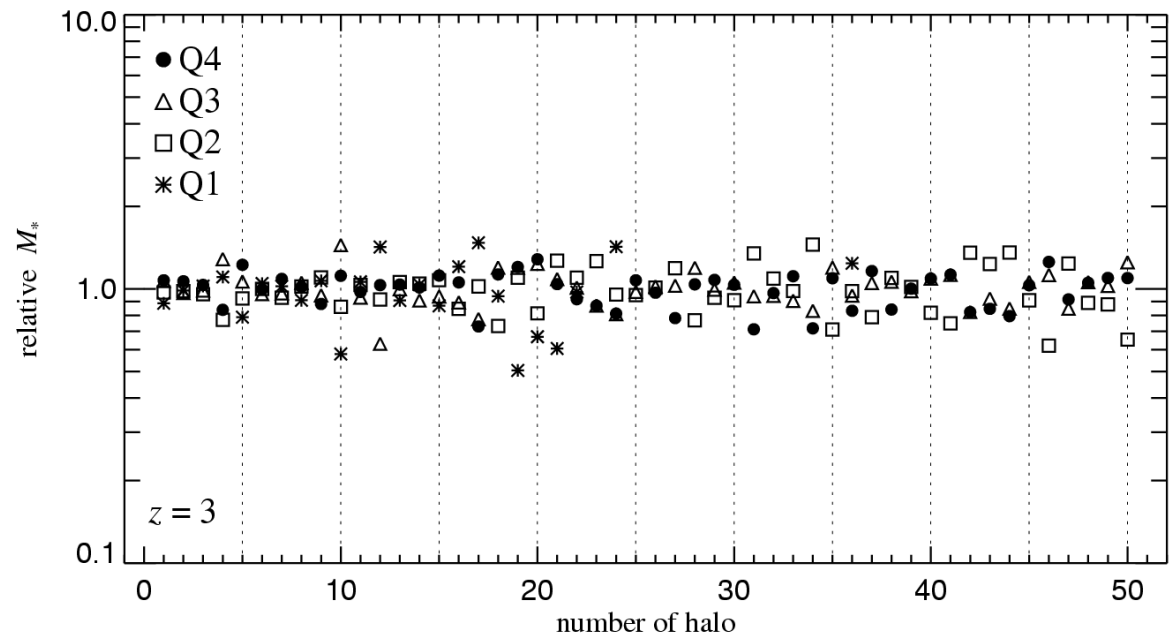
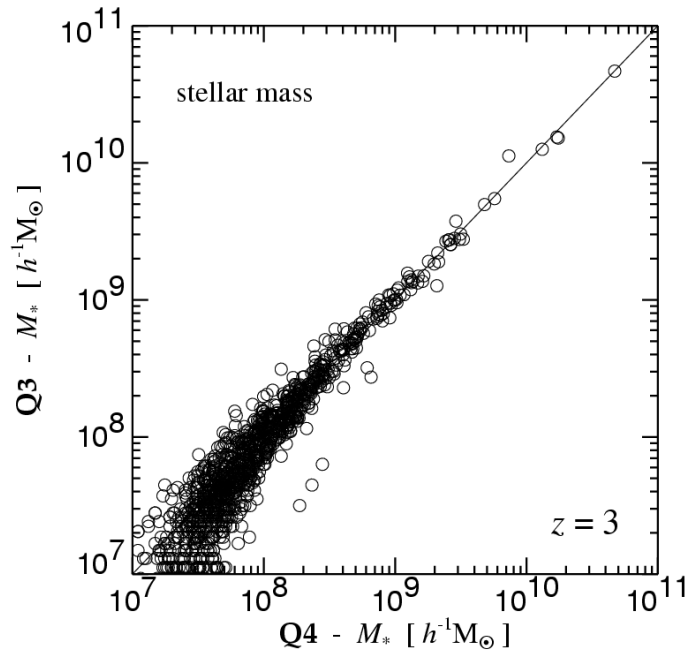
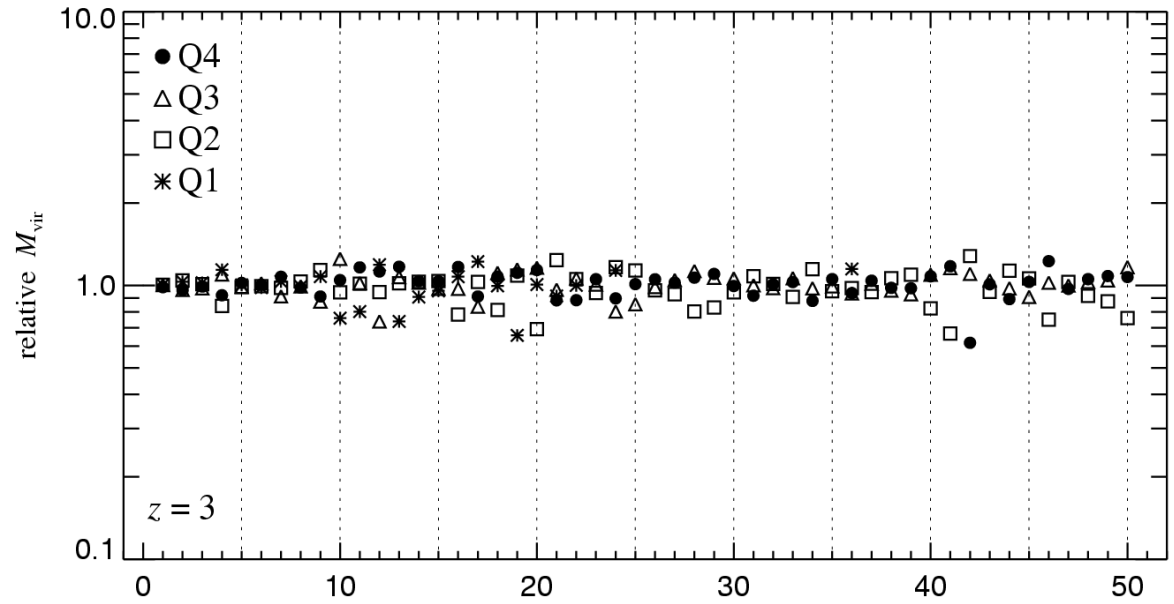
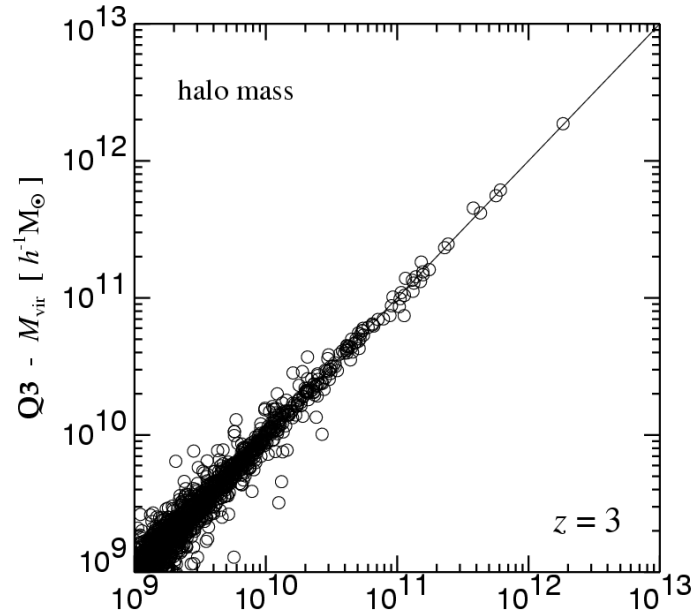
Simulation	$L [h^{-1}\text{Mpc}]$	Resolution	$m_{\text{DM}} [h^{-1}\text{M}_{\odot}]$	$m_{\text{gas}} [h^{-1}\text{M}_{\odot}]$	z_{start}	z_{end}	$\epsilon [h^{-1}\text{kpc}]$
Z1	1.000	2×64^3	2.75×10^5	4.24×10^4	199	6	0.63
Z2	1.000	2×96^3	8.16×10^4	1.25×10^4	199	6	0.42
Z3	1.000	2×144^3	2.42×10^4	3.72×10^3	199	6	0.28
Z4	1.000	2×216^3	7.16×10^3	1.10×10^3	199	6	0.19
R1	3.375	2×64^3	1.06×10^7	1.63×10^6	199	4	2.11
R2	3.375	2×96^3	3.14×10^6	4.84×10^5	199	4	1.41
R3	3.375	2×144^3	9.29×10^5	1.43×10^5	199	4	0.94
R4	3.375	2×216^3	2.75×10^5	4.24×10^4	199	4	0.63
Q1	10.00	2×64^3	2.75×10^8	4.24×10^7	159	2.75	6.25
Q2	10.00	2×96^3	8.16×10^7	1.25×10^7	159	2.75	4.17
Q3	10.00	2×144^3	2.42×10^7	3.72×10^6	159	2.75	2.78
Q4	10.00	2×216^3	7.16×10^6	1.10×10^6	159	2.75	1.85
Q5	10.00	2×324^3	2.12×10^6	3.26×10^5	159	2.75	1.23
D3	33.75	2×144^3	9.29×10^8	1.43×10^8	159	1	9.38
D4	33.75	2×216^3	2.75×10^8	4.24×10^7	159	1	6.25
D5	33.75	2×324^3	8.15×10^7	1.26×10^7	159	1	4.17
G3	100.0	2×144^3	2.42×10^{10}	3.72×10^9	79	0	18.0
G4	100.0	2×216^3	7.16×10^9	1.10×10^9	79	0	12.0
G5	100.0	2×324^3	2.12×10^9	3.26×10^8	79	0	8.00

Higher mass resolution can resolve smaller galaxies



The star formation rate of individual galaxies converges well for sufficient mass resolution

OBJECT-BY-OBJECT RESOLUTION STUDY



The star formation density can be decomposed into contributions coming from different halo mass scales

MULTIPLICITY FUNCTION OF COSMIC STAR FORMATION

The halo mass function:

$$g(M, z) = \frac{dF}{d \log M}$$

Requires large volume to properly sample massive end

The mean normalized star formation rate in halos of given mass:

$$s(M, z) = \frac{\langle \dot{M}_\star \rangle}{M}$$

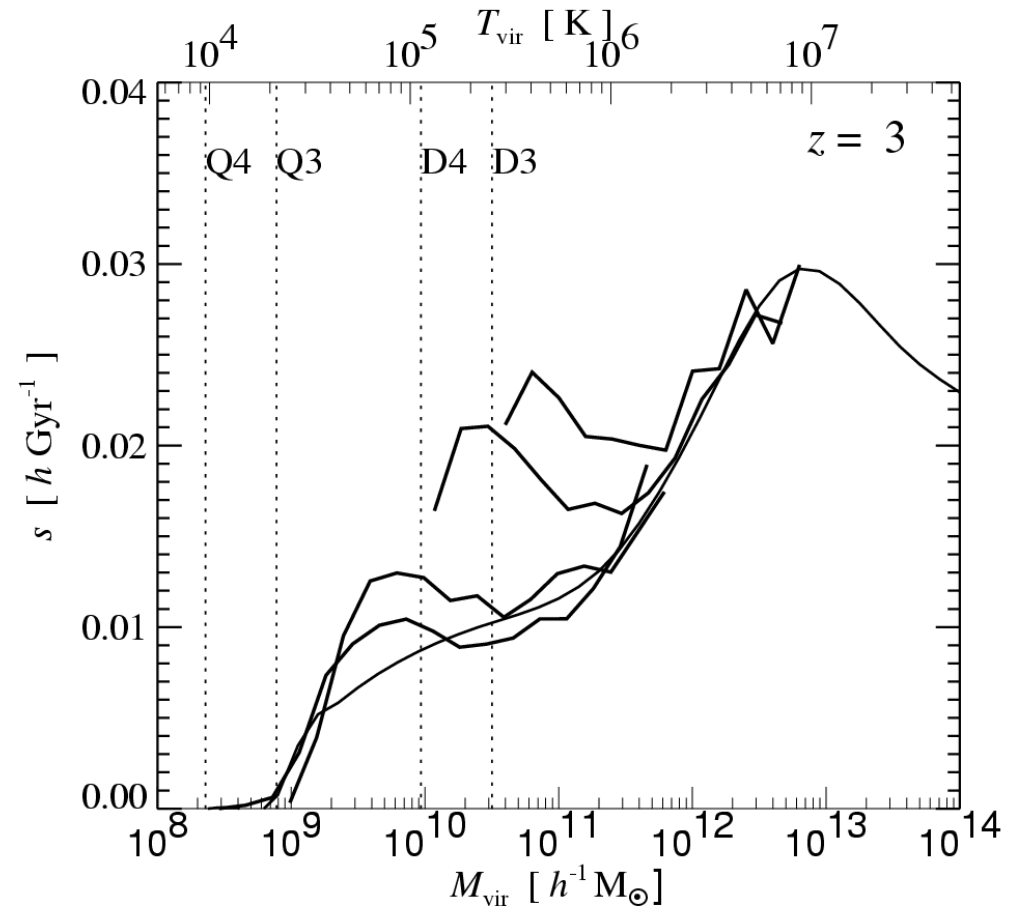
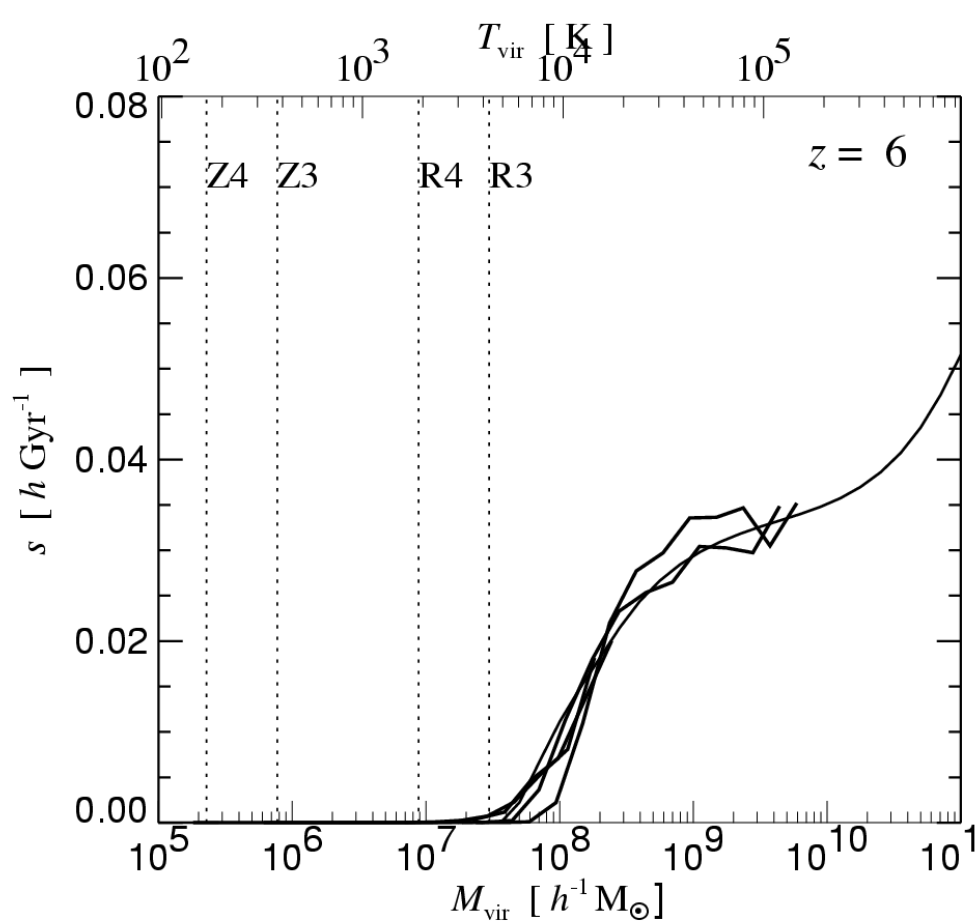
Requires high mass resolution to account for feedback in progenitor halos


$$\dot{\rho}_\star(z) = \bar{\rho}_0 \int g(M, z) s(M, z) d \log M$$

Multiplicity function of cosmic star formation

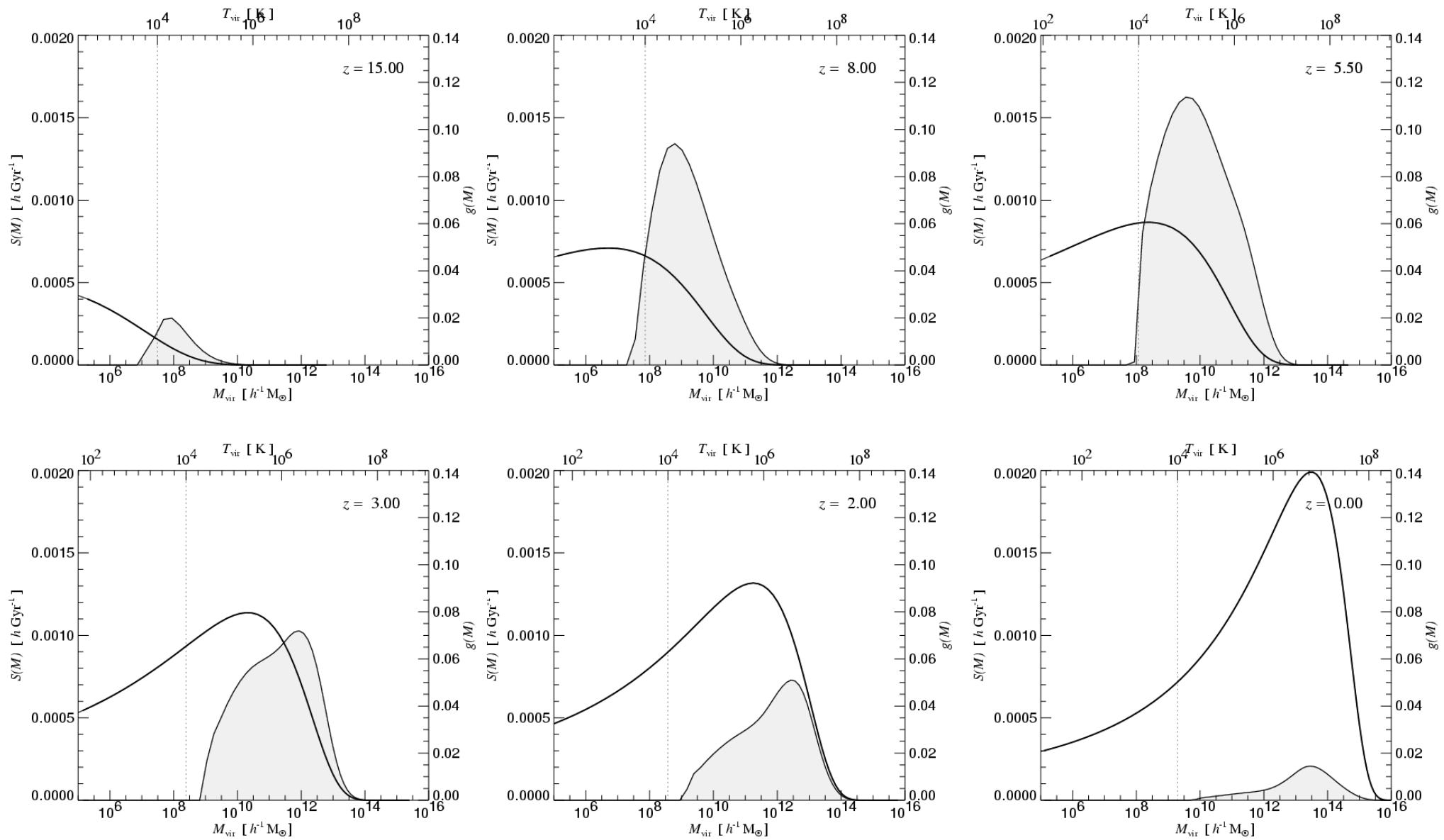
The efficiency of star formation in halos of given mass can be estimated reliably by combining simulations of different resolution

THE EFFICIENCY OF STAR FORMATION IN HALOS OF GIVEN MASS



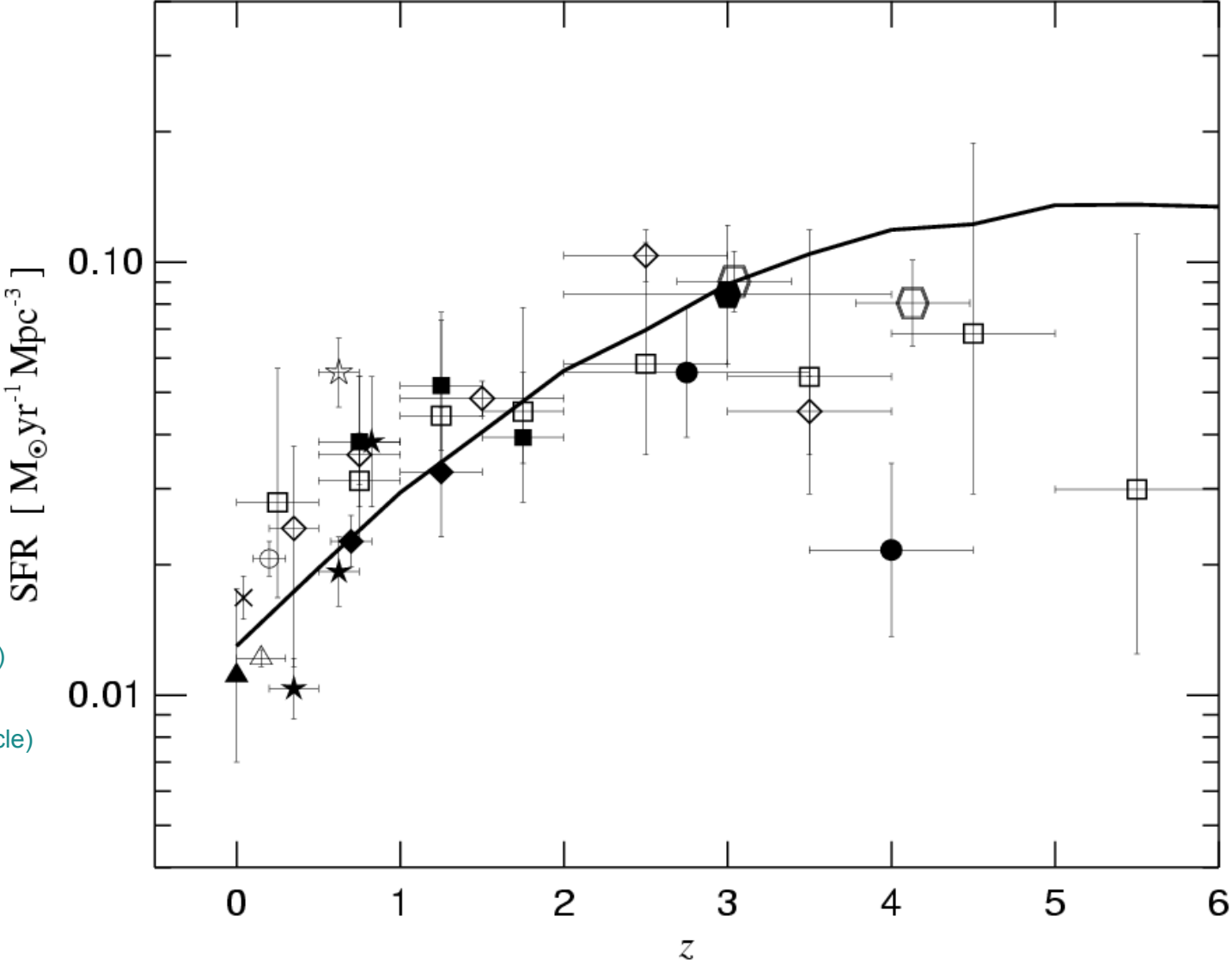
As the universe evolves, star formation shifts to higher mass scales

THE MULTIPLICITY FUNCTION OF STAR FORMATION AT DIFFERENT REDSHIFTS



Comparison of the predicted star formation history with observational results

THE EVOLUTION OF THE COSMIC STAR FORMATION DENSITY

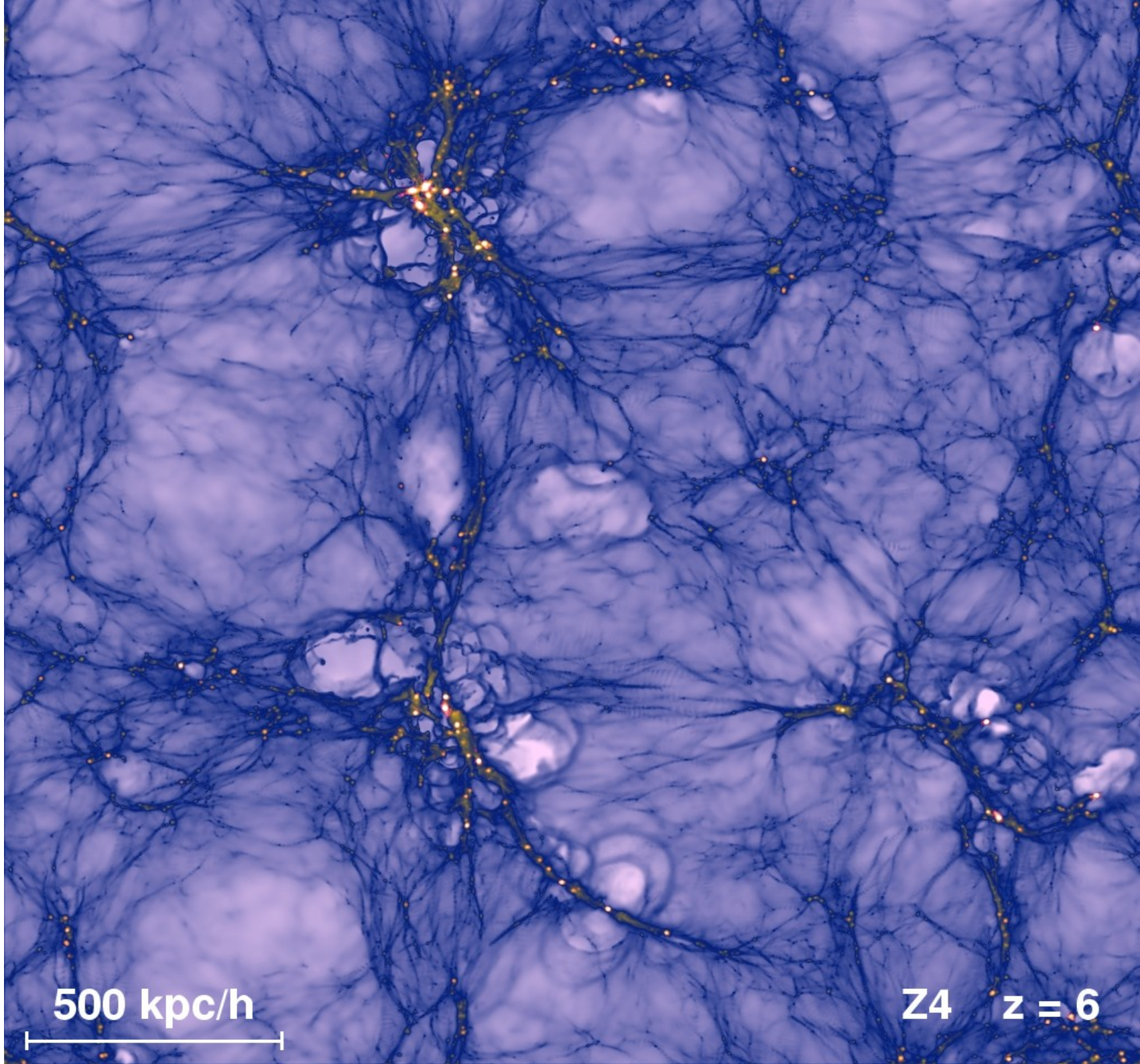


Data points by:

- Gallego et al. (1996, filled triangles)
- Gronwall (1999, diagonal crosses)
- Tryer et al. (1998, open triangle)
- Tresse & Maddox (1998, empty circle)
- Lilly et al. (1996, filled stars)
- Conolly et al. (1997, filled squares)
- Madau et al. (1996, filled circles)
- Pettini et al. (1998, empty squares)
- Flores et al. (1999, empty stars)

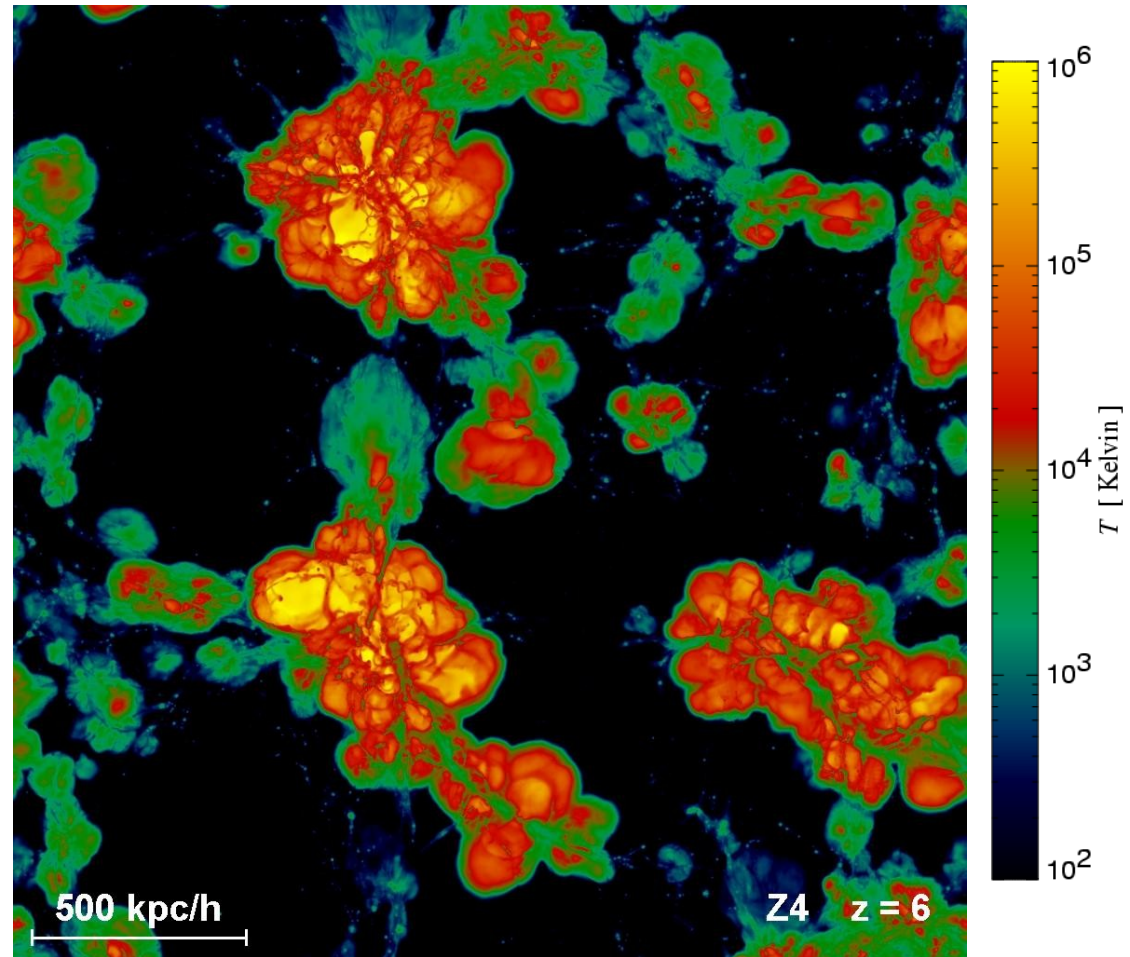
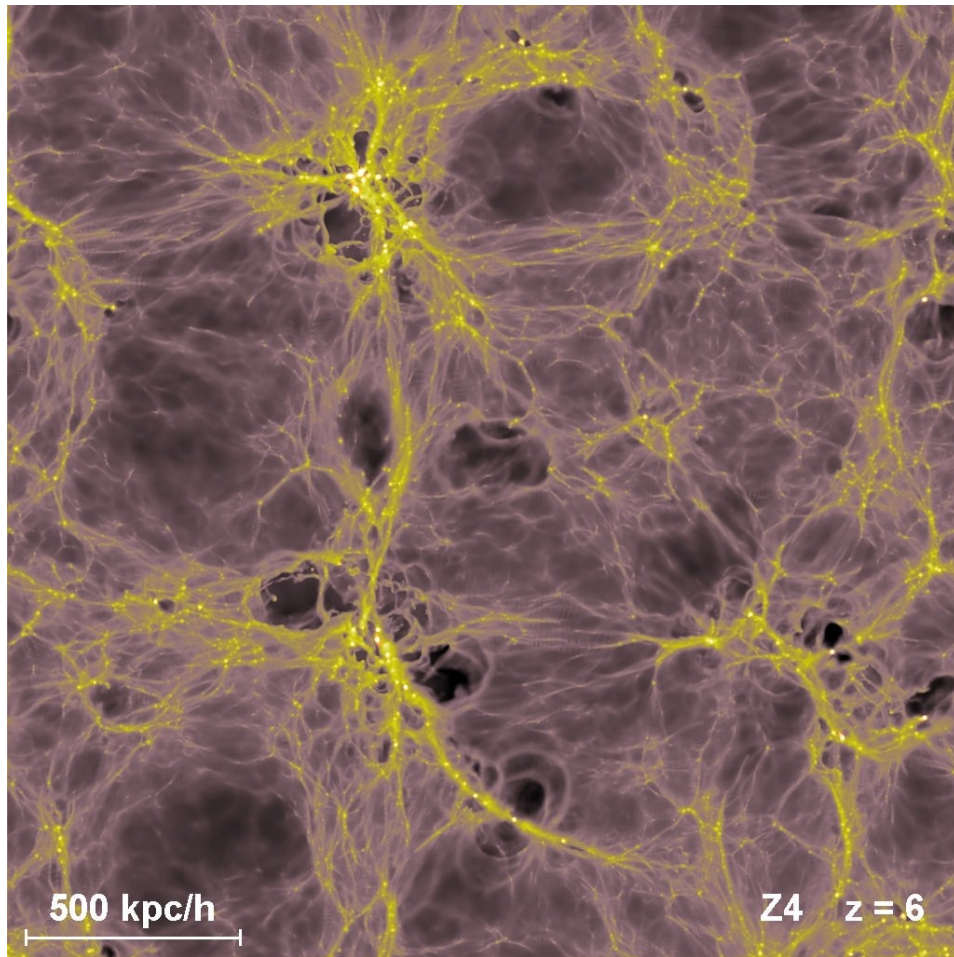
The "large-scale" structure seen at high redshift superficially resembles the morphology of structure seen at low redshift

GAS DISTRIBUTION SEEN IN A SMALL PERIODIC BOX AT REDSHIFT $z=6$

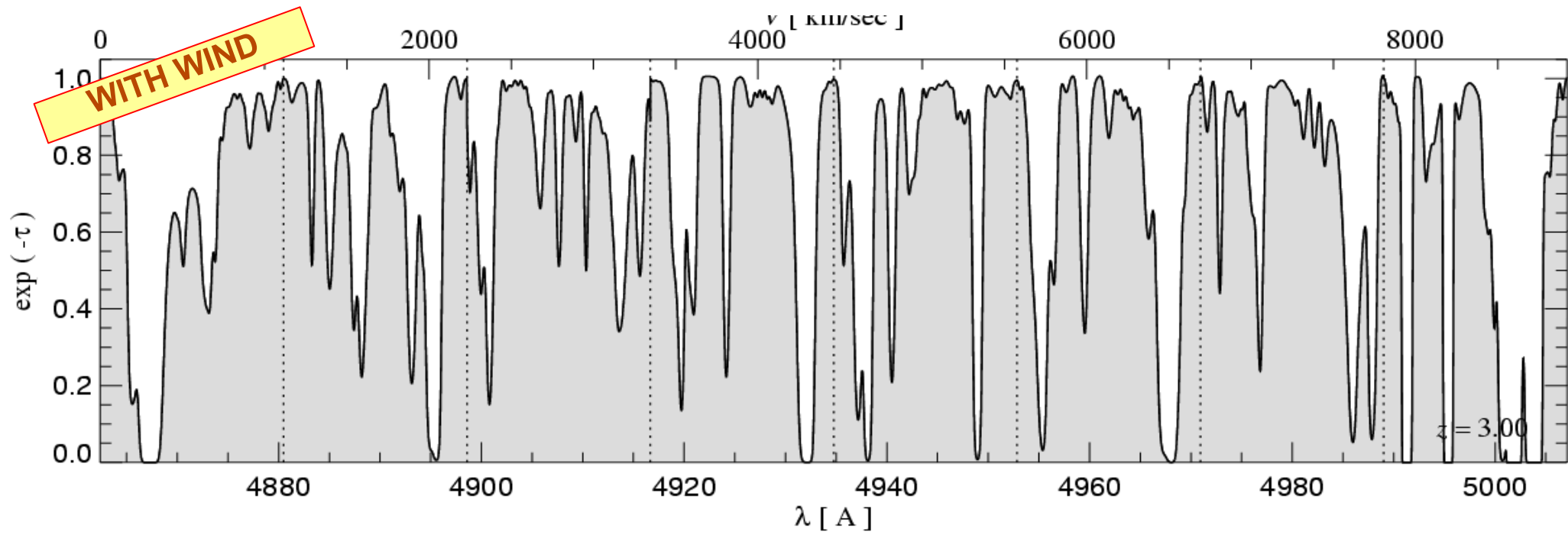
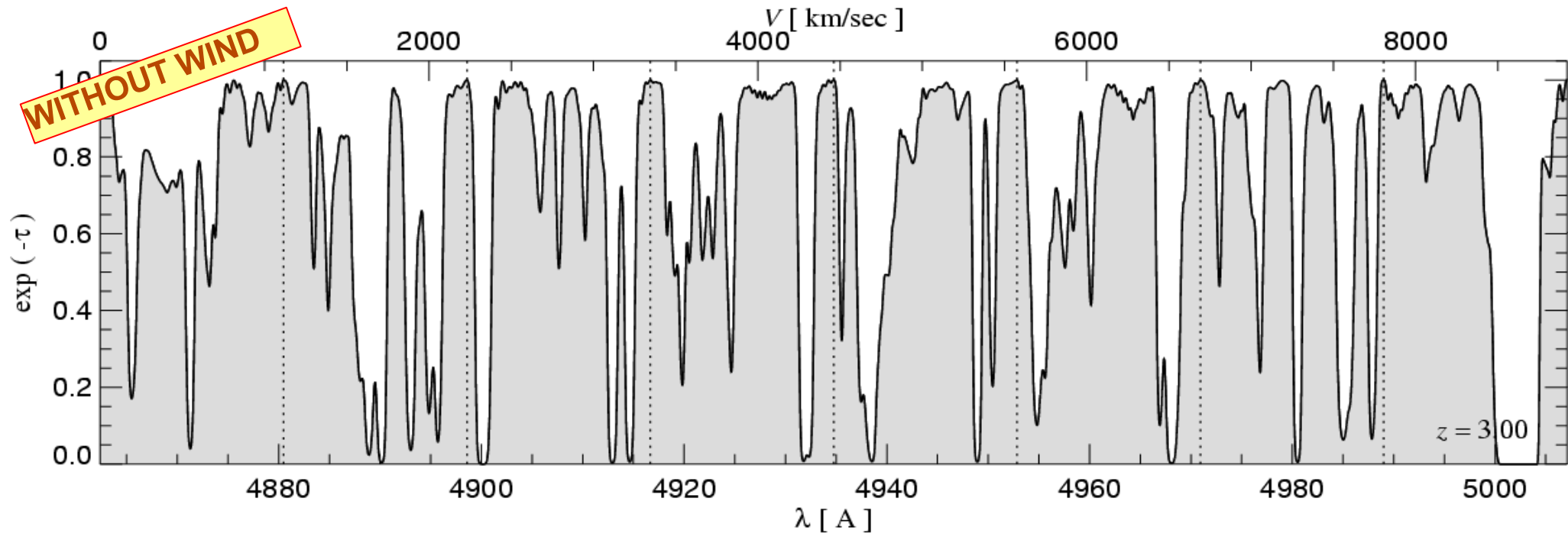


Galactic winds that escape from galaxies are producing shocks in the IGM, dissipating their kinetic energy into heat

HOT BUBBLES IN THE IGM GENERATED BY WINDS



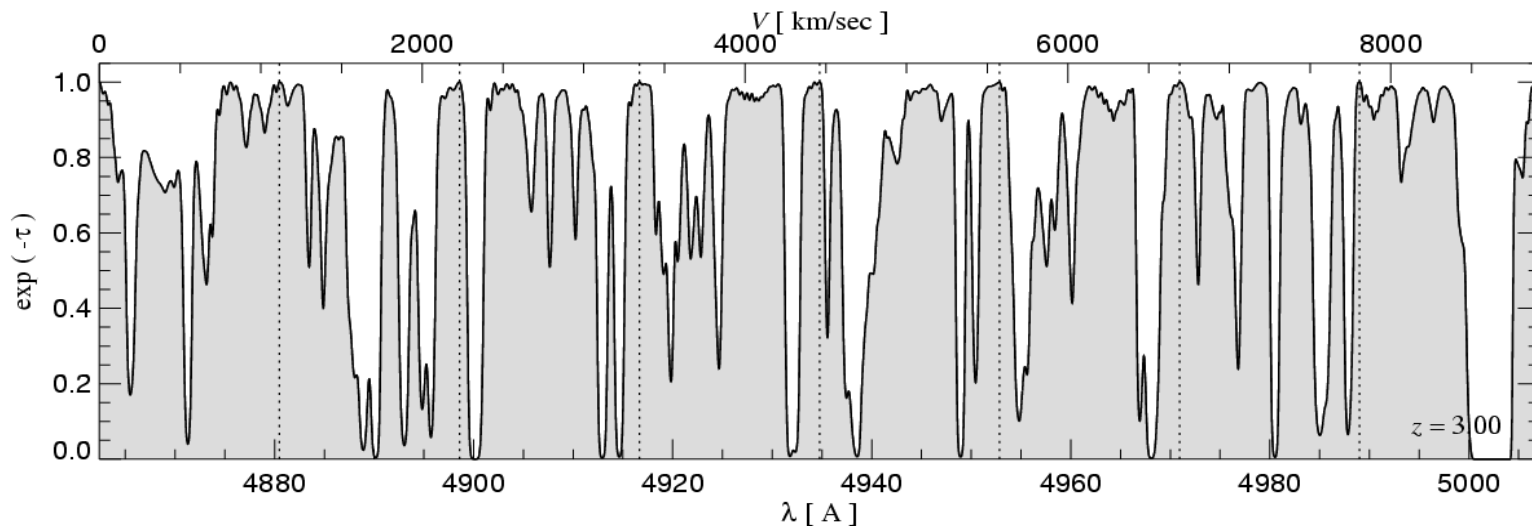
The Lyman alpha forest appears to survive nicely even for strong winds



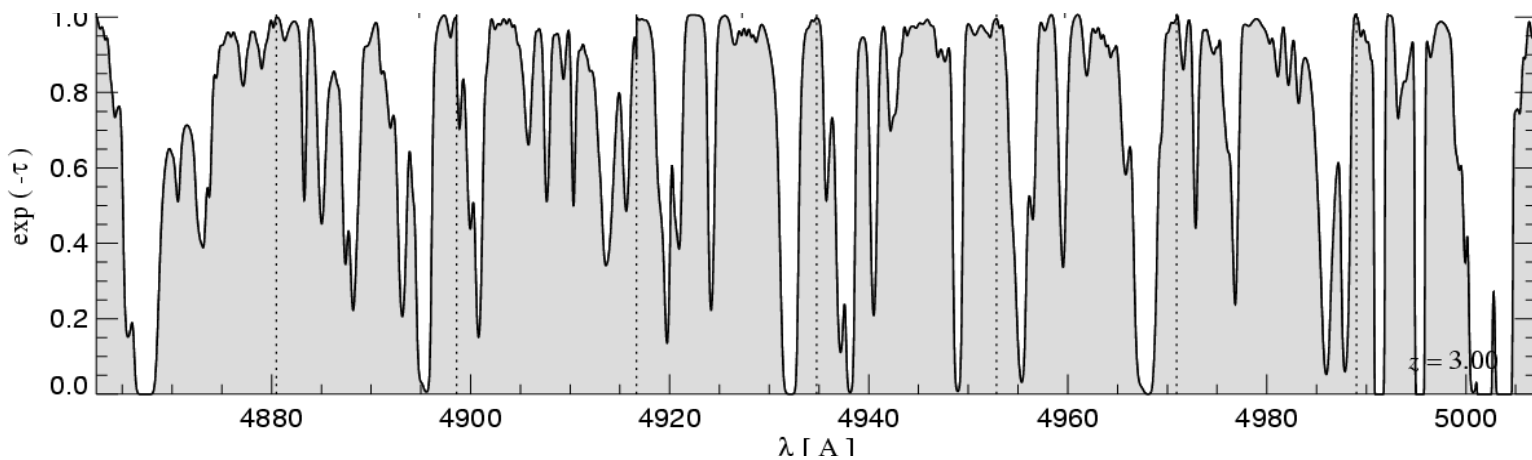
Winds induce differences in transmission

IDENTICAL LINES OF SIGHT

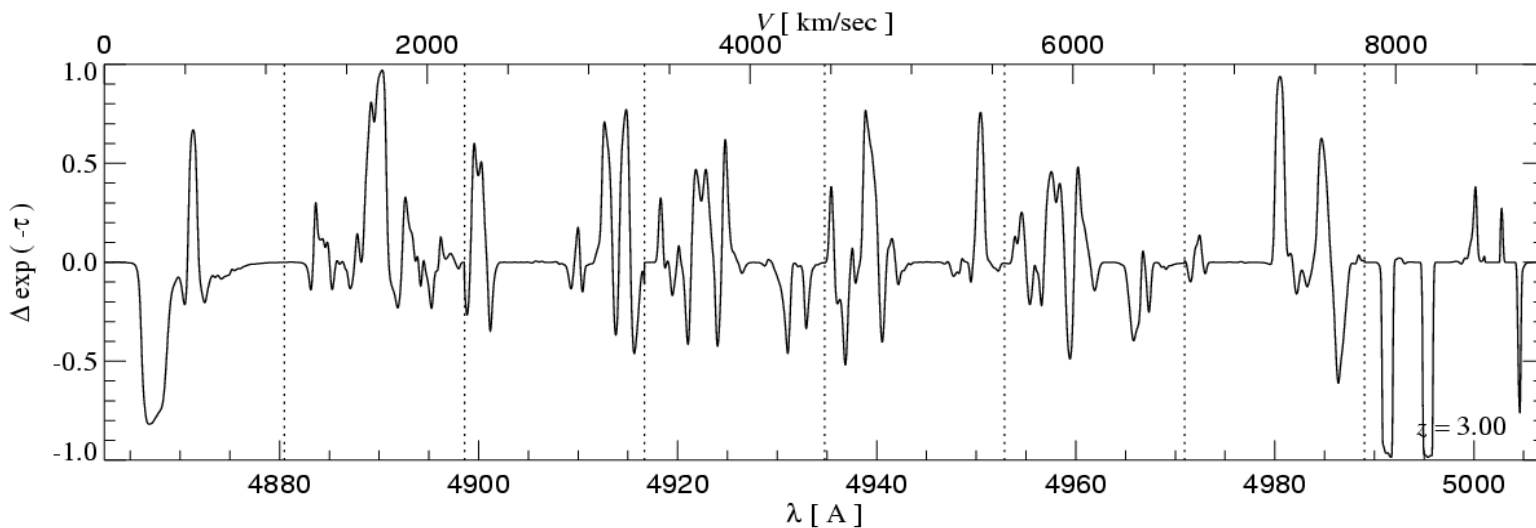
Without wind:



With wind:



Difference in transmission:



(maximum difference selection)

Projected
metallicity
maps
reveal a
highly non-
uniform
enrichment
pattern

PROJECTED
MEAN GAS
METALLICITY

